EFFECT OF VARIOUS GASES ON CO DISINTEGRATION OF MONOLITHIC REFRACTORIES FOR COAL GASIFIERS

by

George E. Wrenn, Jr.

Thesis submitted to the Graduate Faculty of the

Virginia Polytechnic Institute and State University

in partial fulfillment of the requirements for the degree of

MASTER OF SCIENCE

in

Materials Engineering

APPROVED:

J. J. Brown, Jr., Chairman

G. V. Gibbs

W. W. Payne

D. P. H. Hasselman

May, 1979

Blacksburg, Virginia

Acknowledgements

Research is often the combined efforts of many individuals toward a common goal. Many persons participated at all levels in the research program from which this thesis emerged. From apparatus construction to sample preparation, to analysis of sample performance, without the aid of the following individuals, the amount of results represented by this thesis could never have been obtained is so short a time. To

and for help in sample preparation and analysis; to for sample preparation and experimentation in the area of particle size effects; and especially to who was truly a partner at all levels in the research effort for many months, my deepest heartfelt thanks and appreciation.

I would also like to thank of the United States Department of Energy for guidance and support, and to the Department itself for funding the project and the various publications and presentations it has yielded. Thanks as well go to

and for their helpful suggestions and reviews of this thesis, and to for typing it and the many other reports generated in the research program.

My warmest, most special thanks are reserved for three most special people. Thank you mom and dad, for help in getting me to and through school and college, for understanding all the frustrations and problems I have encountered along the way, and always being there. And finally, thanks to a true friend and mentor,

for insight, guidance, and leadership, and for being someone who is more than a teacher or counselor, but an educator. Thanks again to all.

TABLE OF CONTENTS

CONTENTS (CONT'D)

CONTENTS (CONT'D)

CONTENTS (CONT'D)

CONTENTS (CONT'D)

CONTENTS (CONT'D)

CONTENTS (CONT'D)

CONTENTS (CONT'D)

CONTENT (CONT'D)

I. Introduction

A. Objective of Thesis

This thesis examines the effects of CO_2, NH_3, H_2, H_2S and H_2O on CO disintegration of three monolithic refractory compositions for coal gasifiers. These effects have been examined previously for conditions found in blast furnaces. The present study was undertaken to examine the applicability of these results to coal gasifiers conditions.

B. History of Coal Gasification

Combustible gases have been produced from coal for more than 100 years. The earliest major application of coal gas was lighting the streets of London. Coal gasification died out for all practical purposes in the U.S. in early 1900's with the more economical recovery of natural gas and petroleum, which also yielded, in terms of heat content, higher grade fuels. In addition to coal gasification, coal liquefaction was developed during the latter part of the second World War by Germany, which today along with France have major commercial facilities for coal conversion. The largest number of currently operating commercial coal conversion plants is in South Africa. Fifty-eight of the 120 currently operating commercial coal gasifiers world-wide utilize the Lurgi process. Howard-Smith and Werner[1] provide a review of these and the many newer methods of coal gasification that are known. Of the 62 remaining gasifiers, 36 use the Winkler System[1] and 26 Koppers-

Totzek system[1].

In the United States, techniques such as CO_2 Acceptor, HYGAS, and BIGAS, to name a few, which produce higher grade gases are under active consideration[2]. Figure 1 summarizes the overall features of these various techniques in schematic form. These higher grade gases can be boosted to the same grade as natural gas and introduced into the pipeline system carrying natural gas all across the country. This is the goal of the American effort. In order to be "pipeline quality," the gas must also enter the system at 1000 psi, and the feasibility of operating the entire gasification process at this pressure is being considered for efficiency purposes.

C. Refractory Problems in Coal Gasification

Refractories in the new generation coal gasifiers will be exposed to a condition of temperature, pressure, and atmospheric composition that has no analog in other refractory applications. The United States Department of Energy is coordinating a large number of research programs across the country that are examining a variety of refractory materials and the problems they may face in coal gasifiers[3]. Among these DOE-sponsored programs is an investigation of CO disintegration of monolithic refractories for coal gasifiers that began in June, 1977 at V.P.I. and S.U. under the direction of J.J. Brown, Jr.

D. Objectives and Scope of VPI/DOE Program

The primary goal of the VPI/DOE program is to determine whether

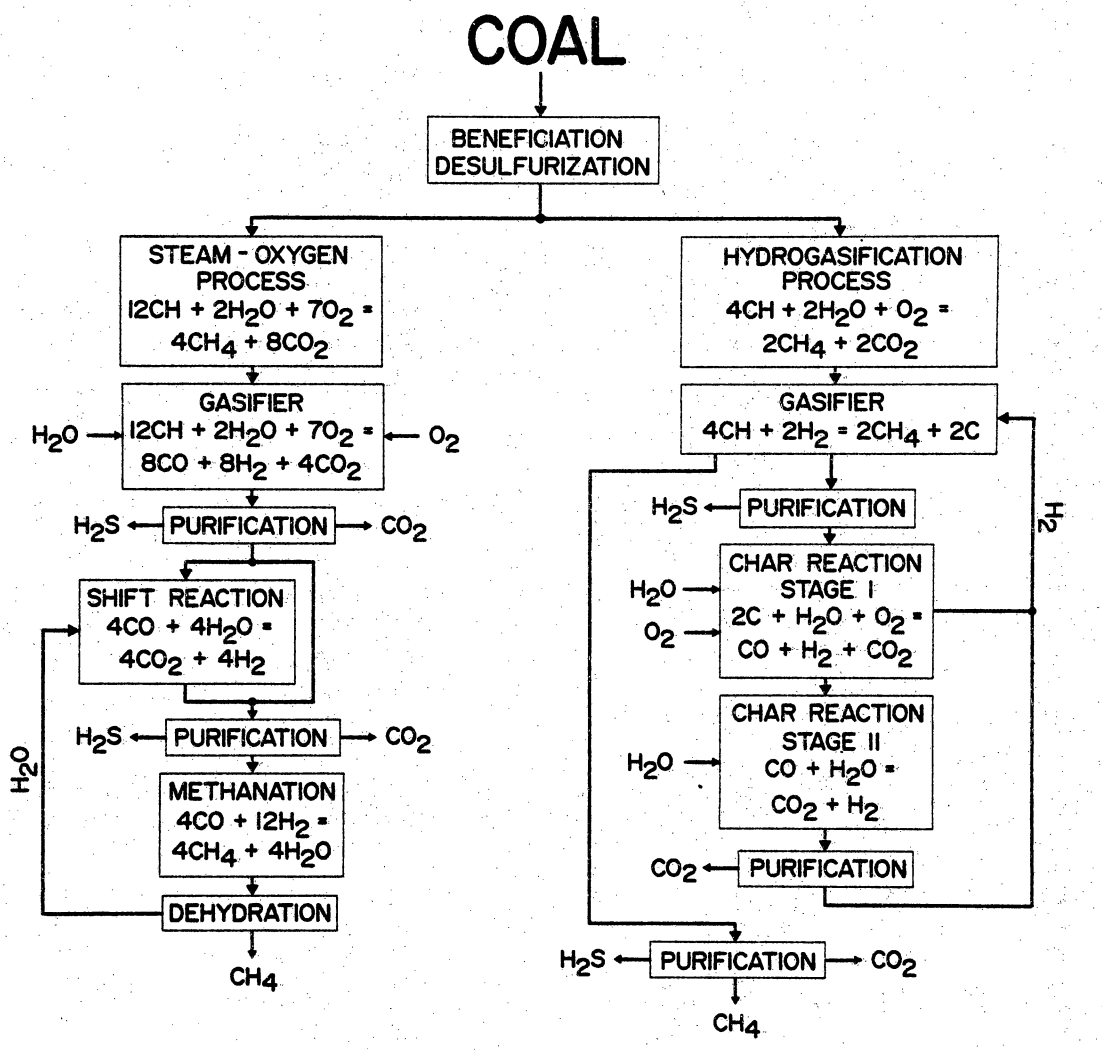

S. KASPER, "A STRATEGY FOR COAL GASIFICATION," SECOND ANNUAL SYMPOSIUM ON COAL GASIFICATION, LIQUEFACTION, AND UTILIZATION; UNIVERSITY OF PITTSBURGH, AUGUST 5-7, 1975

W.W. BODEL, K.C. VYAS, "CLEAN FUELS FROM COAL - INTRODUCTION TO MODERN PROCESSES," IGT - CLEAN FUELS FROM COAL SYMPOSIUM, CHICAGO, ILL., SEPTEMBER 10-14, 1973

Figure 1. Schematic Diagram of Coal Gasification Processes.

or not CO disintegration will be a problem for coal gasifier refractories. A secondary objective is to identify the conditions which do produce CO disintegration. The program was initially divided into six tasks:

Task 1a. Perform 100 Hr. Standard CO Disintegration Test[51] on Laboratory Monoliths to Determine Effect of Fe and Fe_2O_3 Impurities.

Task 1b. Repeat Standard CO Test at Elevated Pressure (500 to 1000 psi) To See If Pressure Affects Disintegration

Task 2. Examine the Effects of Gas Composition on CO Disintegration Using the Following Mixtures:

Gas	%, Balance CO
CO_2	5, 15
NH_3	0.2, 0.8
H_2	20, 40
H_2S	0.2, 0.8
H_2O	20, 40

And Form A Statistical Matrix to Charactize Gas Effects. Repeat These Tests At High Pressure If Task 1b. Results Significant.

Task 3. Perform Confirmation Tests Using DOE Coal Gas Atmospheres:

Gas No.	CO	CO_2	H_2	H_2O	CH_4	H_2S	NH_3	N_2
1	13	12	24	40	4	1.0	1.0	0
2	14	5	45	18	18	0.1	0	0
3	19	6	12	12	0	0.3	0	53

Task 4. Evaluate Selected Commercial Refractories for Resistance to CO Disintegration.

Task 5. Determine Effect of Alkali and Sulfur Impurties on CO Disintegration.

Task 6. Evaluate Clews et. al.[11] Rapid Test for CO Disintegration.

Two tasks have since been added:

Task 7. Examine Effect of Iron-Impurity Particle Size on CO Disintegration.

Task 8. Evaluate the Time-Dependence of CO Disintegration In Selected Refractory Compositions.

Results from Task 8 will be needed before the matrix in Task 2 can be made quantitative.

E. Scope of Thesis

The major portion of this thesis is concerned with Task 1a and the experimental results of Task 2 in the VPI/DOE CO Disintegration Program. Appendix IV and Appendix V contain, respectively, preliminary results from Task 7 and Task 1b. A survey of literature that is related to CO disintegration is also presented.

II. Literature Survey of CO Disintegration

A. Early Investigations

Disintegration of refractories by CO has been recognized as a refractories problem for more than 100 years. Investigations conducted during the mid-1800's yielded conclusions about CO disintegration that have been verified many times since. In 1876, Pattinson[4], found that susceptibility to CO disintegration was greatly increased by the presence of Fe_2O_3 in refractories. Earlier, Stammer[5] observed in 1851 that Fe_3C might have been a catalyst for CO disintegration. Deville[6] showed that the $CO_2 + C = 2CO$ reaction was reversible in 1864, and Bell[7] found that carbon deposition was favored at temperatures less than 800°C.

B. Method of Attack

Refractories are affected by CO by means of carbon deposition. Davis, Rigby, and Slawson[8] observed that the carbon forms as minute vermicular growths 100 Å to 0.2 μ in thickness that can penetrate a considerable distance into the refractory. This work was performed on brickwork for blast furnaces. The carbon is deposited catalytically in a range from about 400°C to 700°C, as shown by Berry, Ames and Snow[9], with many studies[10-14] finding temperature ranges of carbon deposition in blast furnace linings within an overall band of 300°C to 700°C.

Other investigators[15-22] have performed tests at 450-550°C, where CO disintegration is considered most active. These studies, all of which focus on blast furnace refractories or conditions, follow that of Boudouard[23], who carefully investigated the temperature dependency of the $CO_2 + C = 2CO$ reaction.

C. CO Disintegration Catalysts

A number of different Fe-containing materials have been found to cause CO disintegration of refractory materials. In general, these impurities were contained in the raw materials forming the refractory or were introduced through beneficiation. Some studies[24-28] have examined CO disintegration in various blast furnace refractories without naming a specific catalyst, while many studies[12,29-38] have examined only the effects of iron oxide as a catalyst. Other studies[10,19,22,39-42] occurring during the 1930's and 1940's, have examined the catalytic effects of Fe_3O_4, Fe, Fe_2S, FeO, and Fe bound in clay silicates in addition to Fe_2O_3. The closest thing to real agreement between these investigations is that Fe, FeO and Fe_2O_3 are generally more reactive with CO; Fe_2S and the clay-bound iron are less reactive; and Fe_3O_4 falls between the two groups. In the 1950's, Stammer's[5] original proposition that Fe_3C was the CO decomposition catalyst was confirmed. Davis and Rigby[43] found that Fe_2O_3 was converting by and large to Fe_3O_4, but, that small amounts of Fe_3C were present in refractories examined in 1954. Two years later, Berry, Ames, and Snow[4], established that iron carbide, specifically $Fe_{20}C_9$ between

400 and 565°C and Fe_3C between 565 and 700°C, was the catalyst. Other proposed cataylsts, such as Fe and Fe_2O_3, were converted to Fe_3C or $Fe_{20}C_9$ before carbon deposition was catalyzed.

D. CO Disintegration Accelerators and Inhibitors

Along with their identification of iron carbides as the catalyzing agent, Berry, Ames, and Snow[9] showed the effects of some other compounds on CO disintegration. Small amounts, less than 5%, H_2 and H_2O to CO tended to accelerate the deposition of carbon. Gaseous and solid sulfur inhibited the formation of the carbides, thus slowing CO decomposition. Sulfurous compounds were seen as retardants by other investigators[17,37,44-46] as well. Berry, Ames, and Snow[9] also found that small amounts of NH_3 also retarded CO disintegration and that Zn and alkalis tended to poison the effects of sulfur. Ground quartz, phosphates, and chrome have also been identified as inhibitors in various studies[16, 29,38,39,47]. Cyanogen has also been identified as a CO disintegration accelerator by Hibbot and Rees[15]. Diluting the CO with CO_2 has also been shown by Chesters[48], and Rigby, Booth and Green[44] to retard carbon deposition.

E. CO Disintegration Tests

The majority of the studies cited have used tests similar to ASTM C-288, which was proposed in 1950[50] and accepted in 1955[51]. Shea[17] and Trostel[52] outline procedures for test design which are similar to ASTM C-288, while Clews et. al[11] and Pukall[53] designed

tube furnace "rapid tests". Phelps[54] proposed study of a standardized test in 1952 by the Refractories Institute while the ASTM standard was being drawn up. Nadachowski[20] suggested a method based on weight increases of powder concentrates in firebrick samples, similar, it seems to the analytical techniques of the rapid tests.

F. Coal Gas and CO Disintegration

Only one investigation, performed by Towden and Green[55], reports the effect of a coal gas atmosphere on refractories. Firebrick resisted spalling in 200 hr. exposures at 500 and 800°C. Cracking occurred after 72 hr. at 900°C, a temperature at which CH_4, rather than CO tends to dissociate and deposit carbon. Other investigators[14,56] also report the deposition of carbon from CH_4. Westman[57] has also investigated carbon deposition from town gas. This gas could have been either produced from coal or tapped from a natural gas deposit in the earth; Westman does not say.

G. Summary

The volume of literature on CO disintegration in blast furnace refractories is indeed large. The majority of these studies deal with silica or fireclay brick, although the most recent papers[25,26,38] have followed the blast furnace industry into the realm of castables. It should be noted that these investigators observed that castables generally behaved the same as fireclay bricks in regard to CO disintegration. Studies examining CO disintegration in conditions other than

blast furnaces are very rare indeed, and only one, possibly two, investigations have been conducted in coal gas atmospheres.

III. Experimental Procedure

A. Sample Preparation

1. 90+ Wt.% Alumina Castable

This castable is made in 7 kg batches according to the composition shown in the first column of Table I. Batch calculations are made for the various raw materials, some of which need to be screened on a Ro-Tap machine[1] to achieve proper particle size distribution. Screened and as-received materials are then weighed to ± 1 gm. on a scale[2] and combined in an electric mixer[3]. Metallic iron[4] and iron oxide[5] dopants, also weighed to ± 1 gm. are added to the batch and dry-mixed for at least 2 min. For "Effect of Iron-Impurity Particle Size on CO Disintegration," Appendix IV, as-received iron oxide is sintered in mullite crucibles at 1250°C in air, crushed in a steel impact mortar, and screened to required particle size distributions before mixing.

Water is then added and mixing is continued until the batch achieves ball-in-hand consistency. Approximately 650 ml. of water is needed.

---

1. Tyler Company, Ohio
2. Toledo Scales Company, Ohio
3. Hobart Manufacturing Company, Ohio
4. Electrolytic, Fisher Scientific Company, Pennsylvania
5. Certified, Fisher Scientific Company, Pennsylvania

Table I. Castable Compositions for CO Disintegration Tests

Ingredient (Wt.%)	90+ Wt.% Al_2O_3	50+ Wt.% Al_2O_3
Tabular Alumina[6]		
6x10 mesh	25	--
10x20 mesh	20	--
-20 mesh	20	--
Calcined Alumina[6]		
-325 mesh	10	--
Calcined Kaolin[7]		
6x10 mesh	--	25
10x20 mesh	--	20
-20 mesh	--	15
-200 mesh	--	15
Binder (CA-25C)[6]	25	25

6. Aluminum Company of American, Pennsylvania
7. Mulcoa 47, C. E. Minerals, Pennsylvania

The castable is poured into 2 in. x 2 in. x 2 in. aluminum molds that were previously coated with liquid soap[8] to prevent sticking, vibrated for 2 min. to release excess water, and sealed in a plastic bag for 24 hours. The sealed bag creates an atmosphere of 95+ % relative humidity over the samples, allowing them to cure properly. Samples are stored in air after removal from the molds. One 7 kg. batch yields approximately 18 samples.

2. 50+ Wt.% Alumina Castable

This castable is prepared according to the same procedures as the 90+ wt.% alumina castable. The composition is shown in the second column of Table I. A 6 kg. batch yields approximately 20 samples, and, generally requires 700 ml. of water to achieve ball-in-hand consistency.

3. 90+ Wt.% Alumina Phosphate-Bonded Ramming Mix

The ramming mix composition is listed in Table II. Weighing and combining of dry ingredients, including dopants, is the same as for the castable refractories. An 8 kg. (excluding dopants) dry batch is prepared and broken down into 800 gm. batches, which are stored in small plastic bags. Each bag contains enough material for two 2 in. x 2 in. x 2 in. samples.

Forty-eight ml of phosphoric acid and 2 ml water are added to each bag and mixed by hand for 5-10 minutes. Bags may stand for up to

8. Liquinox, Alconox Company, New York

Table II. Ramming Mix Composition for CO Disintegration Test

Ingredient	Wt.%
Tabular Alumina[9]	
6x10 mesh	30
10x20 mesh	20
-20 mesh	15
-48	17
Calcined Alumina, -325 mesh[9]	15
Bentonite (Wyoming)[10]	3
Hydrated Alumina[11]	1 (Added)
Phosphoric Acid, 85%[11]	6 (Added)
Water	0.25 (Added)

9. Alumina Company of America, Pennsylvania
10. Laboratory Grade, Fisher Scientific Company, Pennsylvania
11. Certified, Fisher Scientific Company, Pennsylvania

18 hours after mixing was completed before the samples are formed. The samples are made individually in a mild steel mold on a hydraulic press[12] at 5,000 psi. A 20,000 lb. load is applied through plungers in both ends of the mold by holding the mold 1/2 in. above the bottom of the lower plunger until compacting of the materials has begun. This is done in order to achieve more uniform density in each sample. Samples are cured in air at 250°C for 12 hours and stored in air.

B. Prefiring of Samples

Samples of all three monolithic refractories are prefired at 1100°C for 5 hours in order to drive off water and sulfur-bearing compounds. A separate prefire furnace, described in Appendix II, is used. Samples are prefired within 72 hr. of being used so that only small amounts of water will be re-absorbed prior to testing.

C. Atmospheric Pressure Experiments

1. Preparations

Prefired samples of all three refractories are weighed and then loaded into two atmospheric pressure test furnace chambers. Up to 60 samples may be put in each chamber. After samples are arranged, fibrous insulation[13] is placed in the necks of the furnace liners to prevent both heat loss and failure of o-ring seals due to excessive temperature. Cover plates are then attached while making sure that

12. Midvale-Heppenstal, Pennsylvania
13. Fibrofrax, Aluminum Company of American, Pennsylvania

o-rings seat properly in their guide channels. The coverplates are each secured by twelve bolts that are turned finger-tight and tightened with wrenches in the order shown in Figure 2a as many times as needed in order to assure sealing of the o-rings. Gas and water inlet tubes are attached, along with the gas outlet pipes, which are connected to condensation tanks.

The water inlet tubes and condensation tanks were added for experiments involving the effect of H_2O on CO disintegration and are not included in the original description of apparatus in Appendix II. The condensation tanks are filled or drained to one quarter full of water and steam in the exhaust gas is removed by bubbling it through the water in the tanks.

After all connections are made to the furnaces, exhaust line valves are closed and N_2 gas at approximately 5 psi is added to each furnace to check for leaks. If flowmeters indicate there is no gas flow after pressurization of the reaction chambers and condensation tanks, exhaust valves can be opened and heating of the samples may begin, however, if gas continues to flow, leaks must be located and sealed.

2. Heating Cycle

When preparation for a run are completed, thermocouples are inserted into wells in the coverplates and water flow through furnace liner cooling coils is started. The Master Switch in the control room is turned on. When temperature monitors on the wall of the control

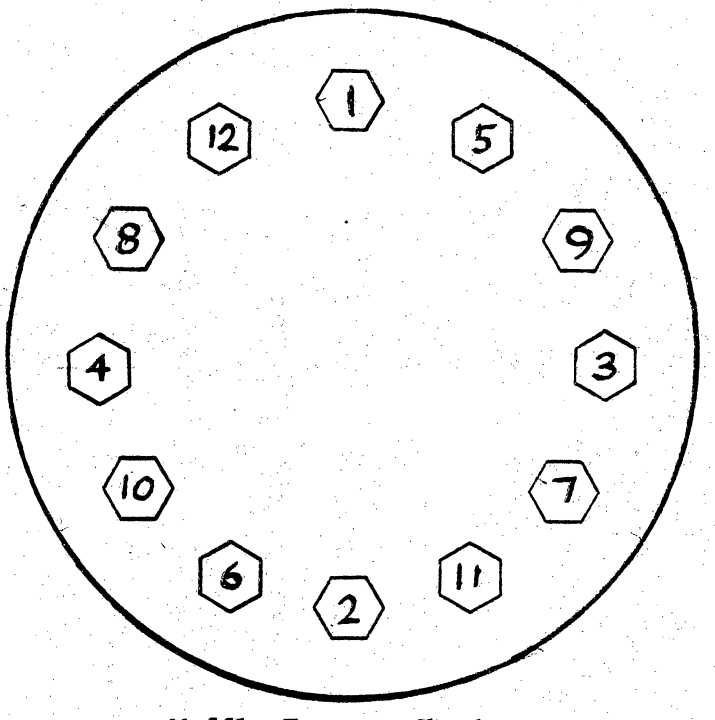

a. Muffle Furnace Chamber

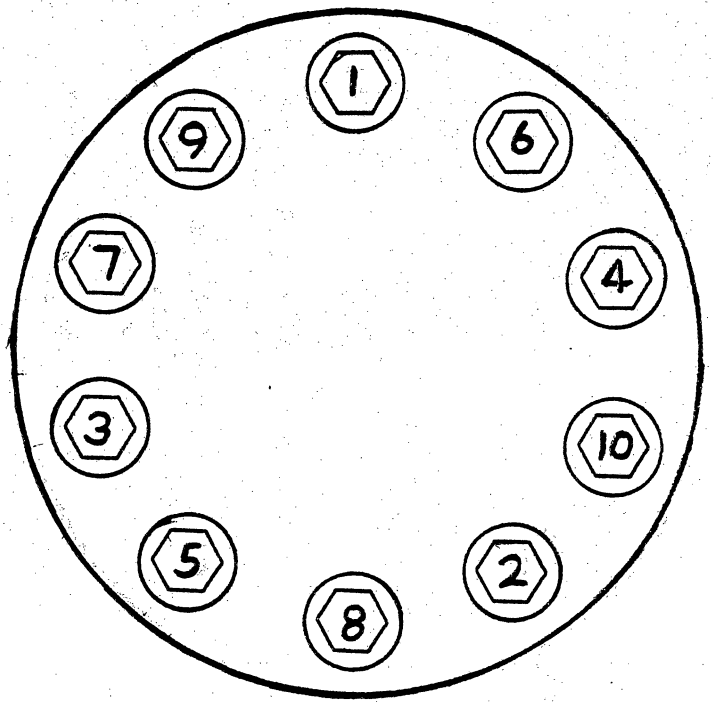

b. High Pressure Furnace Cell

Figure 2. Bolt Tightening Sequences

room have warmed up, the master relay is set in the on position. Furnace controllers are then turned on and set for 500°C. Samples are heated in N_2 at approximately 5 psi which is added at a flow rate of 1 liter/hr. during heating. The furnaces are given at least 12 hr. to heat to 500°C and equilibrate.

3. Exposure to Reaction Gases

After furnaces have equilibrated at 500°C, reaction gases are introduced to the reaction chambers at approximately 5 psi, as was done for N_2. Total flow rate of the reaction gases is set at 5 liters/hr. to each chamber. The experiment is timed beginning with the conversion to reaction gases.

When steam is used as a reactant, flow rate of the other gases is reduced to correspond to their total percentage of the steam-containing atmosphere. For example, a reaction gas containing 80% CO and 20% H_2O would have a CO flow rate of 4 liters/hr., i.e., 80% of 5 liters/hr. Water is added at a rate of 1 ml/hr. for every 1 liter/hr. of steam needed. This rate was calculated based on the volume of liquid H_2O that is needed at 25°C to give the required volume of gaseous H_2O at 500°C. Ideal behavior of gaseous H_2O and other reaction gases was assumed. Errors caused by these assumptions are well within the limits of precision for determining and controlling gas flow rates and can be neglected.

Flow rate of water is controlled by setting the desired flow

rate on the syringe pump[14] in the control room and turning the machine on to infuse. This piece of equipment, as with the condensation tanks, was added for experiments with H_2O.

During the exposure, gas pressure and flow rate are monitored from twice a day to hourly, dawn to dusk, depending on season and weather. Large changes in gas pressure can be caused by heating and cooling of the gas regulator, which is on the roof of the building and exposed to the outdoor environment. In winter, small amounts of moisture may plug the exhaust line due to condensation and freezing. This shows up as zero flow rate combined with full operating pressure. The exhaust line valves for the furnaces are then closed and the section of exhaust tubing extending from the laboratory to the roof is replaced with another warmed tube in the laboratory. From spring through fall, when freezing is not a problem, a curved-top section of tubing is used for extension above roof level so that rainwater will not plug the exhaust line. Carbon plugs also form occasionally in the gas inlet tube in one or the other of the reaction chambers. When this occurs, the tube must be replaced.

The syringe pump is checked daily, and, empty syringes are replaced with full ones as needed. Syringes, themselves, occasionally need replacement due to friction between the plunger and syringe body.

4. Cooling Cycle

At the end of an experiment, the syringe pump is turned off if water is being used. Then N_2 is substituted for the reaction gas.

14. Sage Instruments Division, Orion Research, Inc., Massachusetts.

Power to each furnace is shut off and samples are allowed to cool with N_2 at approximately 5 psi flowing at 1 liter/hr. to each reaction chamber.

When the temperature of the chambers reaches 100°C or less, the thermocouples are removed, followed by the coverplates and fibrous insulation. N_2 flow is stopped and cooling continues to room temperature. Samples or fragments of samples can then be removed from the chambers and weighed.

D. High Pressure Experiments

1. Preparations

The high pressure reaction chamber requires the following maintenance before each experimental run. All carbon residue must be cleaned from the interior face of the cap using a towel or brush and from the entire length of the inlet and outlet tubes with pipe cleaners twisted together. Bolts on the cap nut must be removed and cleaned. After cleaning, oiled bolts are worked in and out of threads in the cap nut to clean these threads. The bolts are then coated with thread lubricant[15] and worked in and out of cap nut threads, recoating bolts with lubricant as needed, until threads in cap nut are also coated with lubricant. The large threads on the interior of the cap nut are also brushed clean and coated with lubricant. The top surface of the body of the reaction chamber is also brushed clean of any powder or debris.

15. Silver Goop, Crawford Fitting Company, Ohio.

Prefired samples are weighed and loaded into the high pressure chamber. This chamber holds up to ten samples. The cap is then fitted to the chamber so that a groove in the cap seats smoothly on a ridge on the top of the chamber body. A thrust washed is put on top of the cap, and the cap nut is then twisted into place. Bolts in the cap nut are then tightened following the pattern shown in Figure 2b to 40 ft. lb., then 80 ft. lb., and finally 85 ft. lb.

Pipes from the gas line are connected to the inlet and outlet ports of the reaction chamber. The entire high pressure system is then checked for leaks with N_2 at 100 psi and later N_2 compressed to 600 psi for the portion of the system containing gas at compressor-elevated pressure. The high pressure system is allowed to stand for 16 hr. to insure reasonable leak-tightness, i.e., a pressure drop of 10 psi or less from 600 psi.

The high pressure system is also fitted with an air-operated failsafe valve near the gas cylinders. In order to get gas to the high pressure system, the master switch and relay must be turned on. The air operated valve is then opened with 140 psi of N_2. The 140 psi limit may not be exceeded due to pressure limitations of the solenoid valve. A gas outlet on a solenoid valve, which provides the electronic link of the failsafe system, must be plugged temporarily with a finger in order for pressurization of the air operated valve to occur. The air operated valve and solenoid valve are then sealed off from the gas line by closing a valve, and a different valve to the high pressure system is opened. Pressure from the regulator is reduced to 100

psi. Pressure in the air-operated valve-solenoid valve link of the line must be recharged occasionally in order to hold the air operated valve open.

2. Heating Cycle

When the system is fully checked out, N_2 pressure is lowered to 30 psi and the furnace is turned on. Temperature is set at 500°F and allowed to equilibrate for 5 hr. The temperature is then reset to 940°F, N_2 pressure is reduced again to 30 psi, and 12 hr. is allowed for equilibration.

While the furnace is heating, the reaction gas cylinder and its regulator fitting are substituted for the N_2. Gases containing H_2S require a stainless steel critical service regulator in addition to a special cylinder fitting.

3. Exposure to Reaction Gases

Once the furnace has equilibrated at 940°F, N_2 is bled from the reaction chamber and it is charged with reaction gas. If steam is to be a constituent of the reaction gas, water is added immediately before pressurizing the chamber with other gases. The amount of water to be added is calculated based on the assumption that all water turns to steam and that both steam and the other reaction gases behave ideally with respect to temperature and pressure. The calculation is based on steam filling its specified percentage of the volume of the reaction chamber. A valve located near the furnace rupture disc is

closed so that the gas compressor can be protected from wetting by H_2O, which can damage the compressor head. Water is added by pressing the tip of a syringe containing the needed amount of water securely into the end of a pipe above the furnace gas inlet. A valve on the pipe is opened, water is then injected into the furnace and the valve is closed. The compressor is turned on and the closed valve near the rupture disc is opened quickly to prevent too much pressure buildup between it and the compressor. Some pressure buildup is desired, as this will reduce the possibility of water vapor flowing toward the compressor. When the desired pressure is obtained, the compressor is turned off and the valve near the rupture disc is again closed.

The reaction gas is bled off from the furnace and replaced 4 hr. after the initial charging and every 8 hr. thereafter. Water, when used, is also added at these same intervals. This quasi-static procedure is necessary due to failure of the adjustable check valve, described in Appendix II, to function properly. This valve was needed in order for gas to flow through the high pressure system continuously, yet be at the desired pressure. Changing the gas every 8 hr. much more than equals the 5 ℓ/hr. flow rate of gas in the atmospheric pressure experiment, however, the gas must be recharged this often due to large decreases in pressure caused by a highly increased rate of CO decomposition at high pressures.

4. Cooling Cycle

Upon conclusion of the exposure time to reaction gases, these gases are bled from the reaction chamber, which is then charged to

100 psi with N_2. The furnace is turned off and the samples are cooled to room temperature in a static N_2 atmosphere.

The high pressure reaction chamber cannot be opened until it has cooled completely to room temperature. At higher temperatures, thermal expansion of its metal parts make the sealing bolts impossible to remove. Even at room temperature, the effects of heating make the bolts difficult to remove. They must be loosened in a minimum of three stages. Immediately after being loosened, in the first stage, each bolt must be retightened to 60 ft. lb. If the last few bolts still appear too difficult to loosen when others are at 60 ft. lb., the other bolts must be tightened back to 85 ft. lb. until all have been loosened and retightened. The 60 ft. lb. step can then be taken, followed by loosening and retightening to 40 ft. lb. and finally loosening from 40 ft. lb. and removing the cap nut. Pipes to the inlet and outlet ports of the chamber must be disconnected prior to loosening the bolts and removing the cap nut and cap. The cap may be difficult to remove, needing the gentle persuasion of a wooden or rubber-tipped mallet. Samples and debris which began as samples can then be removed from the chamber.

E. Analysis

1. Weight Loss Due to Disintegration

Samples are weighed before and after exposure to reaction gases in order to characterize weight changes. Samples are scrubbed with a wire brush prior to weighing after exposure so that all spalled

parts will be removed. Only intact or partially intact samples count toward post-exposure weights.

2. Visible Record of CO Disintegration

Following post-exposure weighing, intact and partially intact samples are photographed. Notation is made in each photograph for samples that completely disintegrated due to exposure.

3. Compressive Strength After Exposure

After being photographed, samples are crushed on a universal testing machine[16] at a crosshead speed of 0.1 in./min. Compressive strengths are calculated and averaged, with completely disintegrated samples being assigned zero compressive strength.

16. ElecTOstatic, Tinius Olsen Testing Machine Company, Pennsylvania.

IV. Experimental Results

Tables I-XXXIII of Appendix I summarize the data collected for 100 hr. exposures of samples of the three refractories to the following gas compositions: 99.99% CO, 95% CO-5% CO_2, 85% CO-15% CO_2, 99.8% CO-0.2% NH_3, 99.2% CO-0.8% NH_3, 80% CO-20% H_2, 60% CO-40% H_2, 99.8% CO-0.2% H_2S, 99.2% CO-0.8% H_2S, 80% CO-20% H_2O, and 60% CO-40% H_2O.

A. Visible Effects of 100 Hr. Exposures to Gas Mixtures

1. 99.99% CO Mixture

a. 90+ Wt.% Alumina Castable

Considerable spalling occurred in one of five samples doped with 0.5 wt.% metallic iron, as shown in Figure 3. As shown in Figures 4, 5, and 6, the severity of the spalling increased with increasing amounts of metallic iron in this refractory. The metallic iron dopant appeared as black specks in the refractory both before and after CO exposure. Considerable surface oxidation of iron particles obviously occurred during prefiring.

Spalling did not occur in any of the samples doped with hematite, however, the dopant caused a change in color of the castable from red or yellow, following prefiring, to dark grey or black following CO exposure.

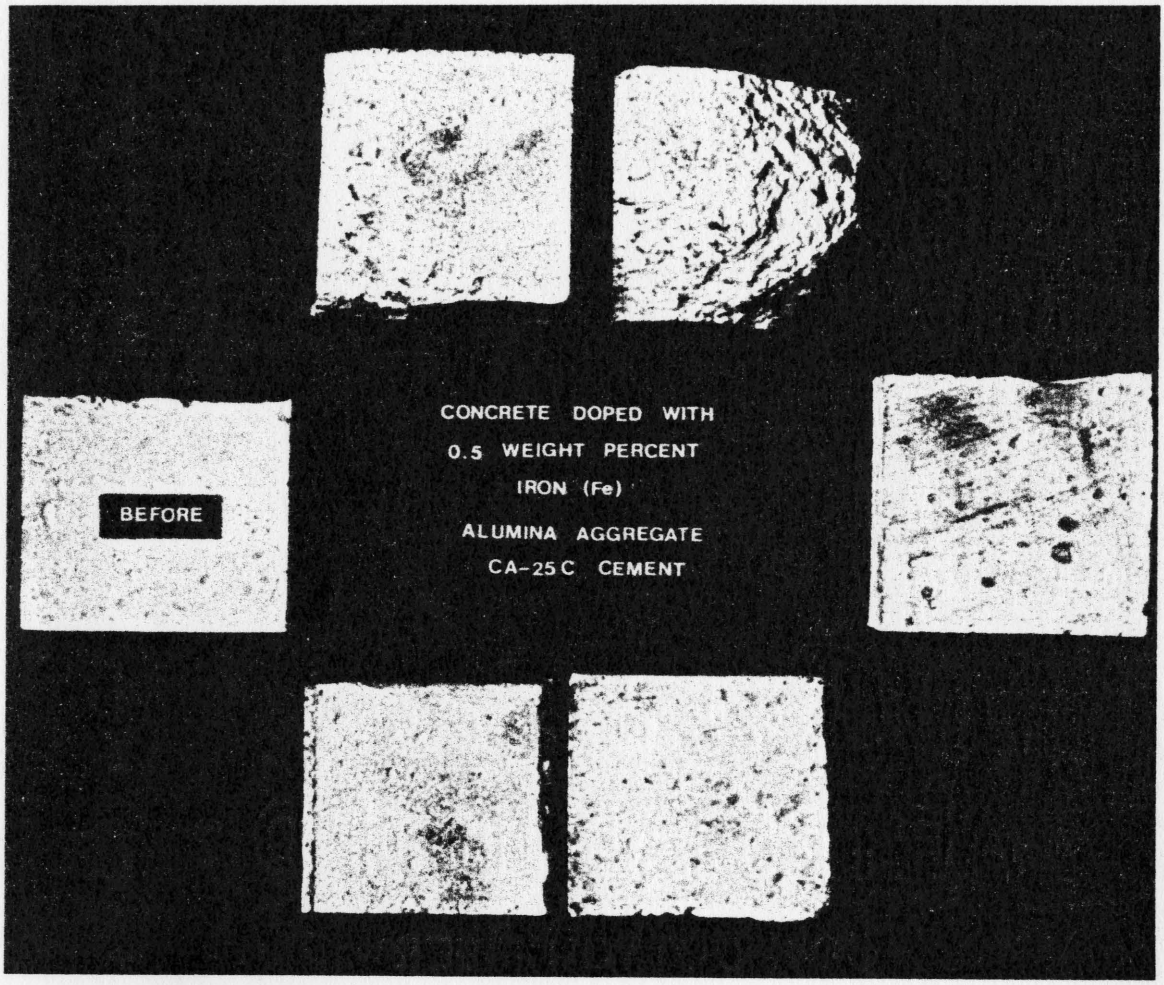

Figure 3. 100 hr. CO Exposure - 90+ wt.% Al_2O_c Castable, 0.5 wt.% Fe.

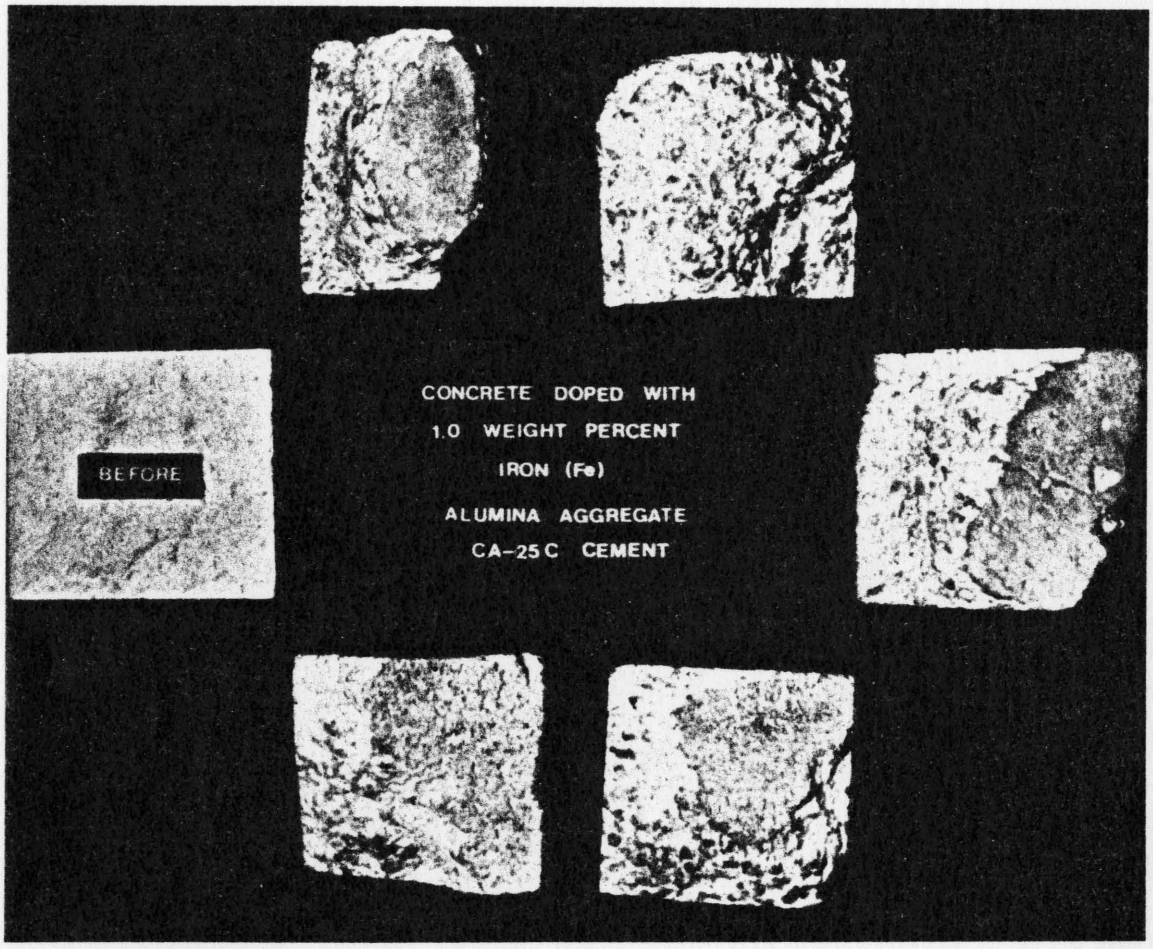

Figure 4. 100 hr. CO Exposure - 90+ wt.% Al_2O_3 Castable, 1.0 wt.% Fe.

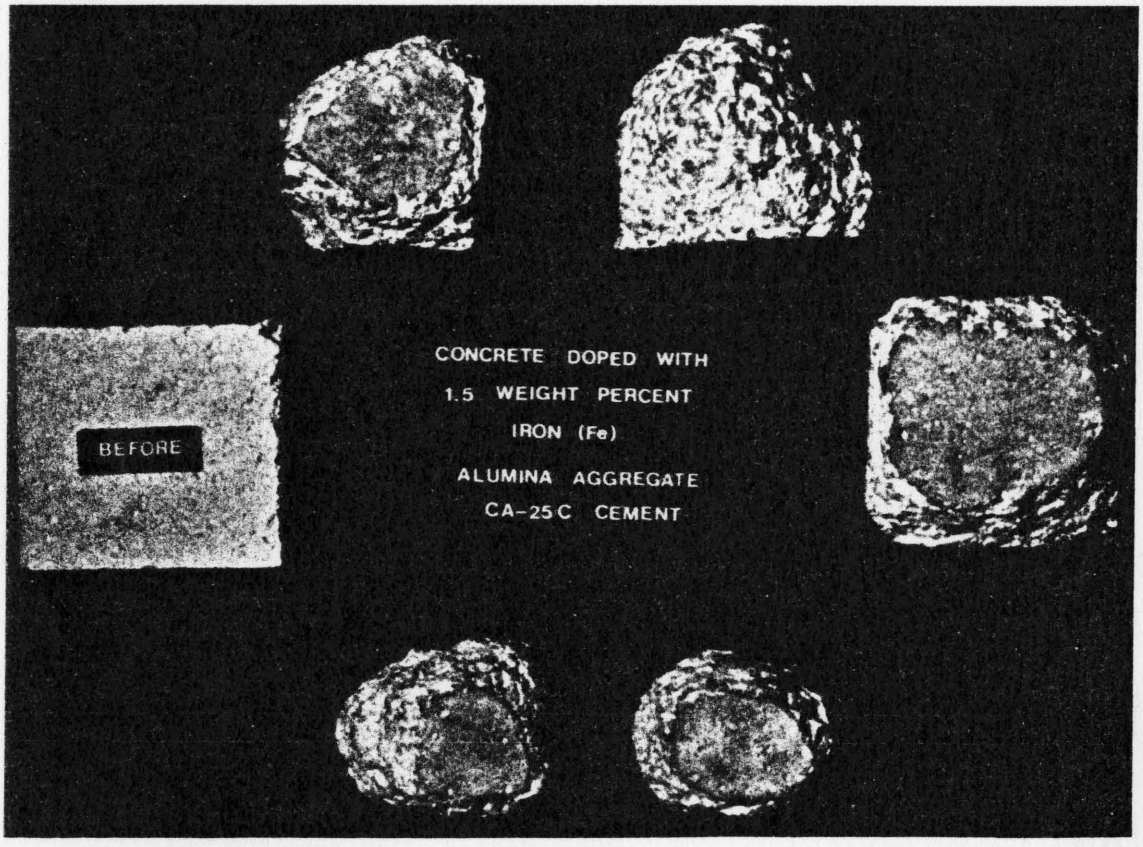

Figure 5. 100 hr. CO Exposure - 90 wt.% Al_2O_3 Castable, 1.5 wt.% Fe.

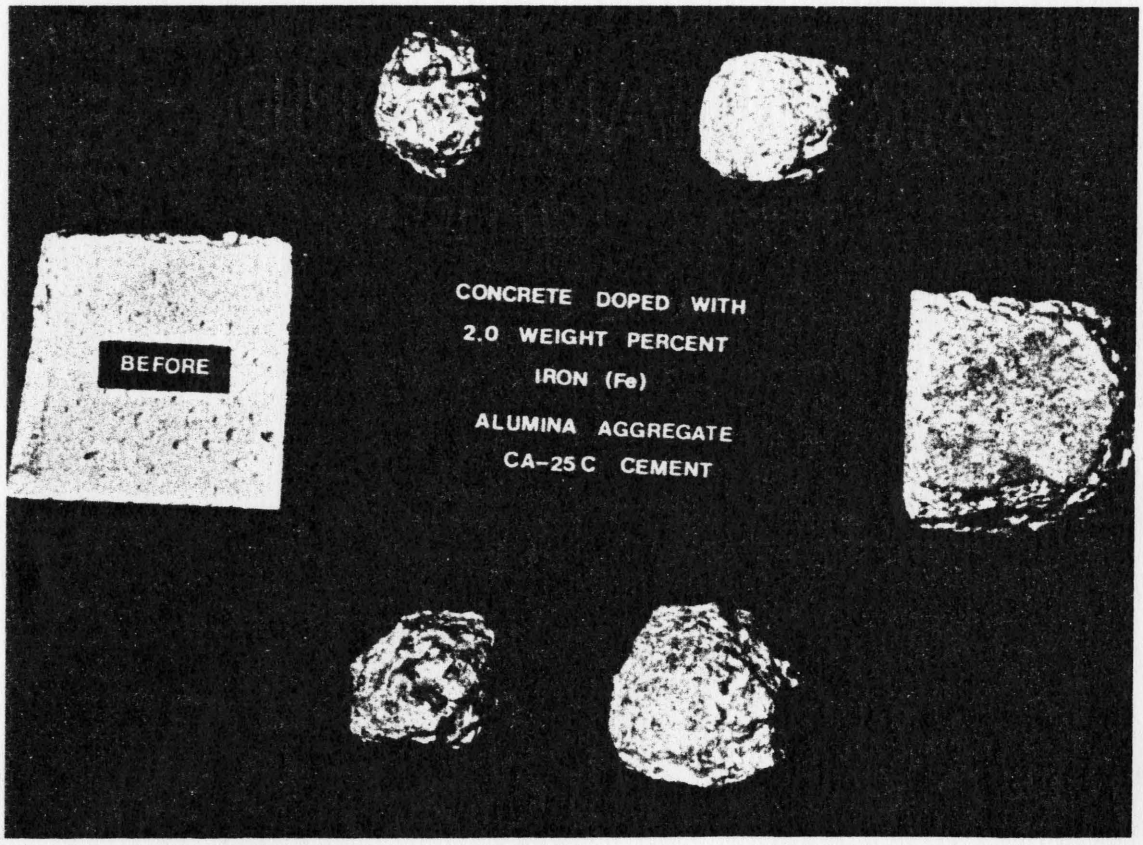

Figure 6. 100 hr. CO Exposure - 90 wt.% Al_2O_3 Castable, 2.0 wt.% Fe.

b. 50+ Wt.% Alumina Castable

A small amount of corner spalling occurred on two of five samples doped with 0.5 wt.% metallic iron, shown in Figure 7. Higher levels of metallic iron in the refractory caused complete disintegration at each dopant level, as shown in Figure 8. Metallic iron appeared as it did in the high-alumina concrete, namely, black specks before and after CO exposure.

The effect of CO on hematite-doped samples of the 50+ wt.% castable alumina was also similar to that of the 90+ wt.% alumina castable. No spalling occurred and the dopant turned dark grey or black. The overall color of the hematite-doped 50+ wt.% alumina castable samples was darker than that for similarly doped 90+ wt.% alumina samples, probably due to the grey rather than white aggregate material.

c. 90+ Wt.% Alumina Phosphate-Bonded Ramming Mix

Advanced states of spalling, i.e. loss of corners or edges, were not apparent on any ramming mix sample. Hairline cracks running nearly the full length of a sample face appeared on two of four samples containing 1.5 and 2.0 Fe wt.% metallic iron and hematite. Metallic iron appeared as black specks in a white matrix material following prefiring. The matrix turned grey during the CO test. The hematite dopant was unchanged by prefiring, but it turned blue or black during CO exposure. Cracking in hematite-doped samples only occurred in cases where the dopant had turned black.

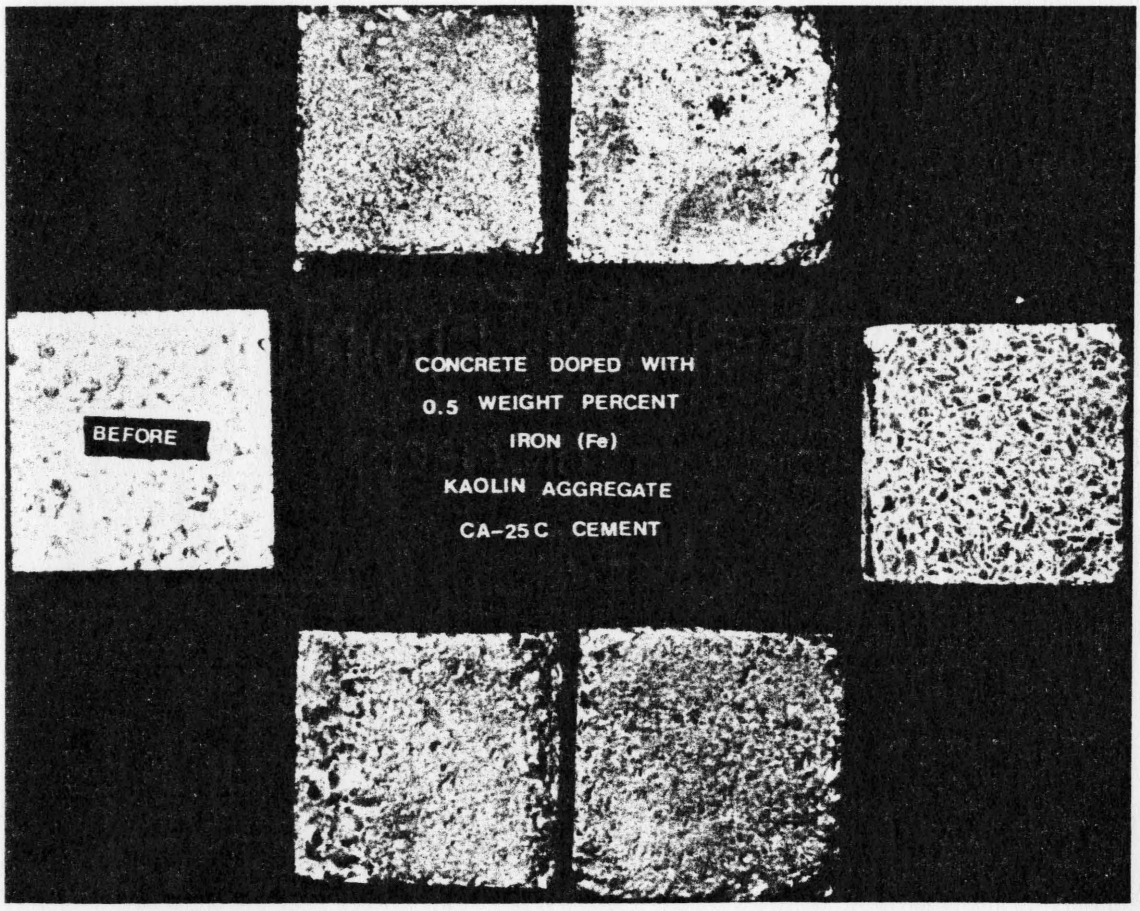

Figure 7. 100 hr. CO Exposure - 50+ wt.% Al_2O_3 Castable, 0.5 wt.% Fe.

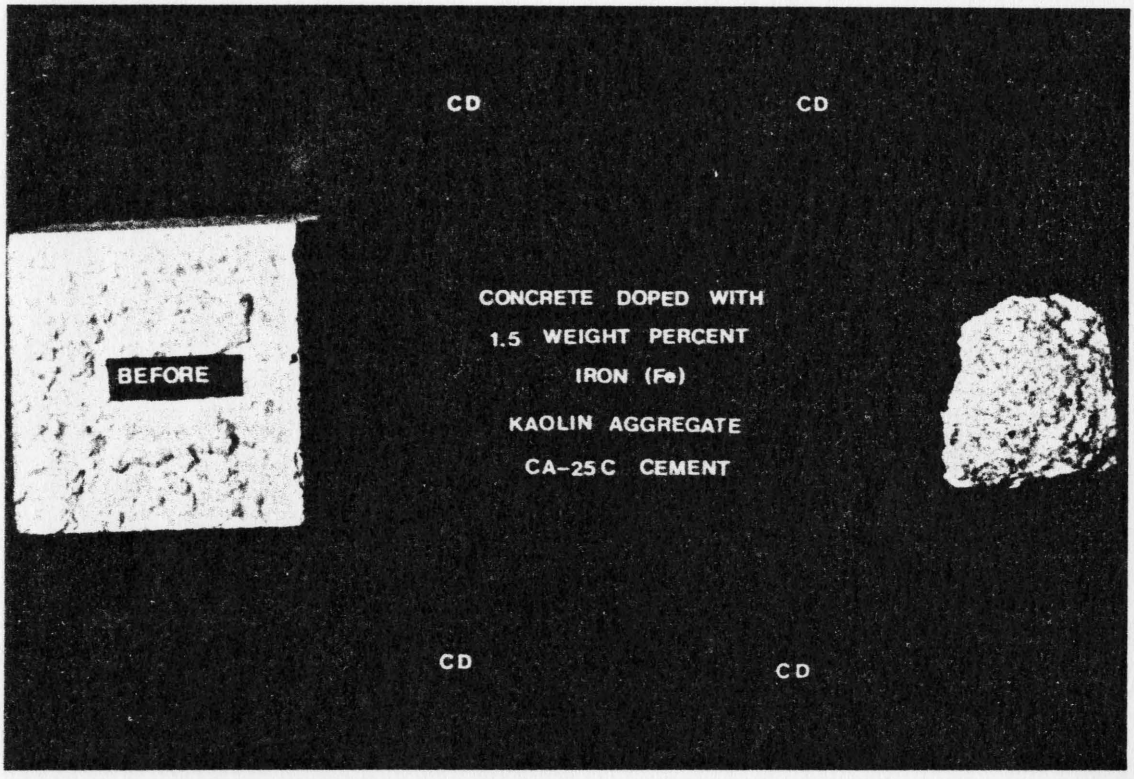

Figure 8. 100 hr. CO Exposure - 50+ wt.% Al_2O_3 Castable, 1.5 wt.% Fe (CD = Complete Disintegration).

2. 95% CO - 5% CO_2 Mixture

a. 90+ Wt.% Alumina Castable

Minor spalling occurred in one of four samples doped with 1.5 wt.% metallic iron in two of four samples doped with 2.0 wt.% Fe. No spalling occurred in iron oxide-doped samples; these samples appeared the same as similarly doped samples exposed to CO.

b. 50+ Wt.% Alumina Castable

Large cracks were formed on two of four samples doped with 0.5 wt.% metallic iron. Higher metallic iron levels caused more severe spalling, with at least two samples at each dopant level suffering complete disintegration. As with the 90+ wt.% alumina castable, iron oxide-doped samples did not spall, and, they appeared the same as samples exposed to CO.

c. 90+ Wt.% Alumina Phosphate-Bonded Ramming Mix

Corner and edge spalling occurred on two of four samples doped with 1.0 wt.% metallic iron. Carbon balls and large cracks were seen on two of four samples doped with 1.5 Fe wt.% iron oxide and significant spalling occurred in three of four samples doped with 2.0 Fe wt.% iron oxide. Undoped samples had red or black colored matrix material, while all doped samples had black matrixes.

3. 85% CO - 15% CO_2 Mixture

a. 90+ Wt.% Alumina Castable

Minor corner or edge spalling was observed for one of four samples doped with 1.0 wt.% metallic iron and for three of four samples doped with 2.0 wt.% metallic iron. Iron oxide-doped samples appeared white to light yellow rather than grey.

b. 50+ Wt.% Alumina Castable

Large cracks formed in one of four samples doped with 2.0 wt.% metallic iron. Color of iron oxide-doped samples varied from off-white for the 0.5 Fe wt.% levels to light grey (lighter than 90+ wt.% alumina castables exposed to CO) for the 2.0 Fe wt.% level.

c. 90+ Wt.% Alumina Phosphate-Bonded Ramming Mix

Corner and edge spalling occurred on three of four samples doped with 1.0 wt.% metallic iron. Higher levels of metallic iron produced significant spalling in at least two of four samples at each level and minor spalling in the remaining samples. Carbon balls were seen in two of four samples doped with 1.0 Fe wt.% iron oxide. Significant spalling occurred in one of four samples at the 1.5 Fe wt.% level, with cracks forming in two of the remaining three samples. One of four samples at the 2.0 Fe wt.% level was affected, having a deep crack accompanied by spalling.

4. 99.8% CO - 0.2% NH_3 Mixture

a. 90+ Wt.% Alumina Castable

Corner spalling occurred on one of four samples doped with 1.0

wt.% metallic iron. Corner and edge spalling was visible on two of four samples at the 1.5 wt.% level and on three of four at the 2.0 wt.% level. Iron oxide-doped samples were somewhat lighter in color than samples exposed to CO.

b. 50+ Wt.% Alumina Castable

Cracking or heavy spalling was observed in three of four samples doped with 1.5 wt.% metallic iron and in all four samples doped with 2.0 wt.% metallic iron. Iron oxide-doped samples appeared the same as when exposed to CO.

c. 90+ Wt.% Alumina Phosphate-Bonded Ramming Mix

Moderate to heavy spalling occurred in three of four samples with 1.0 wt.% metallic iron. One of four samples at the 1.5 wt.% level also had heavy spalling, with two others having minor edge and corner spalling. Two of four samples at the 2.0 wt.% level had corner and edge spalling. No spalling was observed in iron oxide-doped samples, however, a carbon ball was seen on a corner of one sample doped with 2.0 Fe wt.% iron oxide.

5. 99.2% CO - 0.8% NH_3 Mixture

a. 90+ Wt.% Alumina Castable

Moderate spalling occurred on one of four samples at both the 1.0 and 2.0 wt.% metallic iron levels. Two of four samples had moderate spalling at the 1.5 wt.% level. Minor corner or edge spalling occurred

on one of the remaining samples at both the 1.0 and 1.5 wt.% levels. Iron oxide doped samples were slightly darker in appearance than when exposed to CO.

b. 50+ Wt.% Alumina Castable

Heavy spalling occurred on all four samples at both the 1.0 and 2.0 wt.% metallic iron levels. Two of four samples doped with 1.5 wt.% metallic iron were completely disintegrated. Iron oxide-doped samples were lighter in color than when exposed to CO and were also lighter than the iron oxide-doped 90+ wt.% alumina castable samples exposed to 99.2% CO - 0.8% NH_3.

c. 90+ Wt.% Alumina Phosphate-Bonded Ramming Mix

Moderate to heavy spalling occurred in all four samples doped with 1.0 wt.% metallic iron. Two of four samples at both the 1.5 and 2.0 wt.% metallic iron levels suffered moderate spalling. No spalling occurred in iron oxide-doped samples.

6. 80% CO-20% H_2 Mixture

a. 90+ Wt.% Alumina Castable

Three of four samples doped with 2.0 wt.% metallic iron spalled heavily. Samples at other levels of metallic iron doping suffered no spalling damage. The color of iron oxide-doped samples changed to off-white.

b. 50+ Wt.% Alumina Castable

No spalling was observed for this refractory. Samples doped with both iron and iron oxide darkened in color much more than when exposed to CO.

c. 90+ Wt.% Alumina Phosphate-Bonded Ramming Mix

Spalling occurred on two faces of one of four samples doped with 2.0 wt.% metallic iron. Iron oxide doped samples did not spall and remained light grey, rather than turning black as in exposures to CO.

7. 60% CO - 40% H_2 Mixture

a. 90+ Wt.% Alumina Castable

No spalling was observed in any samples doped with either metallic iron or iron oxide. Iron oxide-doped samples turned to a yellowish-white color.

b. 50+ Wt.% Alumina Castable

As with the 90+ wt.% alumina castable, no spalling occurred in any samples of the 50+ wt.% alumina castable. Color of the iron oxide-doped samples ranged from yellowish-white at the 0.5 Fe wt.% Fe_2O_3 level to light grey at the 2.0 Fe wt.% Fe_2O_3 level.

c. 90+ Wt.% Alumina Phosphate-Bonded Ramming Mix

There was no spalling in any samples of this refractory. Iron and

iron oxide-doped samples turned dark grey to black at all dopant levels.

8. 99.8% CO - 0.2% H_2S Mixture

a. 90+ Wt.% Alumina Castable

A large crack formed in one of four samples doped with 1.0 wt.% metallic iron. Moderate spalling occurred on one of four samples at the 1.5 wt.% level of metallic iron. Heavy spalling occurred on two of four samples doped with 2.0 wt.% metallic iron. Iron oxide-doped samples did not spall and ranged in color from off-white at the 0.5 Fe wt.% level to medium grey at the 2.0 Fe wt.% level.

b. 50+ Wt.% Alumina Castable

One of four samples spalled heavily at the 0.5 wt.% metallic iron level. All four samples completely disintegrated at both the 1.0 and 1.5 wt.% metallic iron levels. One of four samples spalled heavily and another completely disintegrated with 2.0 wt.% metallic iron. Iron oxide-doped samples ranged in color from off-white to light grey at the 0.5 Fe wt.% level to dark grey at the 2.0 Fe wt.% level.

c. 90+ Wt.% Alumina Phosphate-Bonded Ramming Mix

Moderate spalling occurred on one of four samples doped with 0.5, 1.5, and 2.0 wt.% metallic iron. Heavy spalling occurred on one and moderate spalling on another of four samples at the 1.0 wt.% metallic iron level. Three of four samples spalled heavily with the fourth com-

pletely disintegrating at the 1.5 Fe wt.% level of iron oxide doping, and two of four samples spalled heavily at the 2.0 Fe wt.% level. The remaining two samples at this level had minor corner and edge spalling.

9. 99.2% CO - 0.8% H_2S

a. 90+ Wt.% Alumina Castable

Moderate spalling damage was observed on one and heavy spalling damage was observed on another of four samples doped with 2.0 wt.% metallic iron. No spalling was seen in other samples. Iron oxide-doped samples ranged in color from off-white at the 0.5 Fe wt.% level to dark grey at the 2.0 Fe wt.% level.

b. 50+ Wt.% Alumina Castable

One of four samples exhibited large cracks following exposure at both the 0.5 and 1.0 wt.% levels of metallic iron doping. At the 1.0 wt.% metallic iron level, two of the remaining three samples cracked into two pieces. All four samples at the 1.5 wt.% metallic iron level cracked into two or more pieces, as did one of four samples doped with 2.0 wt.% metallic iron. Iron oxide-doped samples ranged in color from off-white to light grey at the 0.5 Fe wt.% level to dark grey at the 2.0 Fe wt.% level. Iron oxide-doped samples at the 2.0 Fe wt.% level were no darker than similarly doped samples of the 90+ wt.% alumina castable.

c. 90+ Wt.% Alumina Phosphate-Bonded Ramming Mix

Light spalling occurred on one of four samples doped with 1.0 wt.% metallic iron. All four samples had moderate spalling at the 1.5 wt.% metallic iron level, along with two of the four samples at the 2.0 wt.% metallic iron level. Two of four samples doped with 1.0, 1.5, and 2.0 Fe wt.% iron oxide spalled heavily. The remaining two samples at each of the 1.5 and 2.0 Fe wt.% iron oxide levels suffered complete disintegration.

10. 80% CO - 20% H_2O Mixture

a. 90+ Wt.% Alumina Castable

No samples suffered spalling damage. Iron oxide-doped samples ranged in color from off-white at the 0.5 Fe wt.% level to medium grey at the 2.0 Fe wt.% level.

b. 50+ Wt.% Alumina Castable

As with the 90+ wt.% alumina castable, no samples showed any signs of spalling. Iron oxide-doped samples ranged in color from light grey when doped with 0.5 Fe wt.% iron oxide to medium grey when doped with 2.0 Fe wt.% iron oxide. Samples at the 1.0, 1.5, 2.0 Fe wt.% levels of iron oxide doping also had a yellow tint to their color.

c. 90+ Wt.% Alumina Phosphate-Bonded Ramming Mix

The ramming mix samples suffered no spalling damage when doped with either metallic iron or iron oxide. All doped samples had black matrixes.

11. 60% CO - 40% H_2O Mixture

a. 90+ Wt.% Alumina Castable

No spalling occurred in any of the samples. Iron oxide-doped samples were white at the 0.5 Fe wt.% level, light grey at the 1.0 and 1.5 wt.% levels, and yellow-tinted medium grey at the 2.0 Fe wt.% level.

b. 50+ Wt.% Alumina Castable

There was no visible spalling on any of the 50+ wt.% alumina castable samples. Color of iron oxide-doped samples ranged from light grey at the 0.5 Fe wt.% level to dark grey at the 2.0 Fe wt.% level, with samples at the 1.0, 1.5, and 2.0 Fe wt.% levels tinted yellow.

c. 90+ Wt.% Alumina Phosphate-Bonded Ramming Mix

No spalling was observed in any samples of the ramming mix. Matrix material in all doped samples was black after exposure to the gas mixture.

B. Compressive Strength After 100 Hr. Exposures to Gas Mixtures

1. 99.99% CO Mixture

a. 90+ Wt.% Alumina Castable

The average compressive strength of undoped 90+ wt.% alumina castable is over 10,000 psi following a 100 hr. exposure to CO. Figure 9

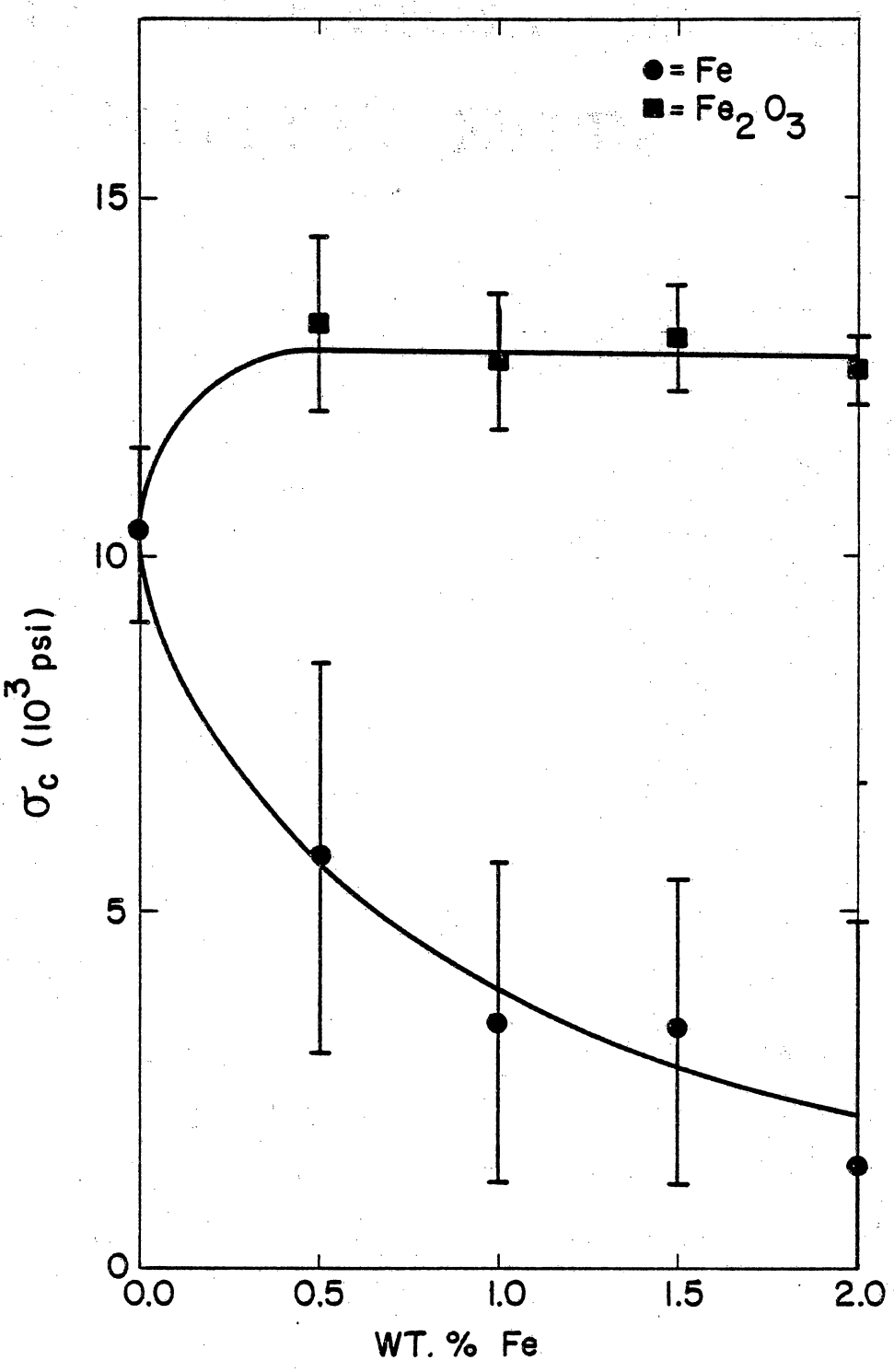

Figure 9. Compressive Strength of 90+ Wt.% Alumina Castable Exposed to CO.

summarizes how the addition of metallic iron and hematite modify this strength. Metallic iron levels of 1.0 wt.% and greater cause the refractory to retain less than 35% of its undoped strength. At the 0.5 wt.% metallic iron level, less than 60% of the undoped strength is retained. Doping the high-alumina concrete with hematite results in a 25% increase in strength. This increase is seen at all four dopant levels.

b. 50+ Wt.% Alumina Castable

The undoped 50+ wt.% alumina castable has an average compressive strength of nearly 7,000 psi after being exposed to CO. At the 0.5 wt.% level of metallic iron dopant, the refractory retains over 75% of strength, as seen in Figure 10. Metallic iron levels of 1.0 wt.% and greater cause complete disintegration of the refractory, and thus no retained strength.

Doping and 50+ wt.% alumina castable with hematite causes no significant change in compressive strength.

c. 90+ Wt.% Alumina Phosphate-Bonded Ramming Mix

An average compressive strength of nearly 14,000 psi is exhibited by the undoped ramming mix after CO exposure. As seen in Figure 11 the refractory retains less than 50% of this strength when doped with 1.5 wt.% metallic iron. Higher and lower levels of metallic iron in the ramming mix yield strength retentions of about 70%. Addition of 0.5 or 1.0 wt.% hematite leave the after-CO exposure strength of the

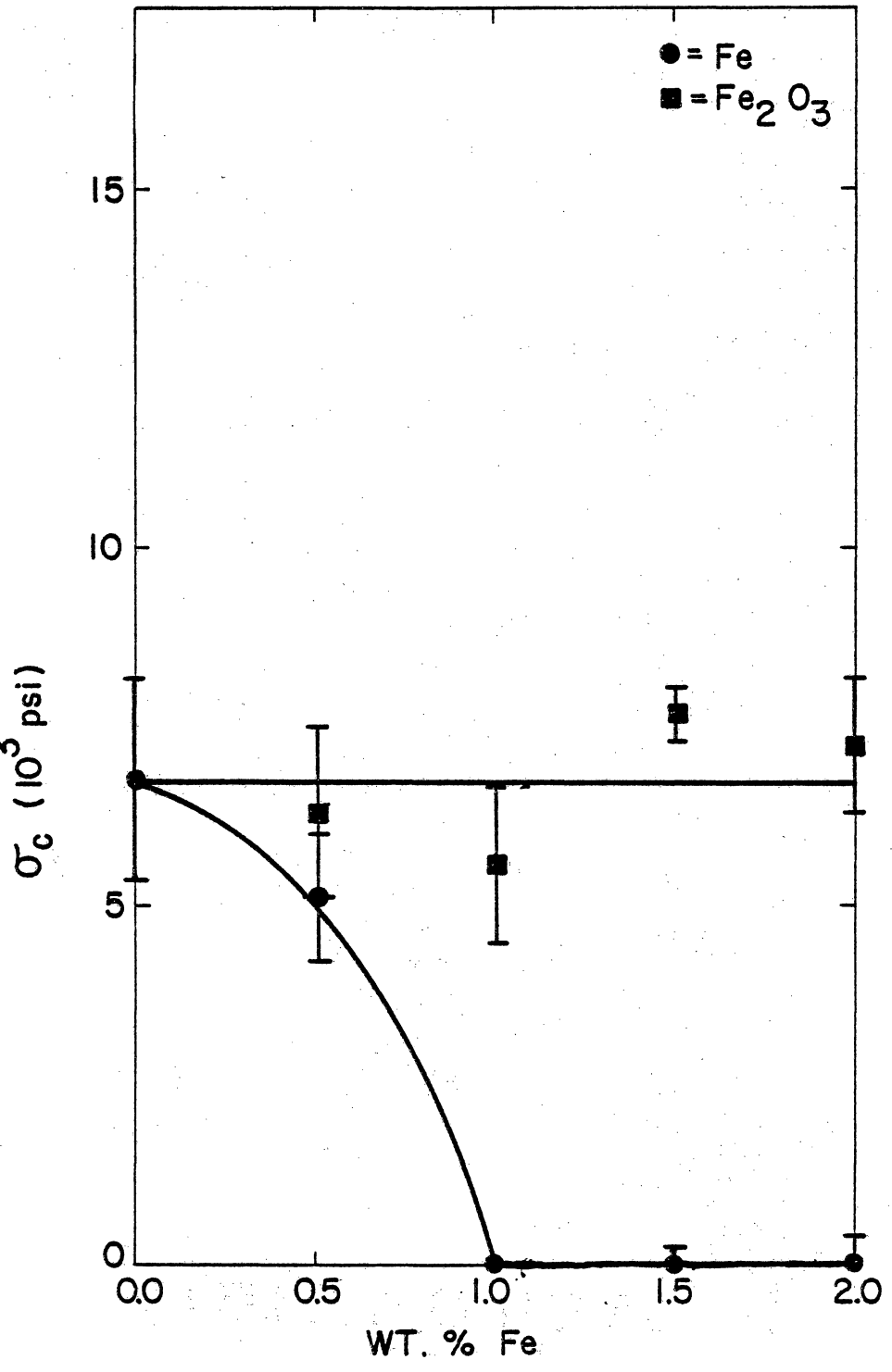

Figure 10. Compressive Strength of 50+ Wt.% Alumina Castable Exposed to CO.

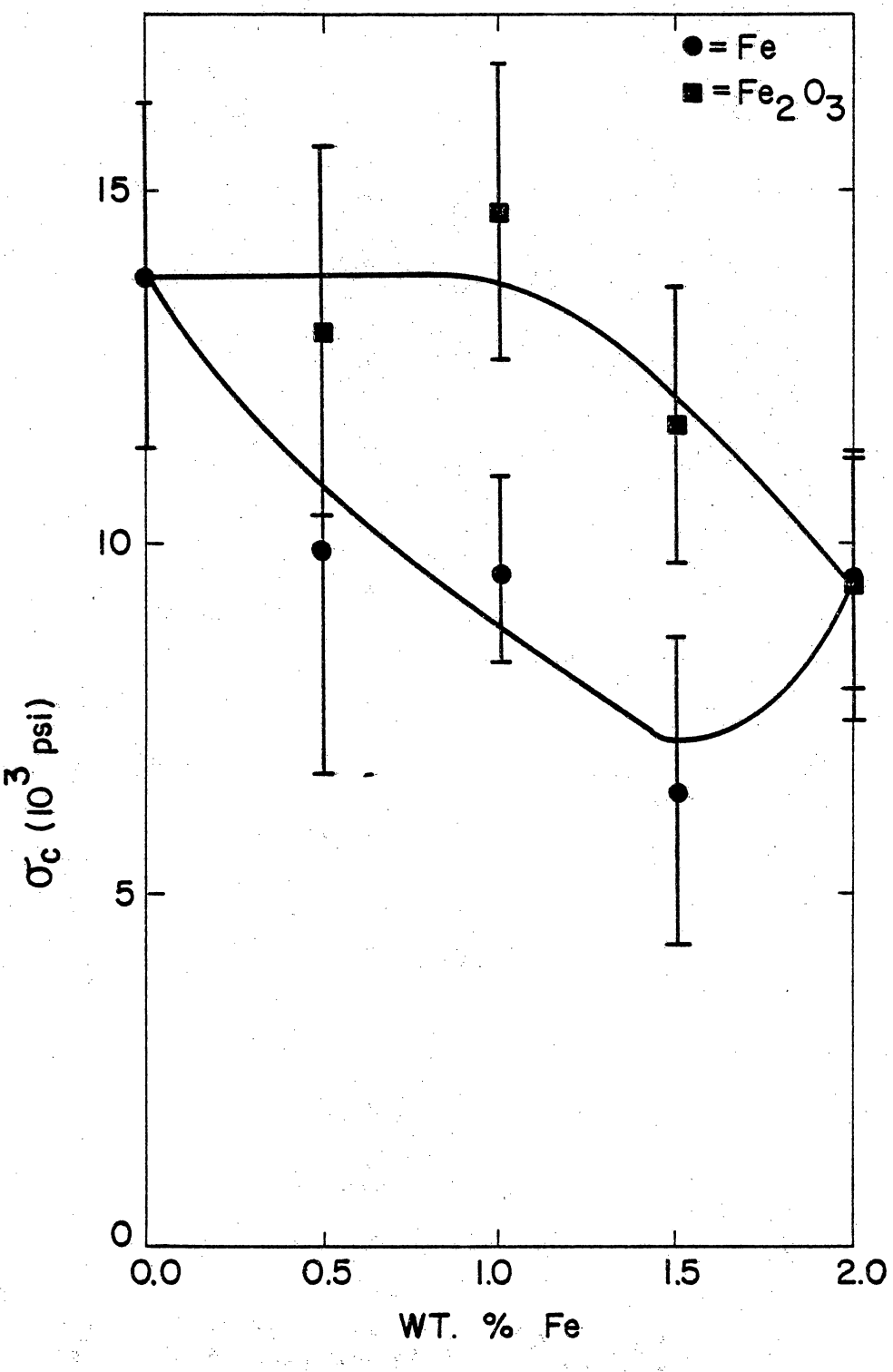

Figure 11. Compressive Strength of 90+ Wt.% Alumina Ramming Mix Exposed to CO.

refractory essentially unchanged. Higher levels of hematite cause moderate strength losses. At the 2.0 Fe wt.% level, metallic iron and hematite doped ramming mix samples have approximately the same strength.

2. 95% CO - 5% CO_2 Mixture

a. 90+ Wt.% Alumina Castable

The average undoped strength of the 90+ wt.% alumina castable is 5,800 psi after exposure to the 95% CO-5% CO_2 mixture. Strength losses from this level did not occur until the castable was doped with 1.5 wt.% metallic iron, as shown in Figure 12. The refractory retained 80% of its undoped strength at the 1.5 wt.% metallic iron level and 75% of its undoped strength at the 2.0 wt.% metallic iron level. The refractory was at least 20% stronger when doped with up to 2.0 Fe wt.% iron oxide than when undoped.

b. 50+ Wt.% Alumina Castable

The 50+ wt.% alumina castable had an average undoped strength of 4,450 psi after exposure. Metallic iron at the 0.5 wt.% level caused the refractory to retain only 71% of its undoped strength, while metallic iron levels of 1.0 and 1.5 wt.% yielded no retained strength, shown in Figure 13. Some strength retention, approximately 40% of the undoped strength, occurred when the refractory was doped with 2.0 wt.% metallic iron. Strengths of the iron oxide-doped samples did not differ significantly from the average undoped strength.

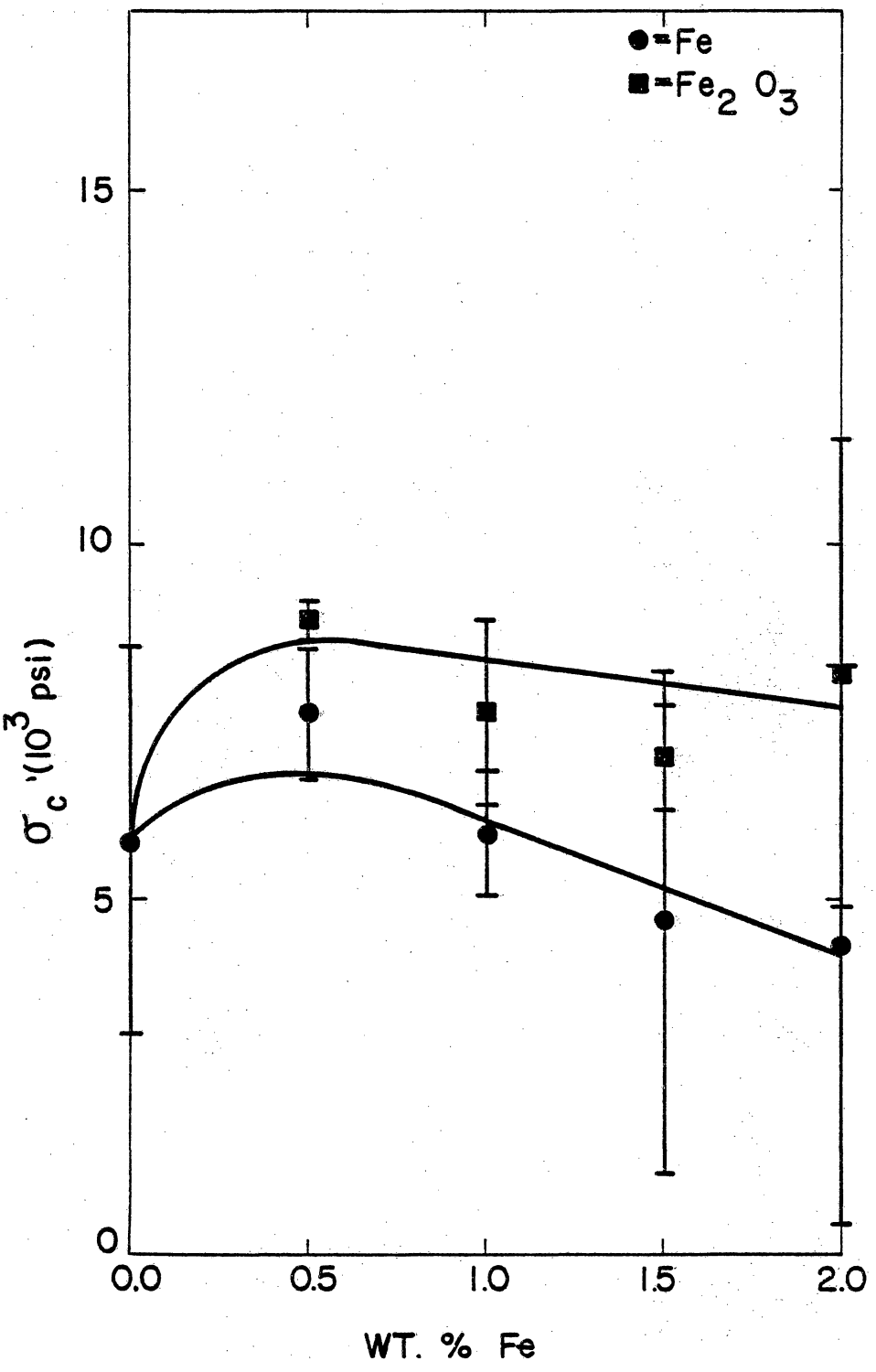

Figure 12. Compressive Strength of 90+ Wt.% Alumina Castable Exposed to 95% CO-5% CO_2.

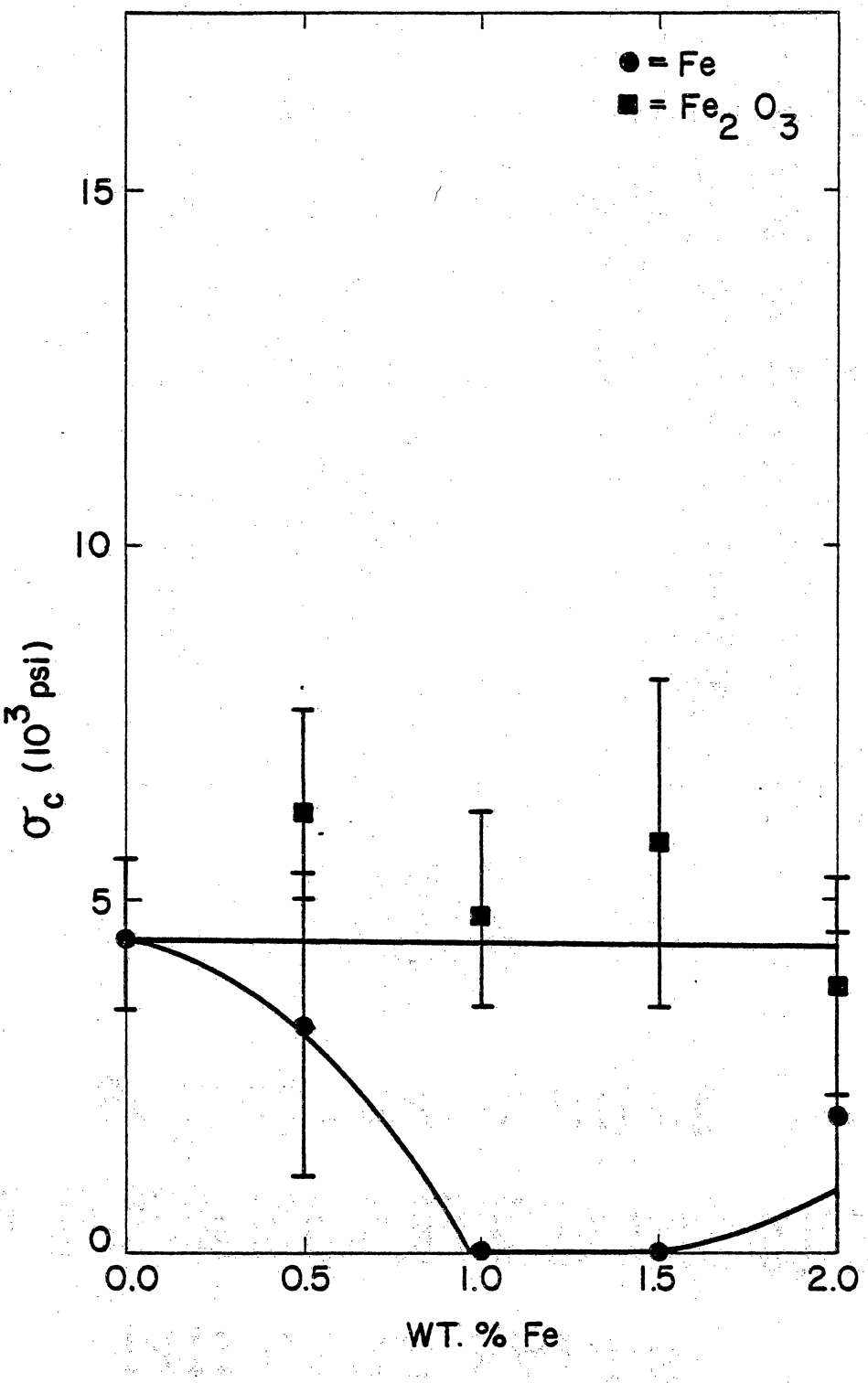

Figure 13. Compressive Strength of 50+ Wt.% Alumina Castable Exposed to 95% CO-5% CO_2.

c. 90+ Wt.% Alumina Phosphate-Bonded Ramming Mix

The ramming mix exhibited an undoped strength of 8,075 psi following exposure to the gas mixture. When doped with metallic iron, the strength of this refractory remained very close to the undoped strength, as shown in Figure 14. The iron oxide-doped ramming mix was stronger than the undoped ramming mix except at the 2.0 Fe wt.% level, where a large strength loss was observed. The refractory retained only 31% of its undoped strength at this level of iron oxide doping.

3. 85% CO - 15% CO_2 Mixture

a. 90+ Wt.% Alumina Castable

The 90+ wt.% alumina castable had an average undoped strength of 7,025 psi after being exposed to the 85% CO - 15% CO_2 gas. Little deviation from this strength occurred for the refractory when it was doped with either metallic iron or iron oxide, as shown in Figure 15.

b. 50+ Wt.% Alumina Castable

An average undoped strength of 4,425 psi was exhibited by the 50+ wt.% alumina castable following exposure to this gas composition. A general increase in strength was observed as dopant levels increased, shown in Figure 16, with metallic iron and iron oxide-doped samples nearly the same average strengths at each dopant level.

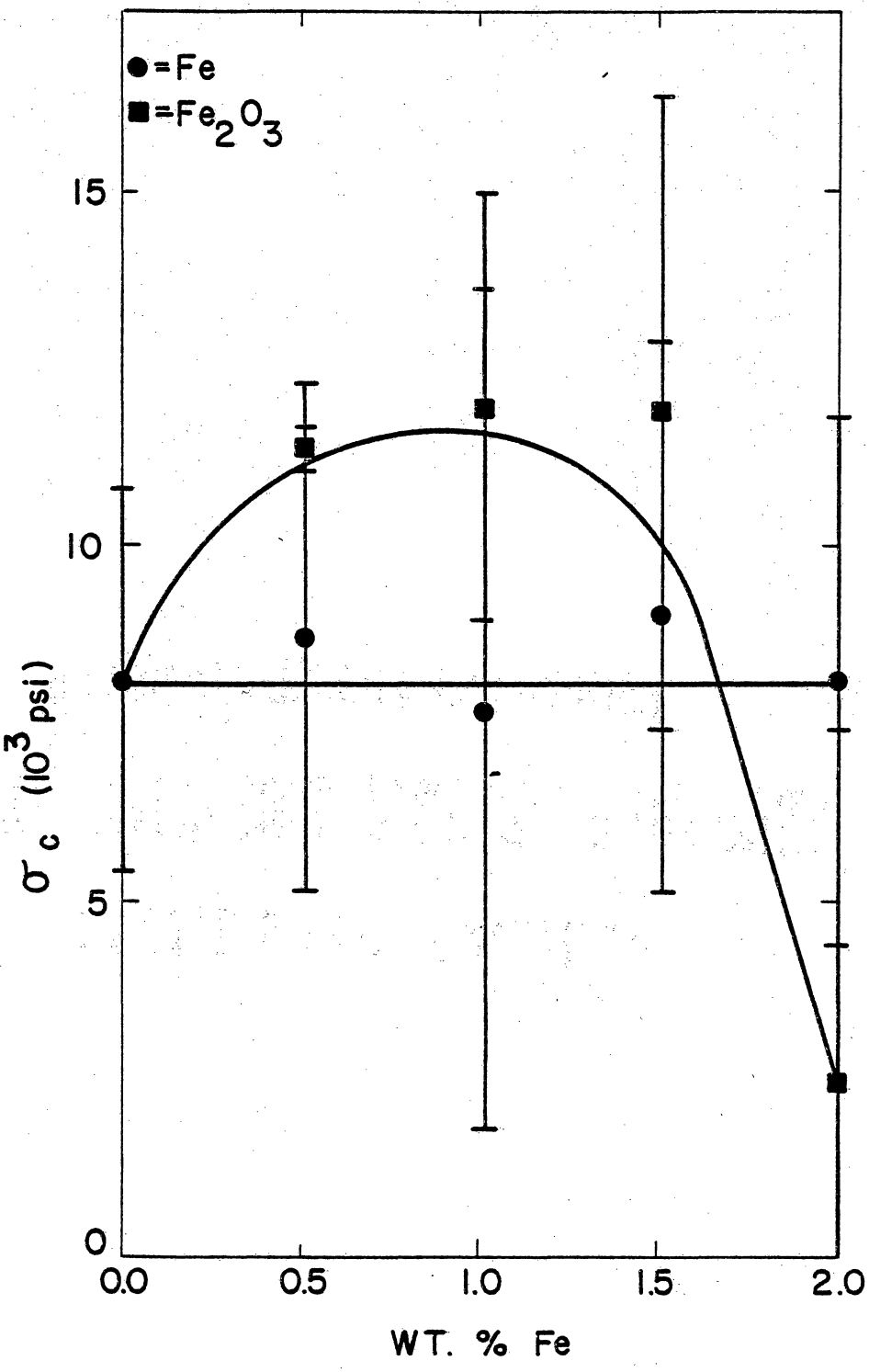

Figure 14. Compressive Strength of 90+ Wt.% Alumina Ramming Mix Exposed to 95% CO-5% CO_2.

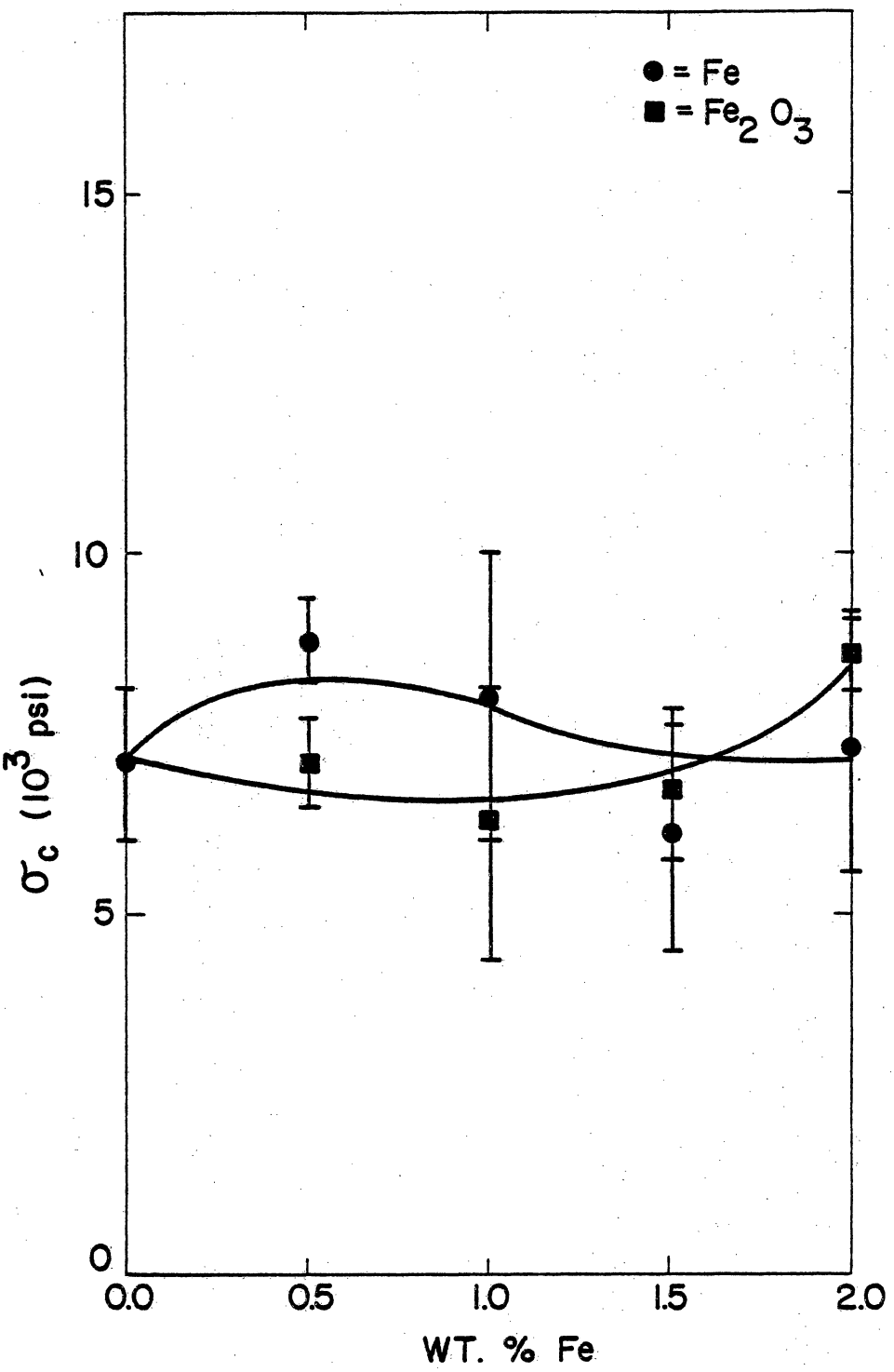

Figure 15. Compressive Strength of 90+ Wt.% Alumina Castable Exposed to 85% CO-15% CO_2.

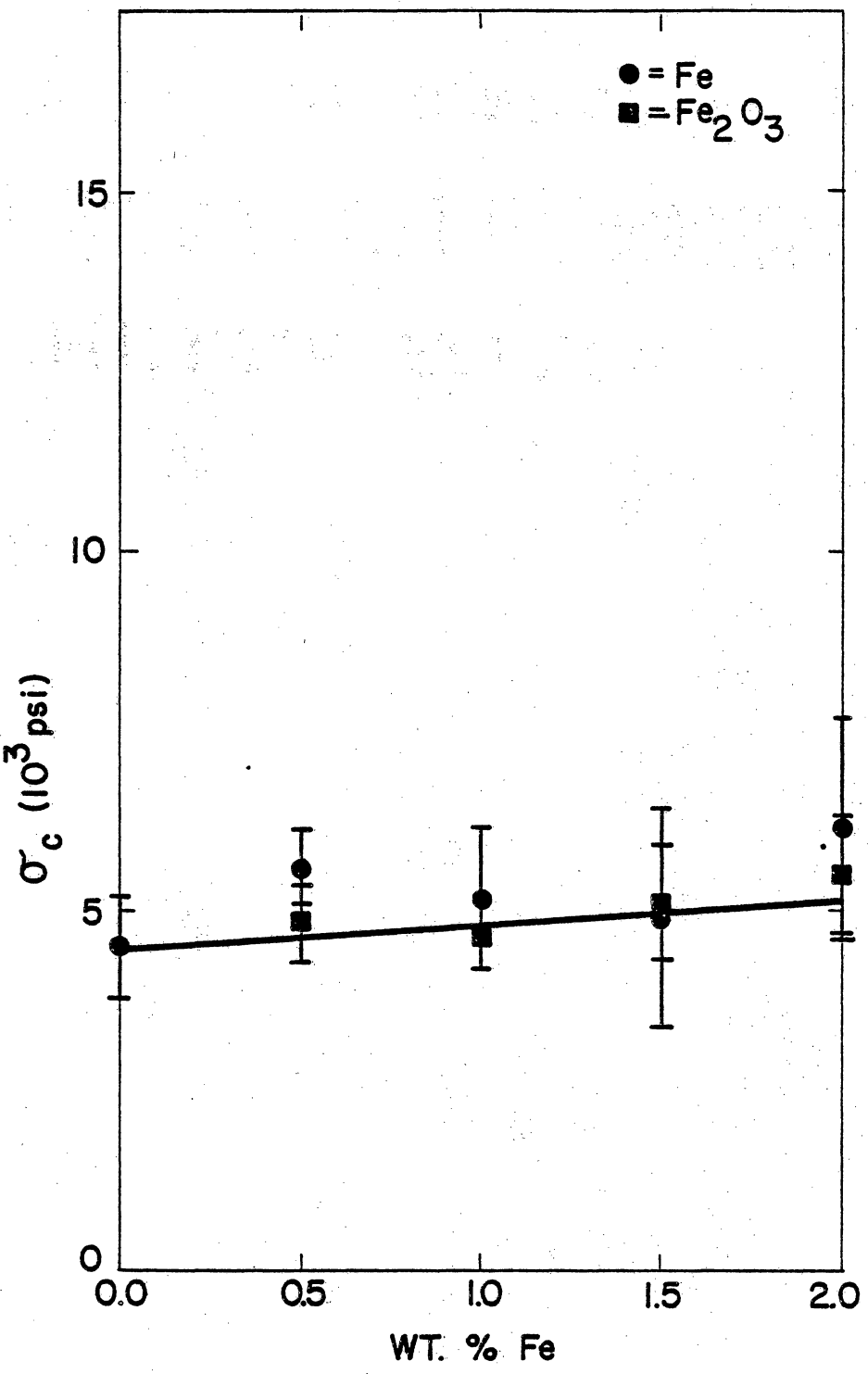

Figure 16. Compressive Strength of 50+ Wt.% Alumina Castable Exposed to 85% CO-15% CO_2.

c. 90+ Wt.% Alumina Phosphate-Bonded Ramming Mix

The average undoped strength of the ramming mix was 11,625 psi after being exposed to the 85% CO - 15% CO_2 gas. Addition of up to 1.5 wt.% metallic iron produced progressive degradation of this strength, as shown in Figure 17, to a minimum of 41% of the undoped strength, at 1.5 wt.% metallic iron. Strength of the refractory at the 2.0 wt.% metallic iron level was somewhat greater: 58% of the undoped strength. The strength of the ramming mix doped with 0.5 Fe wt.% iron oxide was nearly the same as its undoped strength. Higher levels of iron oxide-doping caused progressive strength loss, shown again in Figure 17, to a minimum of 43% of the undoped strength at the 2.0 Fe wt.% level.

4. 99.8% CO - 0.2% NH_3 Mixture

a. 90+ Wt.% Alumina Castable

After exposure to the 99.8% CO - 0.2% NH_3 composition, the average undoped strength of the 90+ wt.% alumina castable was 6,100 psi. A general decrease in strength accompanied the addition of increasing amounts of metallic iron, as shown in Figure 18. A large decrease in strength was noted for samples of the refractory doped with 0.5 Fe wt.% iron oxide. The average strength of these samples wes only 67% of the undoped strength. Higher levels of iron oxide doping resulted in strengths approximately the same as the undoped strength.

b. 50+ Wt.% Alumina Castable

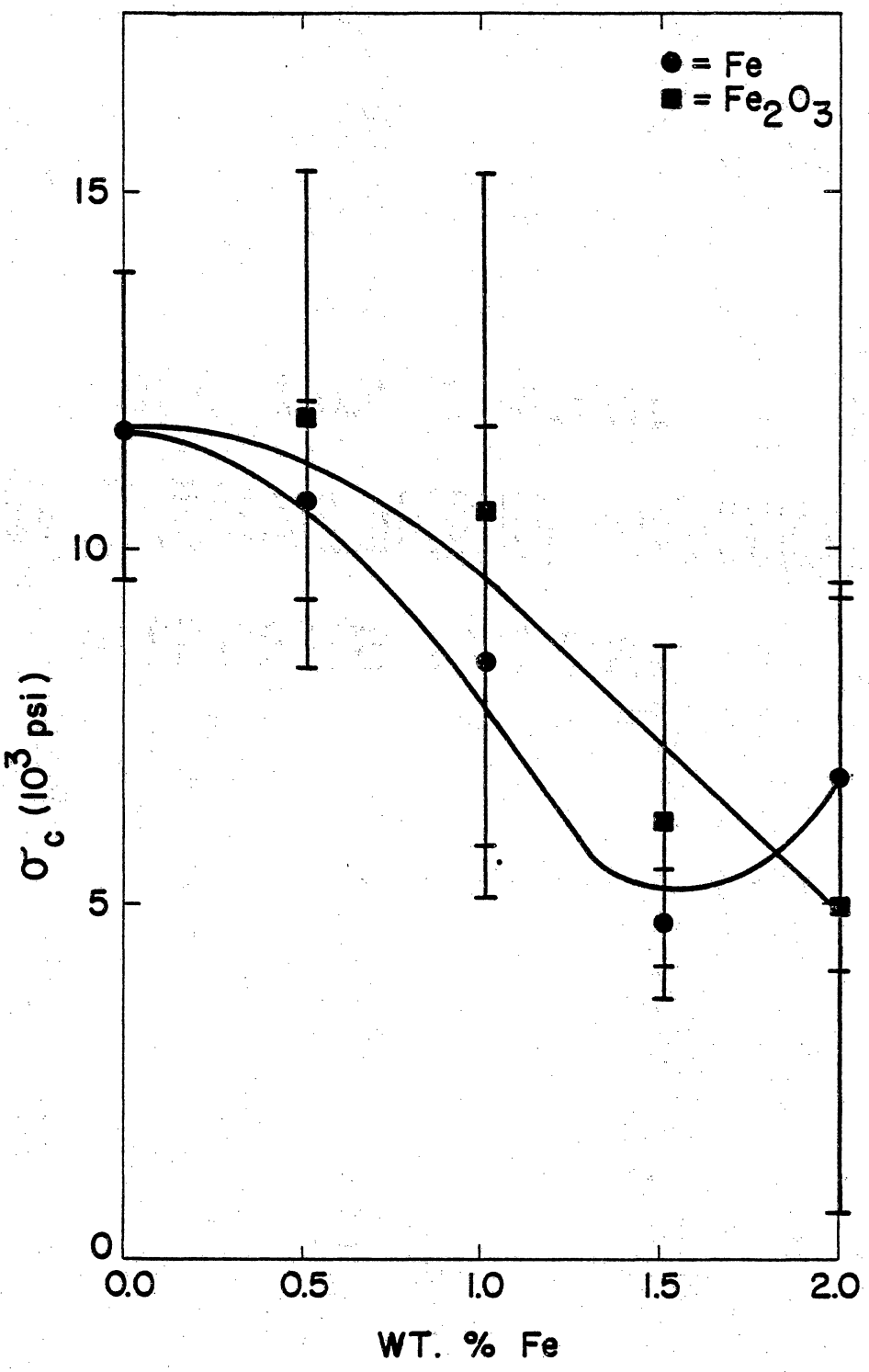

Figure 17. Compressive Strength of 90+ Wt.% Alumina Ramming Mix Exposed to 85% CO-15% CO_2.

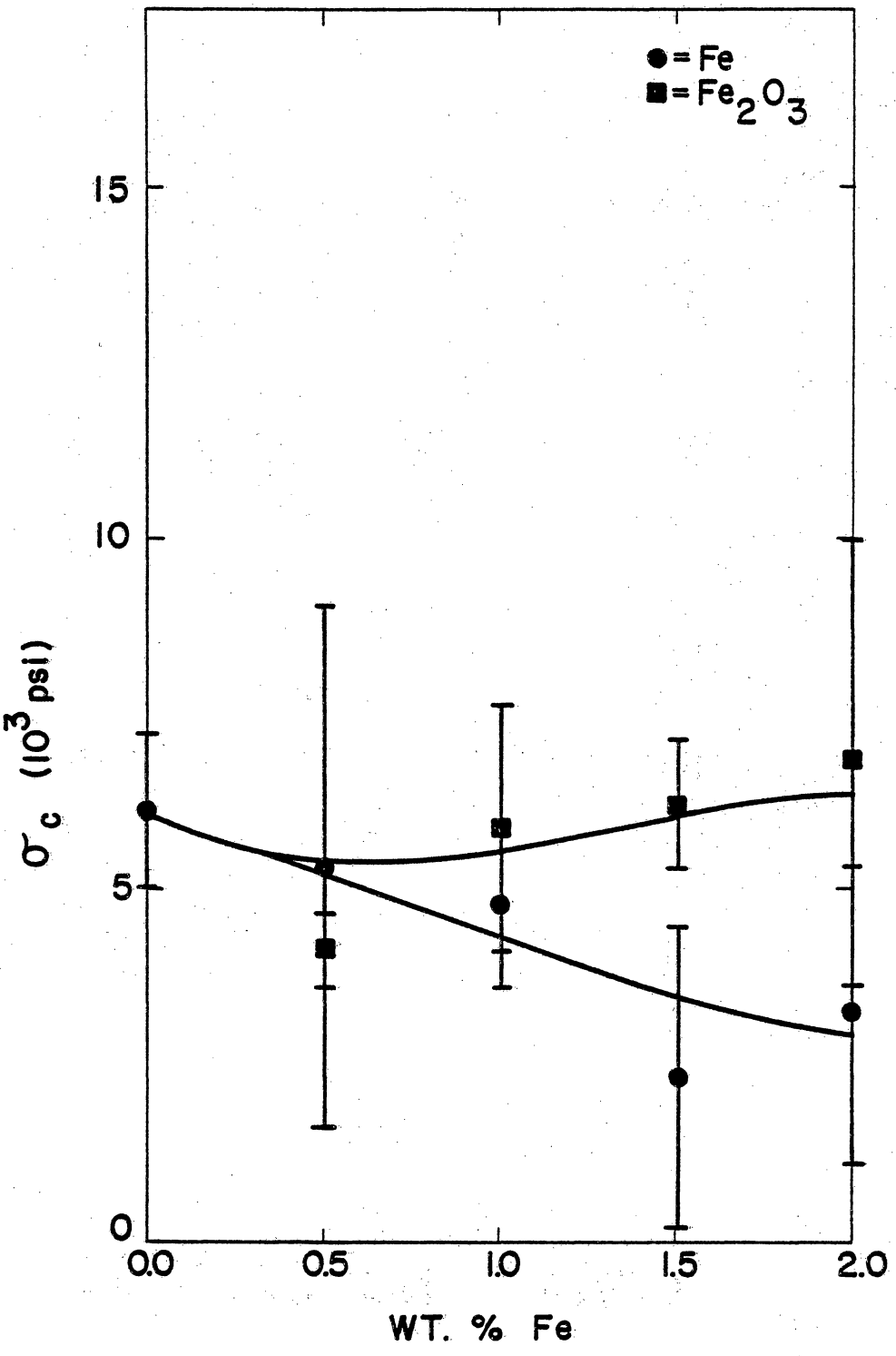

Figure 18. Compressive Strength of 90+ Wt.% Alumina Castable Exposed to 99.8% CO-0.2% NH_3.

The average undoped strength of the 50+ wt.% alumina castable was 4,875 psi following exposure. Strength decreased only slightly from this level when the refractory was doped with 0.5 wt.% metallic iron, with 95% of the undoped strength being retained. Greater amounts of metallic iron caused progressively greater decreases in strength, as shown in Figure 19, with the 2.0 wt.% metallic iron-doped refractory retaining essentially no strength. Strength of the refractory increased slightly as increasing amounts of iron oxide were added to it. This is also shown in Figure 19.

c. 90+ Wt.% Alumina Phosphate-Bonded Ramming Mix

The average undoped strength of the ramming mix exposed to 99.8% CO - 0.2% NH_3 was 14,950 psi. Strength of the ramming mix decreased rapidly when doped with metallic iron to a minimum of 35% of the undoped strength at the 1.0 wt.% Fe level. Greater amounts of metallic iron dopant caused small increases from this minimum level, as shown in Figure 20. Iron oxide at the 0.5 Fe wt.% level caused essentially no change in the strength of the refractory. Greater amounts of iron oxide caused progressively decreasing strength. A minimum of 58% of the undoped strength of the iron oxide-doped refractory was reached at the 2.0 Fe wt.% level.

5. 99.2% CO - 0.8% NH_3

a. 90+ Wt.% Alumina Castable

An average undoped strength of 6,350 psi was obtained for the 90+

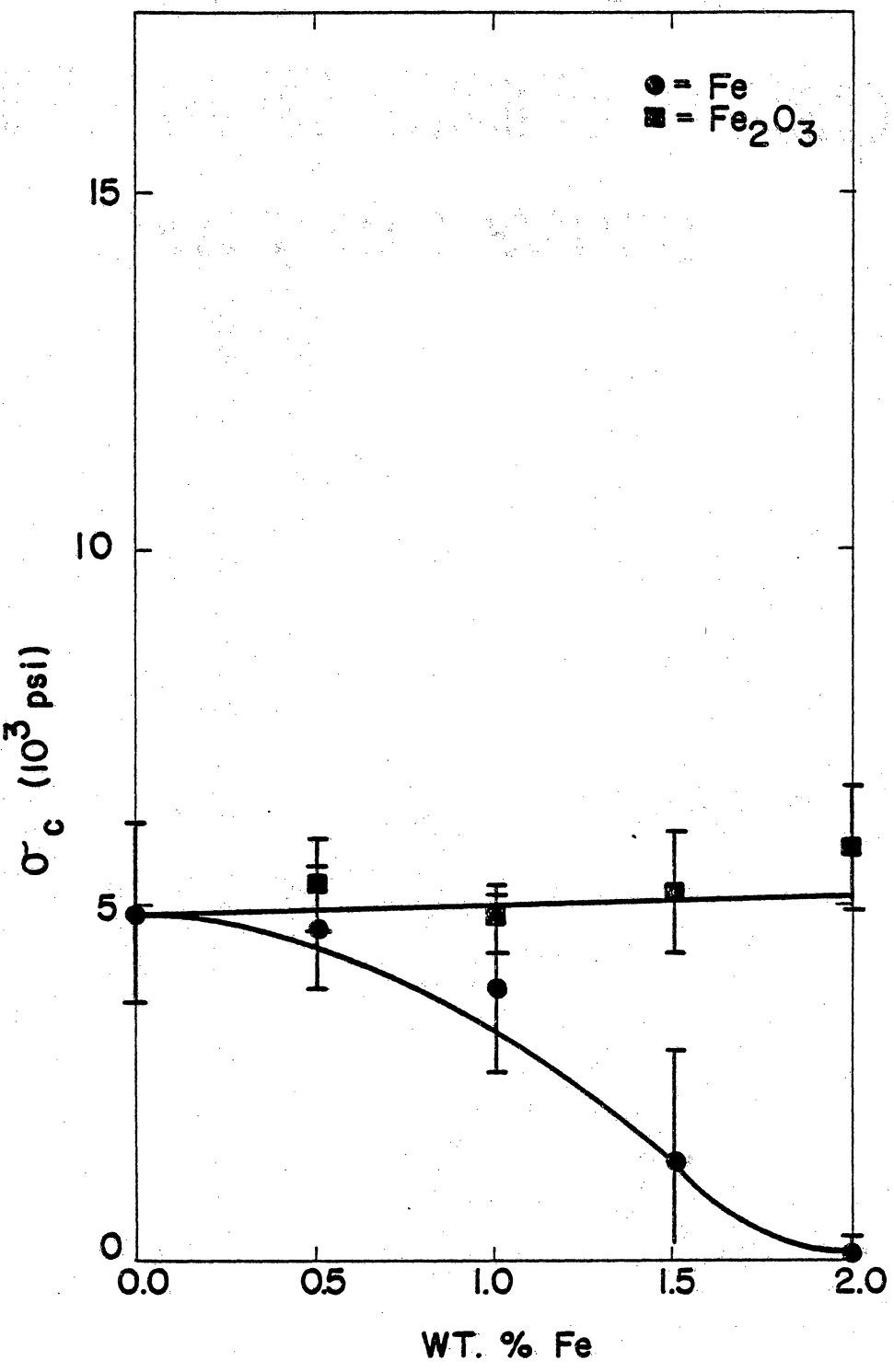

Figure 19. Compressive Strength of 50+ Wt.% Alumina Castable Exposed to 99.8% CO-0.2% NH_3.

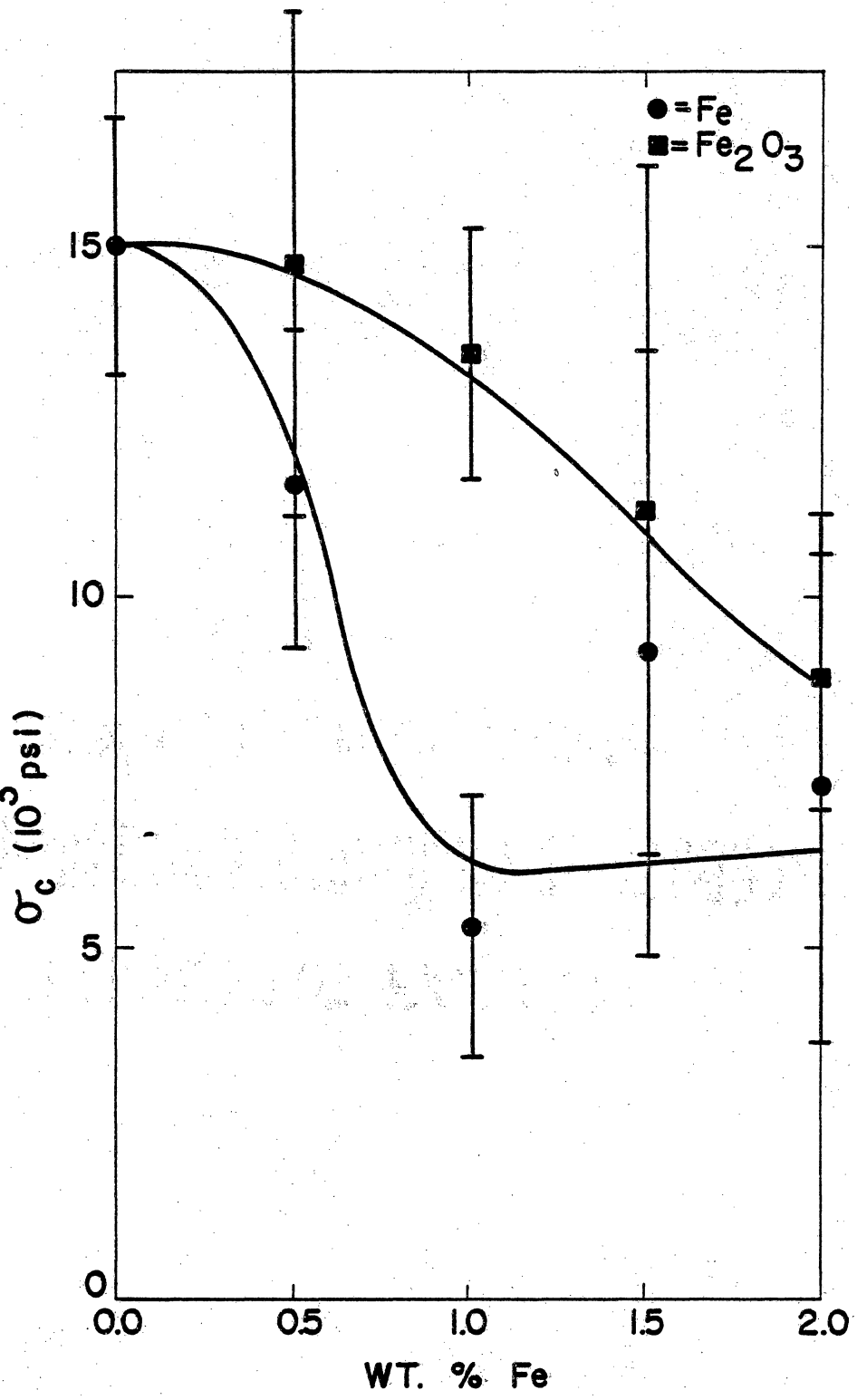

Figure 20. Compressive Strength of 90+ Wt.% Alumina Ramming Mix Exposed to 99.8% CO-0.2% NH_3.

wt.% alumina castable after being exposed to 99.2% CO - 0.8% NH_3. An average minimum of 68% of the undoped strength was retained by samples doped with 1.0 wt.% metallic iron. Strengths at 0.5 and 2.0 wt.% metallic iron were essentially the same as the undoped strength, as shown in Figure 21. Iron oxide-doped samples retained at least 94% of the undoped refractory strength.

b. 50+ Wt.% Alumina Castable

The 50+ wt.% alumina castable exhibited an average undoped strength of 3,925 psi following exposure to the 99.2% CO - 0.8% NH_3 gas composition. At the 0.5 Fe wt.% level, both the metallic iron and iron oxide-doped refractories had more strength than the undoped refractory. Higher levels of metallic iron produced considerable strength degradation, as shown in Figure 22, while higher levels of iron oxide further improved average refractory strength.

c. 90+ Wt.% Alumina Phosphate-Bonded Ramming Mix

The average undoped strength of the ramming mix was 12,150 psi after exposure. A small strength decrease, to 88% of the undoped strength, occurs at the 0.5 wt.% level of metallic iron doping. Greater amounts of metallic iron caused larger strength losses, with a minimum strength of 39% of the undoped strength at 1.0 wt.% metallic iron, as shown in Figure 23. Iron oxide-doped samples retained an average of at least 90% of the undoped strength.

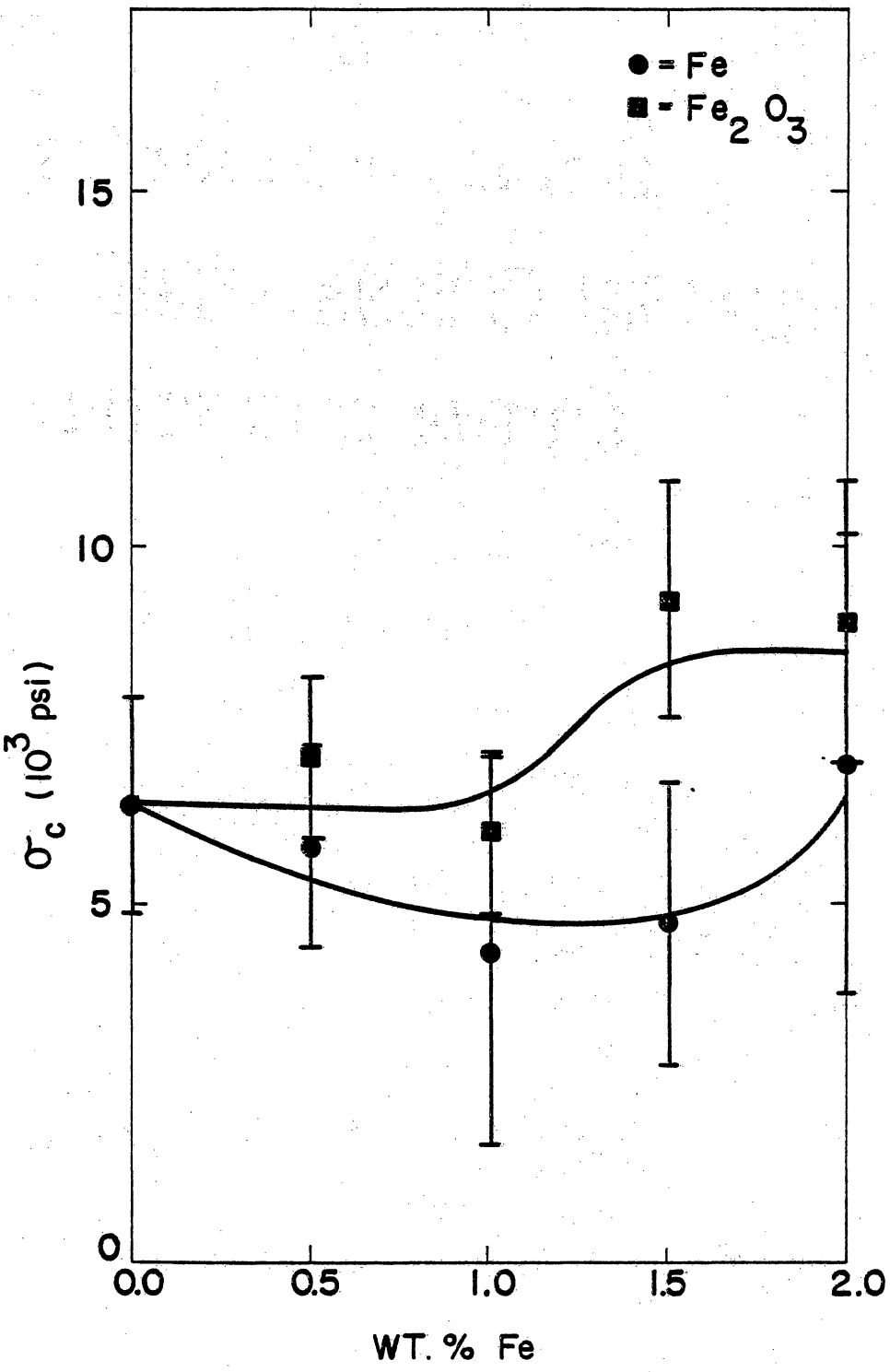

Figure 21. Compressive Strength of 90+ Wt.% Alumina Castable Exposed to 99.2% CO-0.8% NH_3.

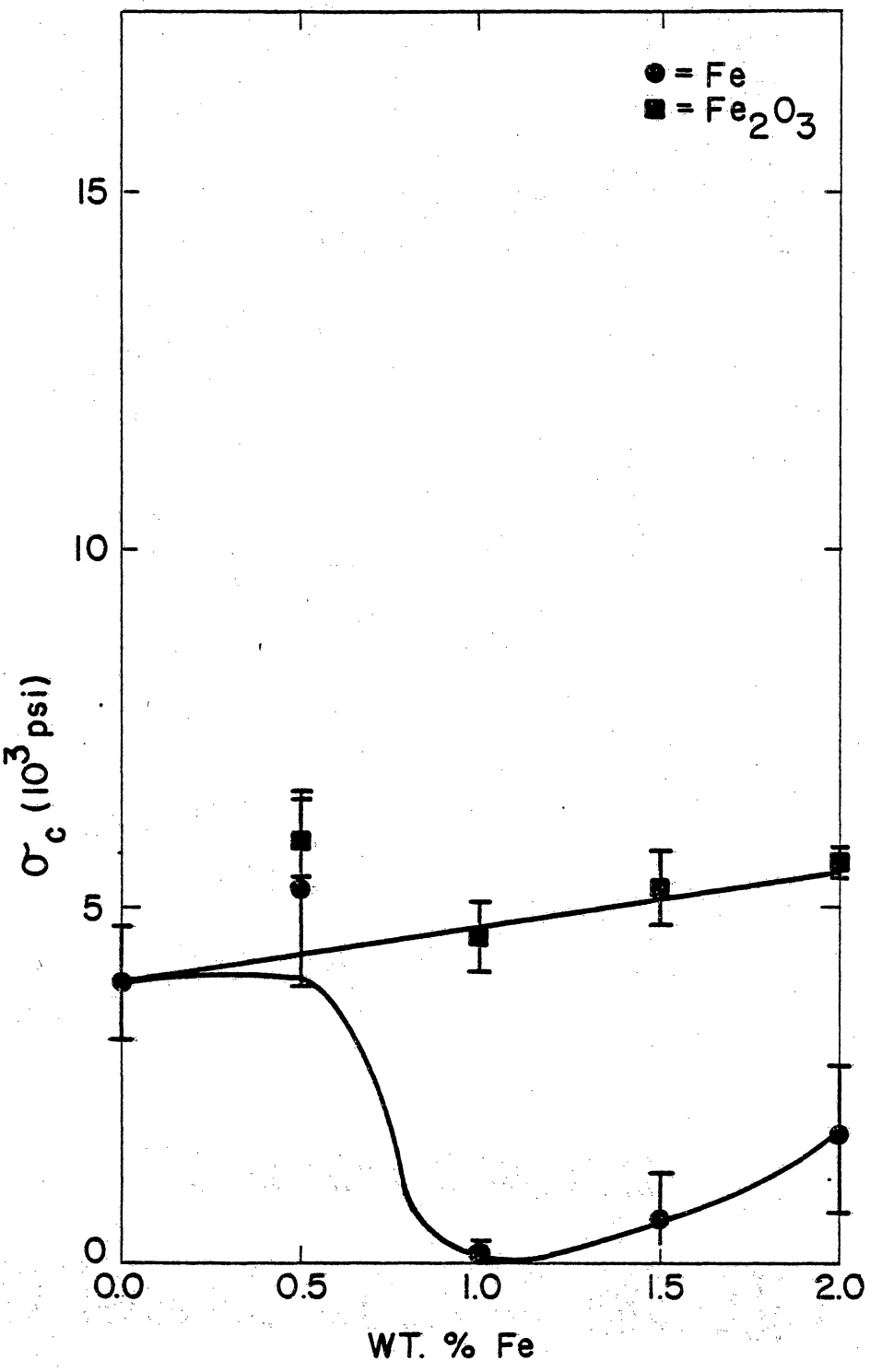

Figure 22. Compressive Strength of 50+ Wt.% Alumina Castable Exposed to 99.2% CO-0.8% NH_3.

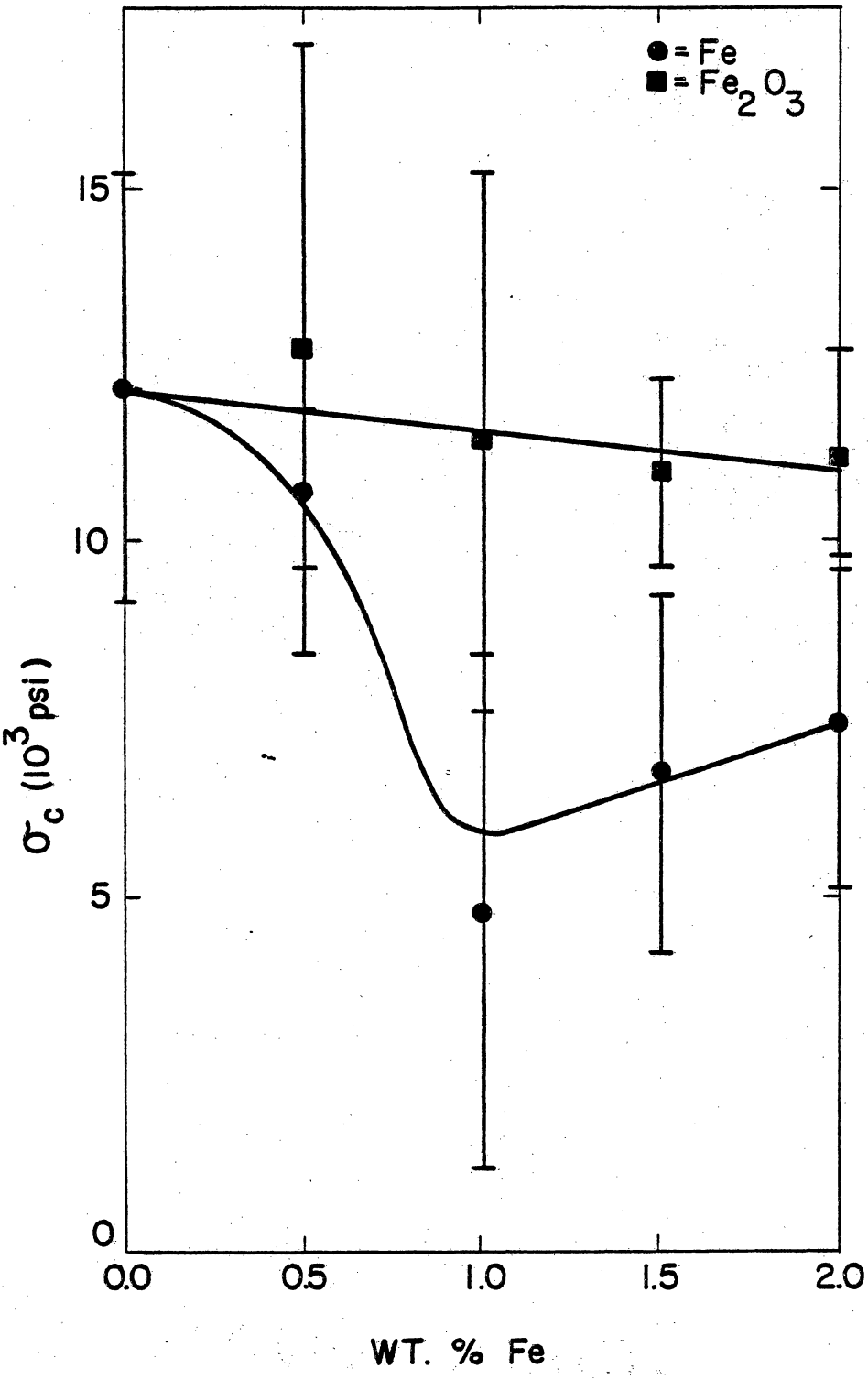

Figure 23. Compressive Strength of 90+ Wt.% Alumina Ramming Mix Exposed to 99.2% CO-0.8% NH_3.

6. 80% CO - 20% H_2 Mixture

a. 90+ Wt.% Alumina Castable

The 90+ wt.% alumina castable retained an average of 5,325 psi after exposure to the 80% CO - 20% H_2 gas. The refractory retained at least 91% of its undoped strength when doped with metallic iron and more than 140% of this undoped strength when doped with iron oxide, as shown in Figure 24.

b. 50+ Wt.% Alumina Castable

The 50+ wt.% alumina castable had an average undoped strength of 5,100 psi. When doped with 0.5 Fe wt.% metallic iron and iron oxide, the refractory was approximately 15% stronger than when undoped. Higher levels of both dopants produced strengths greater than double that of the undoped refractory, shown in Figure 25.

c. 90+ Wt.% Alumina Phosphate-Bonded Ramming Mix

The undoped phosphate-bonded ramming mix exhibited 12,000 psi after exposure to the gas mixture. It retained approximately 82% of this strength when doped with 0.5 wt.% metallic iron. Greater amounts of metallic iron in the refractory caused progressive strength increases, with the 2.0 wt.% strength being slightly greater than the undoped strength, as shown in Figure 26. Strength of the iron oxide-doped ramming mix was at least as great as the undoped strength at the 0.5, 1.0, and 1.5 Fe wt.% levels. Strength decreased to less than 70% of the un-

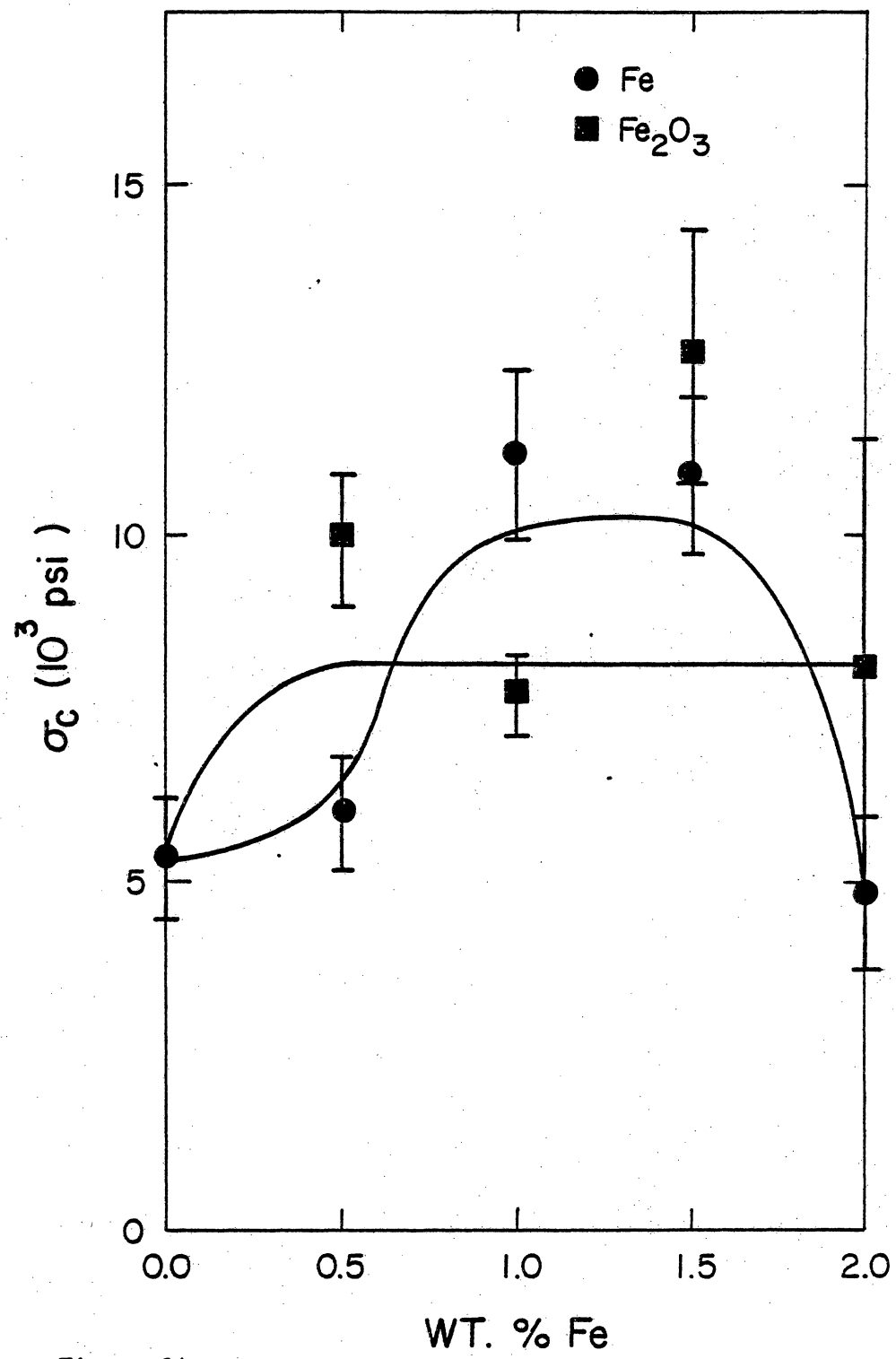

Figure 24. Compressive Strength of 90+ wt.% Alumina Castable Exposed to 80% CO-20% H_2.

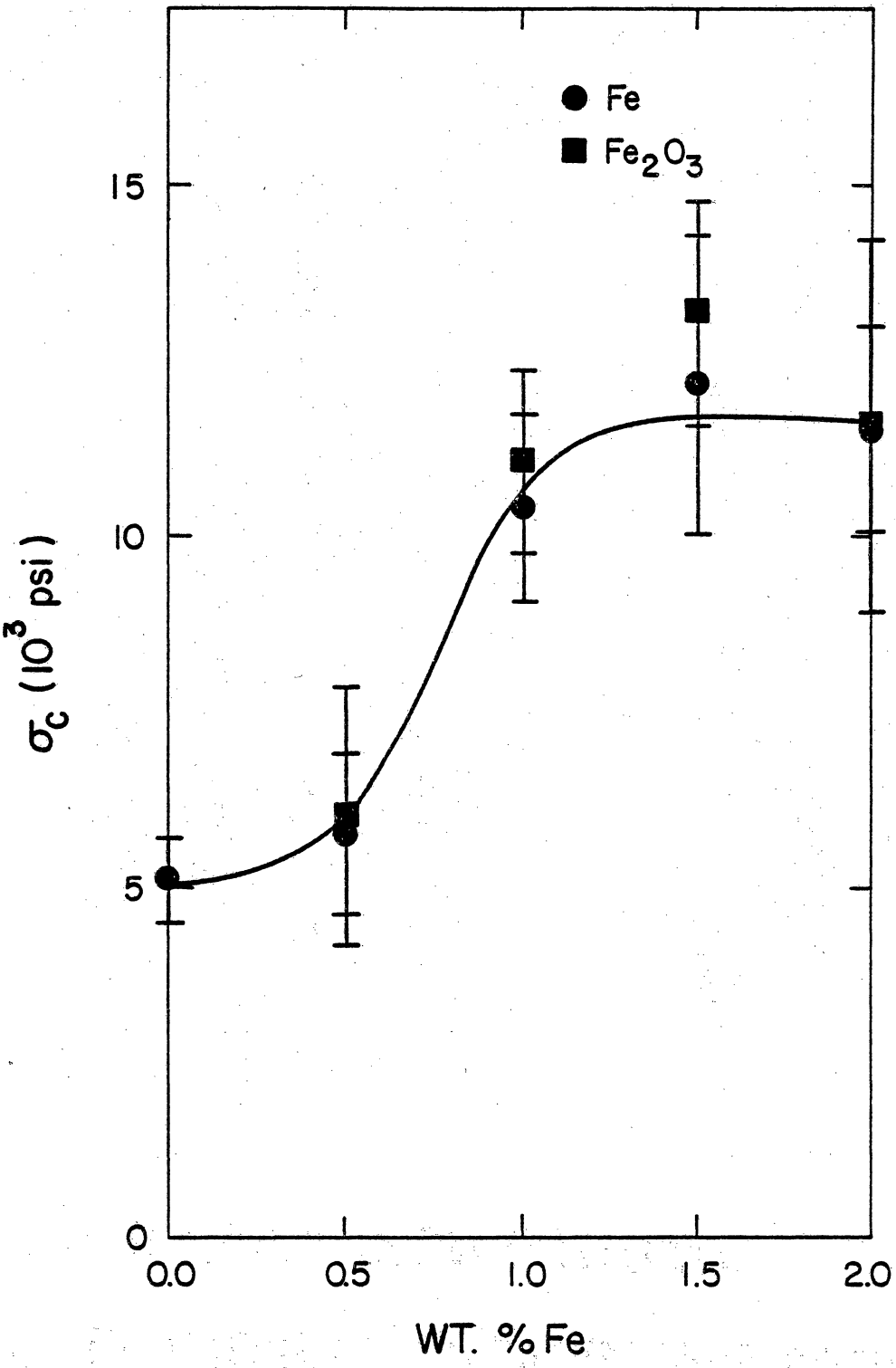

Figure 25. Compressive Strength of 50+ Wt.% Alumina Castable Exposed to 80% CO–20% H_2.

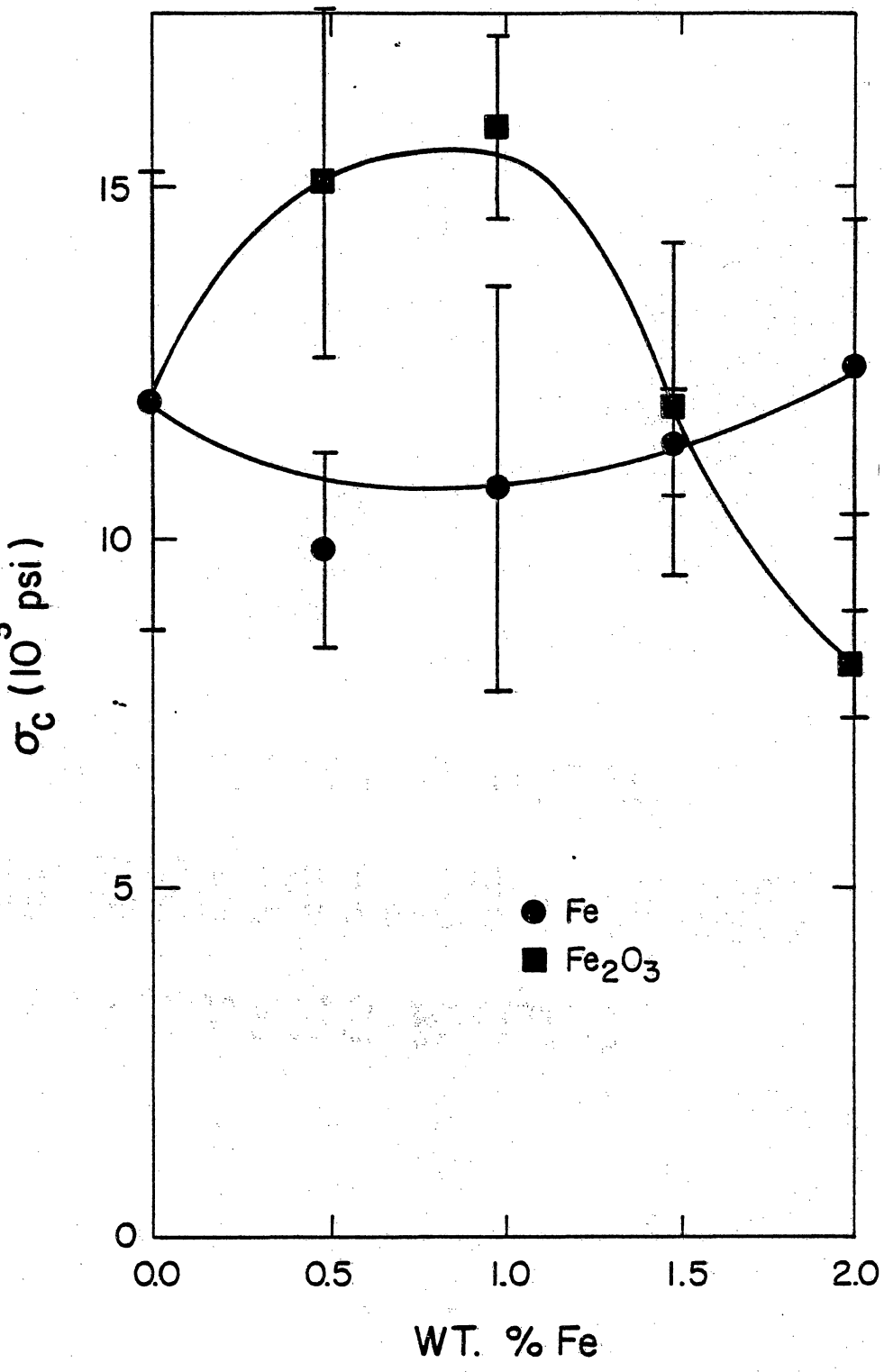

Figure 26. Compressive Strength of 90+ Wt.% Alumina Ramming Mix Exposed to 80% CO-20% H2.

doped strength at the 2.0 Fe wt.% iron oxide level, shown in Figure 26.

7. 60% CO - 40% H_2 Mixture

a. 90+ Wt.% Alumina Castable

An average strength of 6,975 psi was obtained for the undoped 90+ wt.% alumina castable after exposure. The refractory retained at least 97% of this strength when doped with 0.5 wt.% metallic iron. Higher levels of metallic iron and all levels of iron oxide-doping produced strength greater than the undoped strength, as shown in Figure 27.

b. 50+ Wt.% Alumina Castable

The 50+ wt.% alumina castable has an undoped strength of 5,125 psi after exposure to the 60% CO - 40% H_2 mixture. A minimum of 79% of this strength, which occurred at the 0.5 wt.% metallic iron level, was retained by the refractory. Metallic iron at levels of 1.0 wt.% and greater produced strengths at least equal to the undoped strength, as shown in Figure 28. Strength of the iron oxide-doped refractory, also shown in Figure 28, varied from 17% less to 22% greater than the undoped strength.

c. 90+ Wt.% Alumina Phosphate-Bonded Ramming Mix

The undoped ramming mix exhibited an average strength of 10,450 psi following exposure. When doped with metallic iron, the refractory has a minimum of 83% of the undoped strength at the 0.5 wt.% level. Higher levels of metallic iron yielded strengths approximately equal to

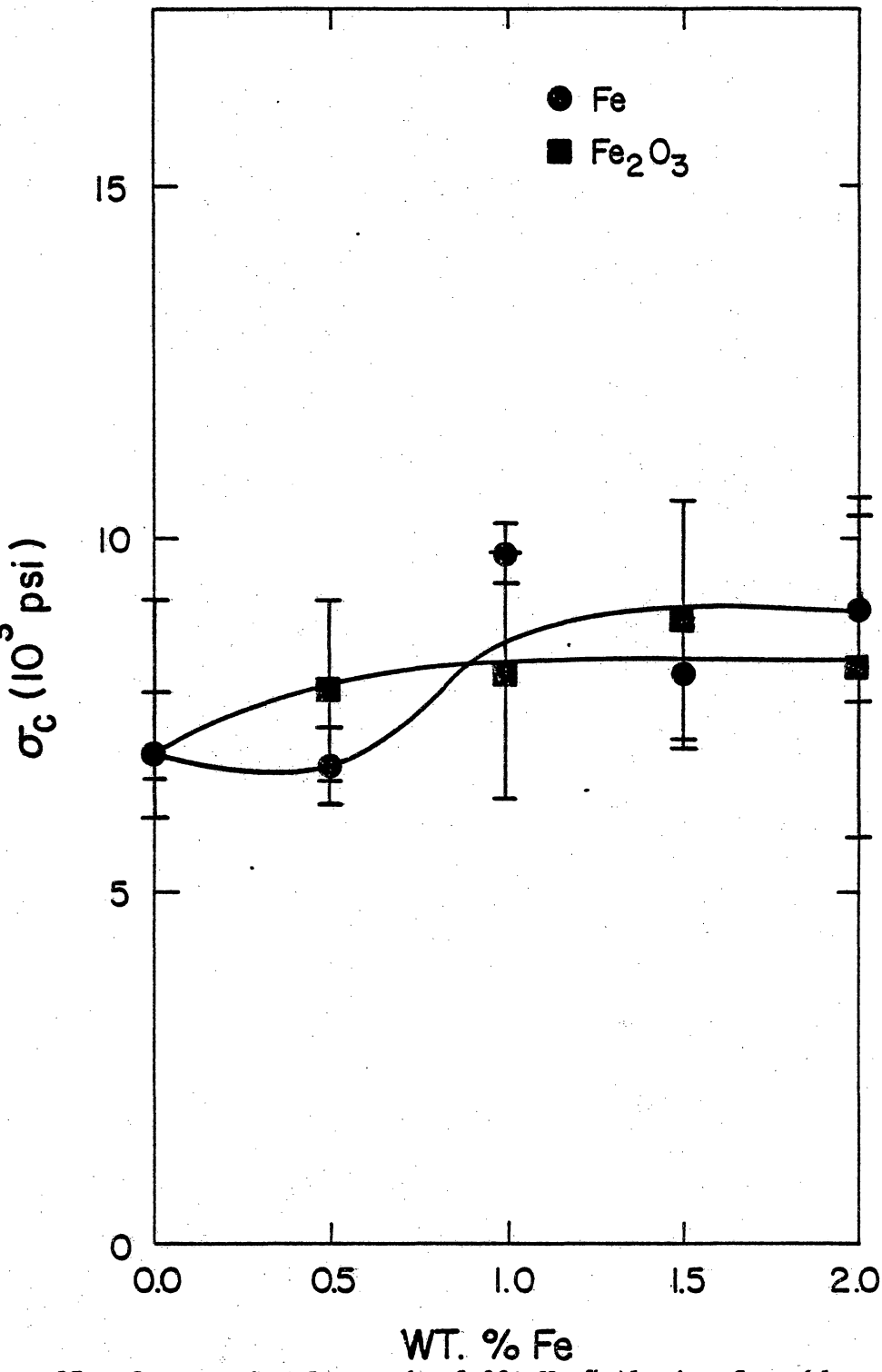

Figure 27. Compressive Strength of 90+ Wt.% Alumina Castable Exposed to 60% CO-40% H_2.

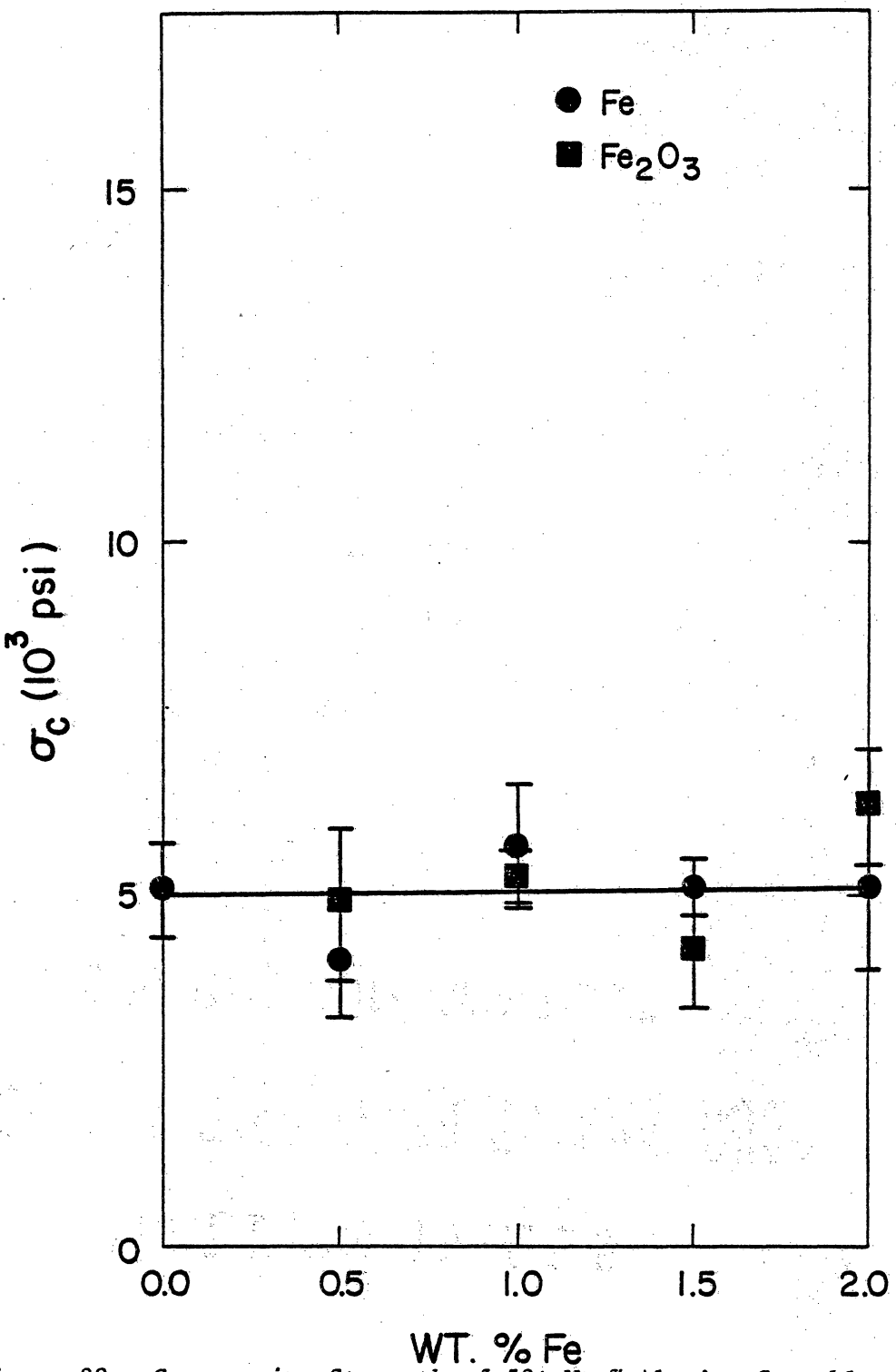

Figure 28. Compressive Strength of 50+ Wt.% Alumina Castable Exposed to 60% CO-40% H_2.

the undoped strength, as shown in Figure 29. The iron oxide-doped refractory retained at least 92% of its undoped strength.

8. 99.8% CO - 0.2% H_2S

a. 90+ Wt.% Alumina Castable

The 90+ wt.% alumina castable had an average undoped strength of 7,200 psi. It retained a minimum of 75% of this strength when doped with 1.0 wt.% metallic iron, as shown in Figure 30. Metallic iron levels of 0.5 wt.% and 1.5 wt.% yielded strengths greater than 95% of the undoped strength, while the 2.0 wt.% level exhibited 87% of the undoped strength. Doping the refractory with iron oxide yielded strengths that averaged 17% greater than the undoped strength.

b. 50+ Wt.% Alumina Castable

An average of 4,375 psi was retained by the undoped 50+ wt.% alumina castable. The refractory retained only 36% of its undoped strength when doped with 0.5 wt.% metallic iron. Metallic iron levels of 1.0 and 1.5 wt.% caused the refractory to retain no strength, as shown in Figure 31. Doping the refractory with 2.0 wt.% metallic iron resulted in a retention of 65% of the undoped strength. When doped with iron oxide, the refractory exhibited at least 98% of its undoped strength.

c. 90+ Wt.% Alumina Phosphate-Bonded Ramming Mix

After exposure to the 99.8% CO - 0.2% H_2S mixture, the ramming mix

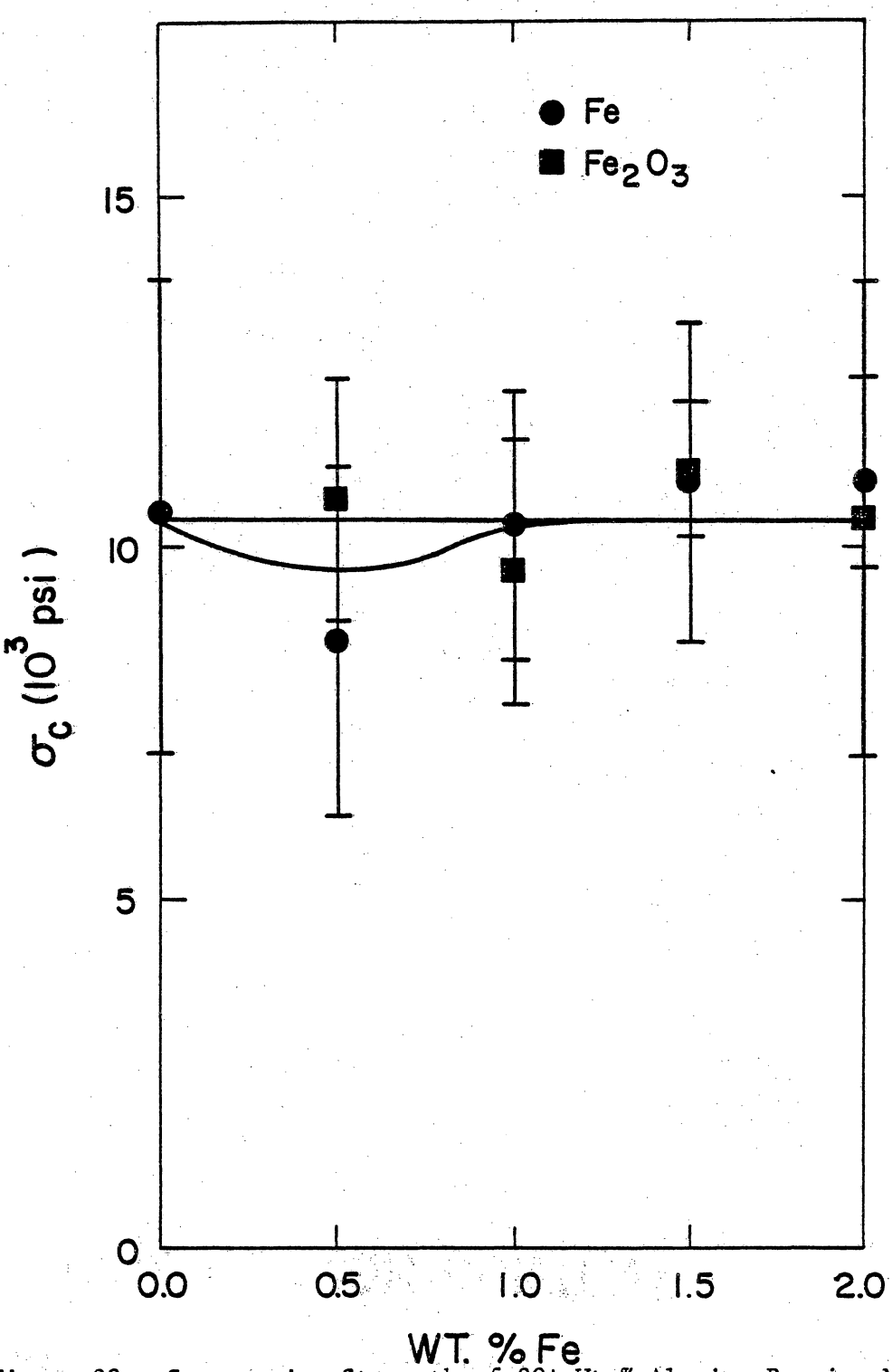

Figure 29. Compressive Strength of 90+ Wt.% Alumina Ramming Mix Exposed to 60% CO-40% H_2.

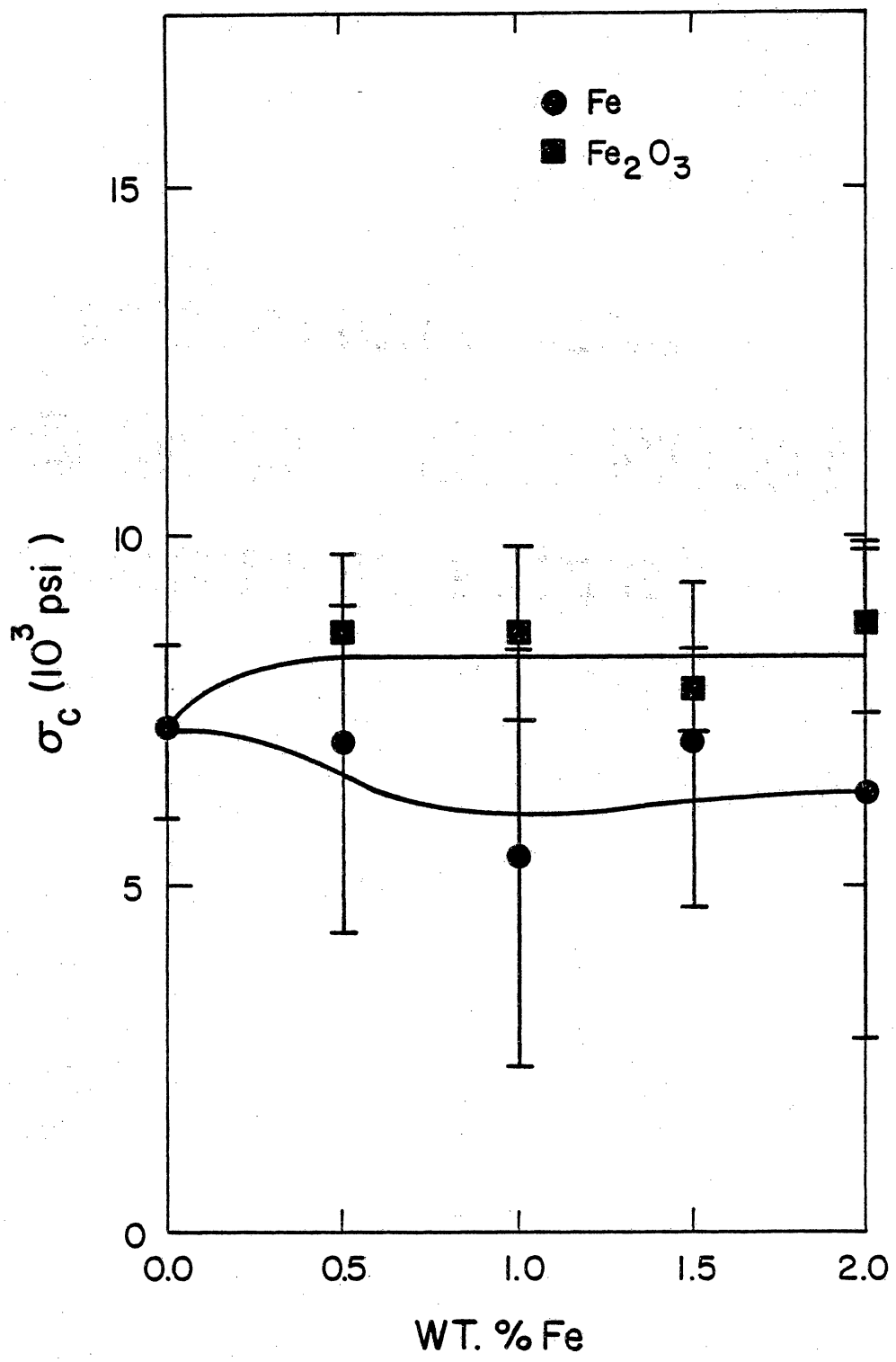

Figure 30. Compressive Strength of 90+ Wt.% Alumina Castable Exposed to '99.8% CO-0.2% H_2S.

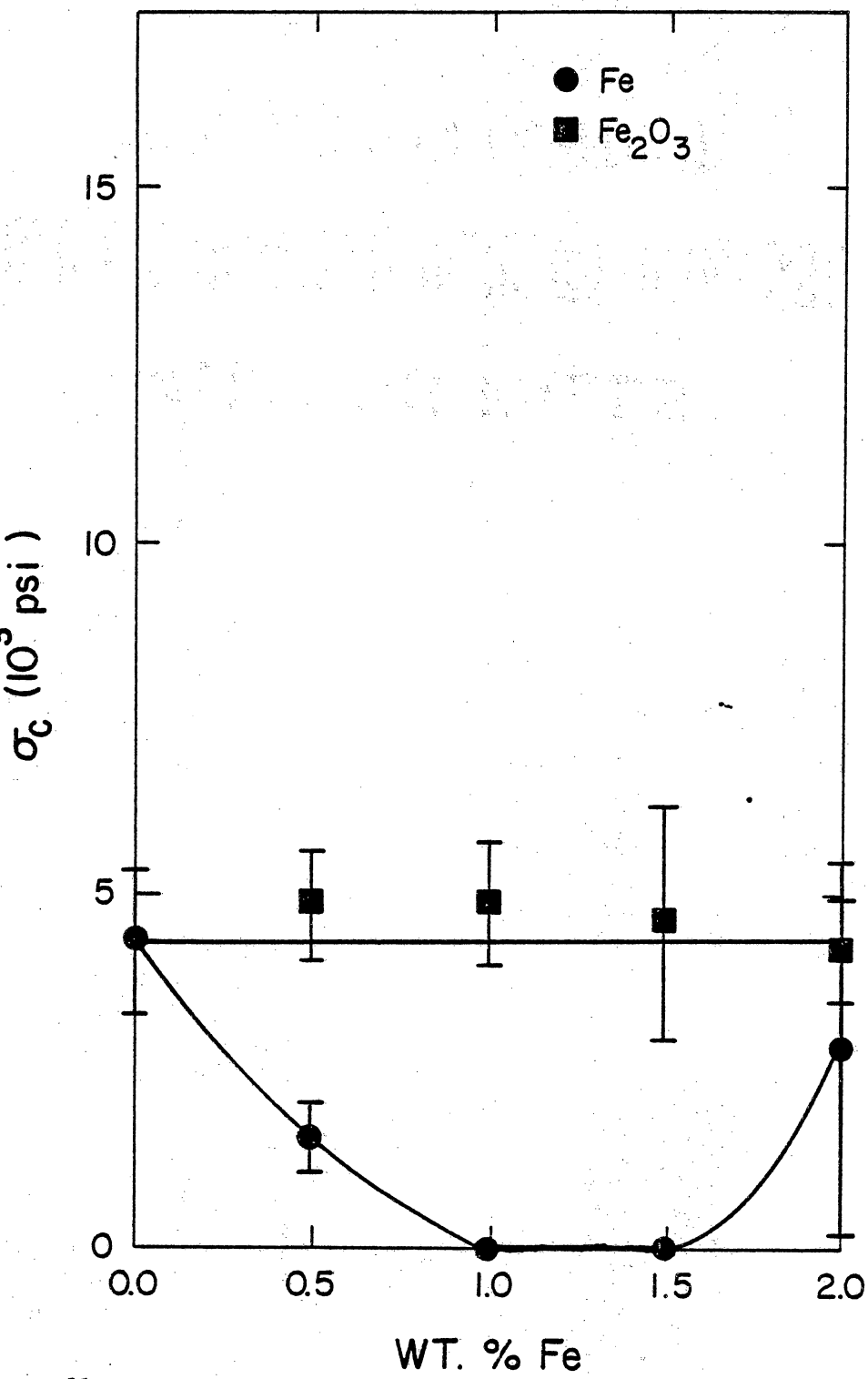

Figure 31. Compressive Strength of 50+ Wt.% Alumina Castable Exposed to 99.8% CO-0.2% H_2S.

had an average undoped strength of 8,250 psi. It retained 73% of this strength when doped with 0.5 wt.% metallic iron. Greater amounts of iron resulted in strengths of 60 to 65% of the undoped strength, as shown in Figure 32. When doped with 0.5 and 1.0 Fe wt.% iron oxide, the refractory was stronger than when undoped, however, iron oxide levels of 1.5 and 2.0 Fe wt.% caused the refractory to retain less than 30% of its undoped strength.

9. 99.2% CO - 0.8% H_2S Mixture

a. 90+ Wt.% Alumina Castable

The 90+ wt.% alumina castable had an average undoped strength of 7,475 psi after exposure. The refractory retained all of its undoped strength when doped with 0.5, 1.0, and 1.5 wt.% metallic iron, but had only 55% of this strength when doped with 2.0 wt.% metallic iron, as shown in Figure 33. When doped with iron oxide, the castable retained a minimum of 95% of its undoped strength.

b. 50+ Wt.% Alumina Castable

The average strength of the undoped 50+ wt.% alumina castable was 5,450 psi after exposure to the gas mixture. The refractory retained 73% of this strength when doped with 0.5 wt.% metallic iron. Metallic iron dopant levels of 1.0 and 1.5 wt.% reduced strength further, to 48% and 10% of the undoped strength, respectively, as shown in Figure 34. At the 2.0 wt.% level of metallic iron doping, the refractory retained 90% of its undoped strength, however, this value had a large standard

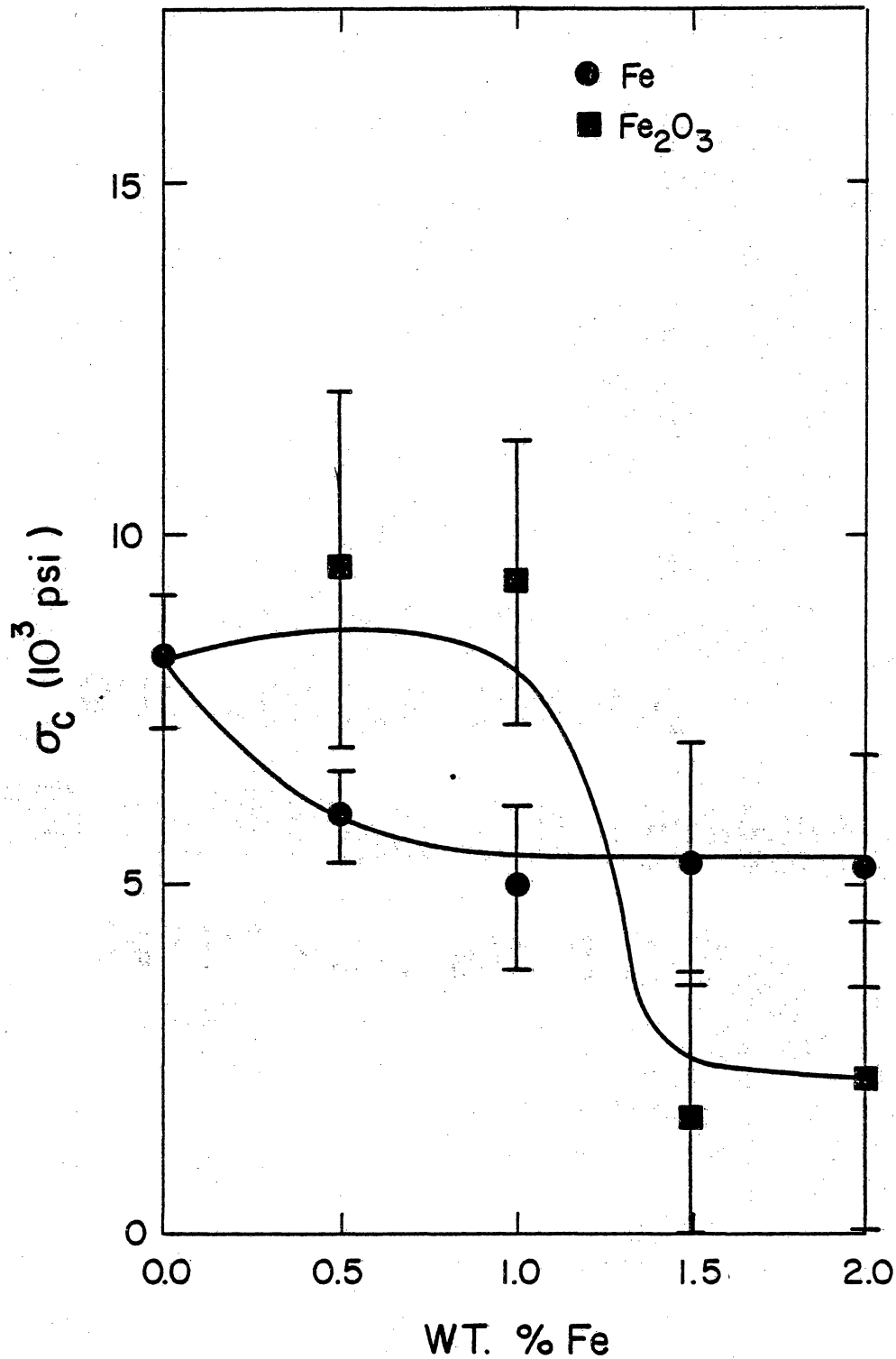

Figure 32. Compressive Strength of 90+ Wt.% Alumina Ramming Mix Exposed to 99.8% CO-0.2% H_2S.

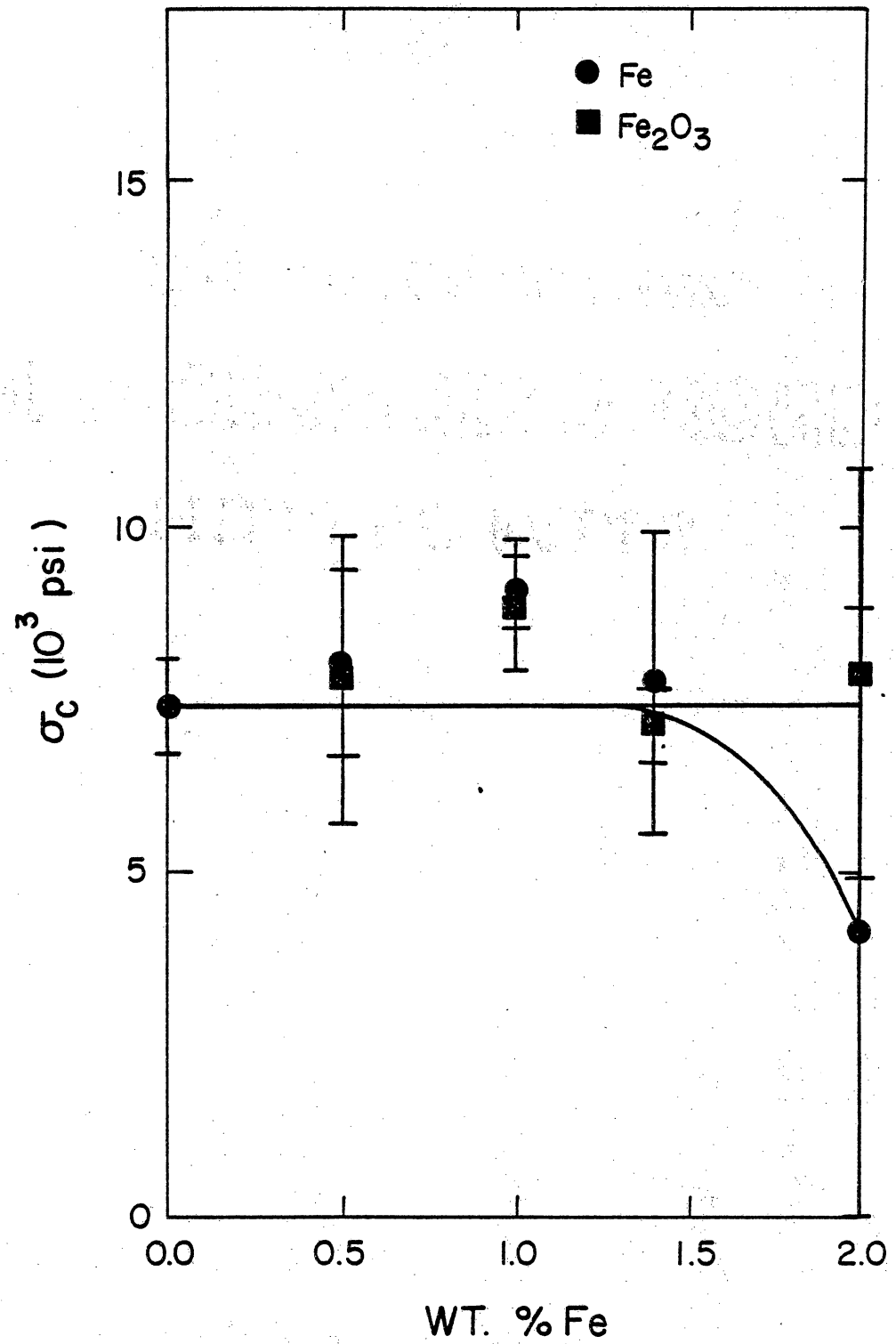

Figure 33. Compressive Strength of 90+ Wt.% Alumina Castable Exposed to 99.2% CO-0.8% H_2S.

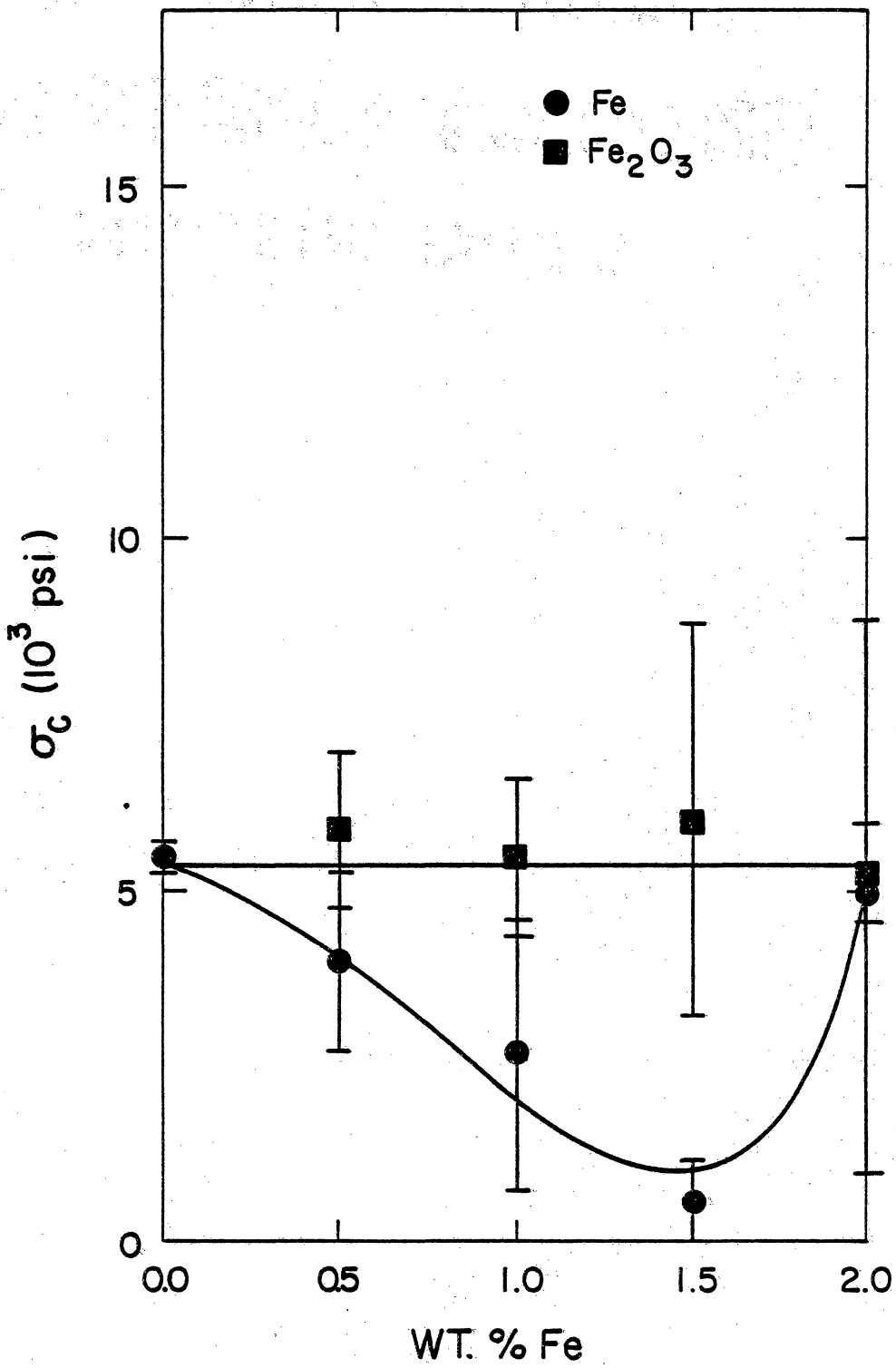

Figure 34. Compressive Strength of 50+ Wt.% Alumina Castable Exposed to 99.2% CO-0.8% H_2S.

deviation, as shown in Figure 34. The castable exhibited over 95% of its undoped strength when doped with iron oxide.

c. 90+ Wt.% Alumina Phosphate-Bonded Ramming Mix

The 90+ wt.% alumina ramming mix had an average undoped strength of 5,700 psi following exposure to the 99.2% CO - 0.8% H_2S gas mixture. The refractory retained at least 100% of this strength when doped with metallic iron and 0.5 Fe wt.% iron oxide. When doped with 1.0 Fe wt.% iron oxide, the ramming mix retained less than 45% of its undoped strength. Iron oxide levels of 1.5 and 2.0 Fe wt.% caused the refractory to retain 0% and 12%, respectively, of its undoped strength, as shown in Figure 35.

10. 80% CO - 20% H_2O Mixture

a. 90+ Wt.% Alumina Castable

The 90+ wt.% alumina castable exhibited a 6,775 psi average undoped strength after exposure to this gas mixture. The refractory was 25 to 55% stronger when doped with metallic iron, as shown in Figure 36. When doped with iron oxide, the castable had 134 to 260% of its undoped strength, also shown in Figure 36.

b. 50+ Wt.% Alumina Castable

An average undoped strength of 3,475 psi was obtained for the 50+ wt.% alumina castable following exposure to the 80% CO - 20% H_2O mixture. The castable retained 93% of this strength when doped with 0.5

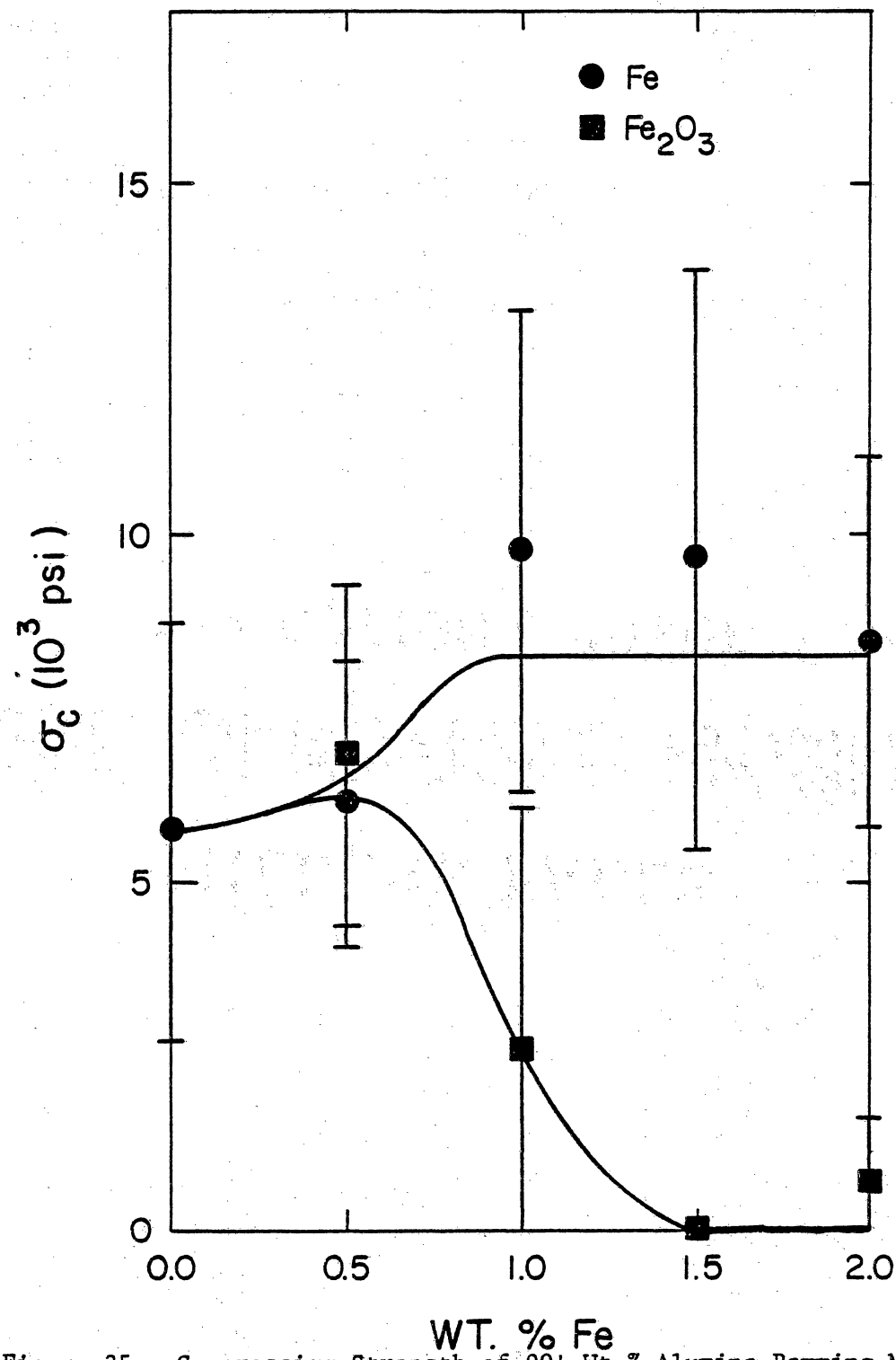

Figure 35. Compressive Strength of 90+ Wt.% Alumina Ramming Mix Exposed to 99.2% CO-0.8% H_2S.

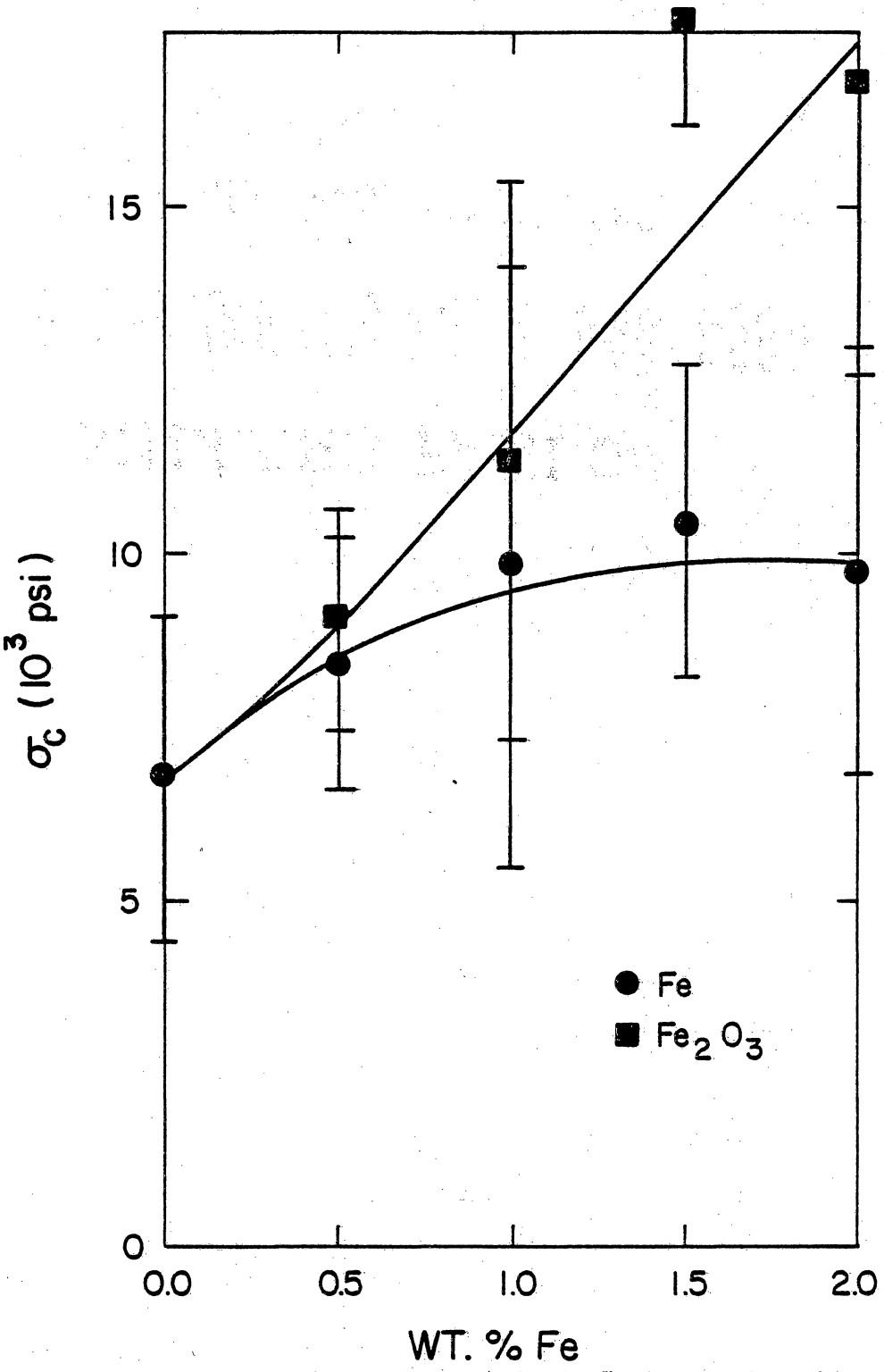

Figure 36. Compressive Strength of 90+ Wt.% Alumina Castable Exposed to 80% CO-20% H_2O.

wt.% metallic iron. Greater amounts of this dopant caused the refractory to have 27 to 53% more strength than when undoped, as shown in Figure 37. Doping the refractory with iron oxide resulted in strengths 17 to 76% greater than the undoped strength.

c. 90+ Wt.% Alumina Phosphate-Bonded Ramming Mix

The strength of the undoped ramming mix averaged 6,725 psi following exposure. The refractory retained 95% of this strength when doped with 0.5 wt.% metallic iron, and only 72% of this strength when doped with 1.0 wt.% metallic iron, as shown in Figure 38. Metallic iron dopant levels of 1.5 and 2.0 wt.% caused the refractory to exhibit greater strength than when undoped. Doping the refractory with up to 1.5 Fe wt.% iron oxide resulted in strengths that exceeded the undoped strength by at least 20%, however, the refractory retained only 89% of its undoped strength when 2.0 Fe wt.% iron oxide was added.

11. 60% CO - 40% H_2O Mixture

a. 90+ Wt.% Alumina Castable

The 90+ wt.% alumina castable had an undoped strength of 8,700 psi after exposure. The castable retained at least 89% of this strength when doped with metallic iron, as shown in Figure 39. When doped with iron oxide, the refractory was as strong or stronger than when undoped.

b. 50+ Wt.% Alumina Castable

The undoped 50+ wt.% alumina castable exhibited a strength of

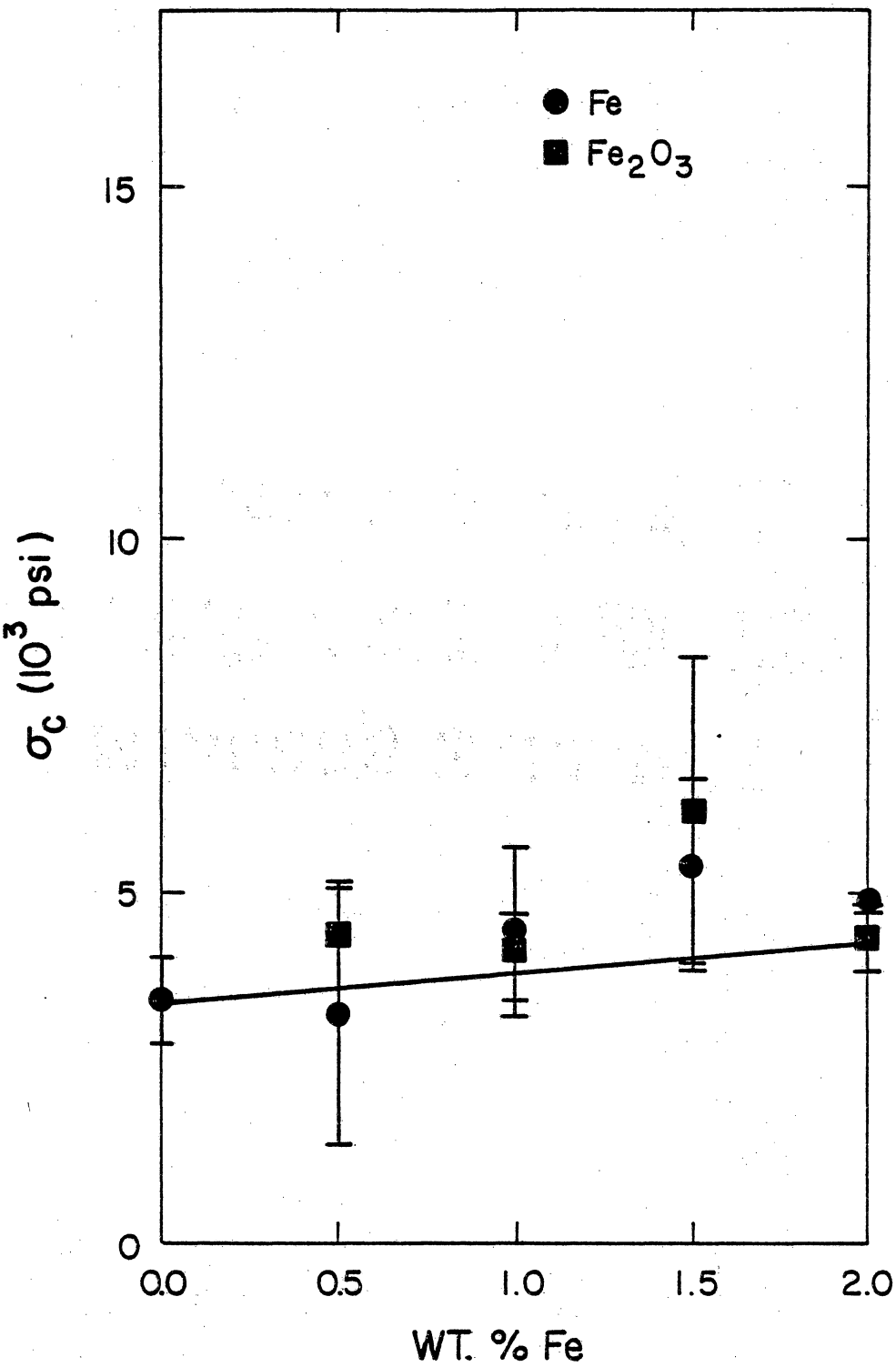

Figure 37. Compressive Strength of 50+ Wt.% Alumina Castable Exposed to 80% CO-20% H_2O.

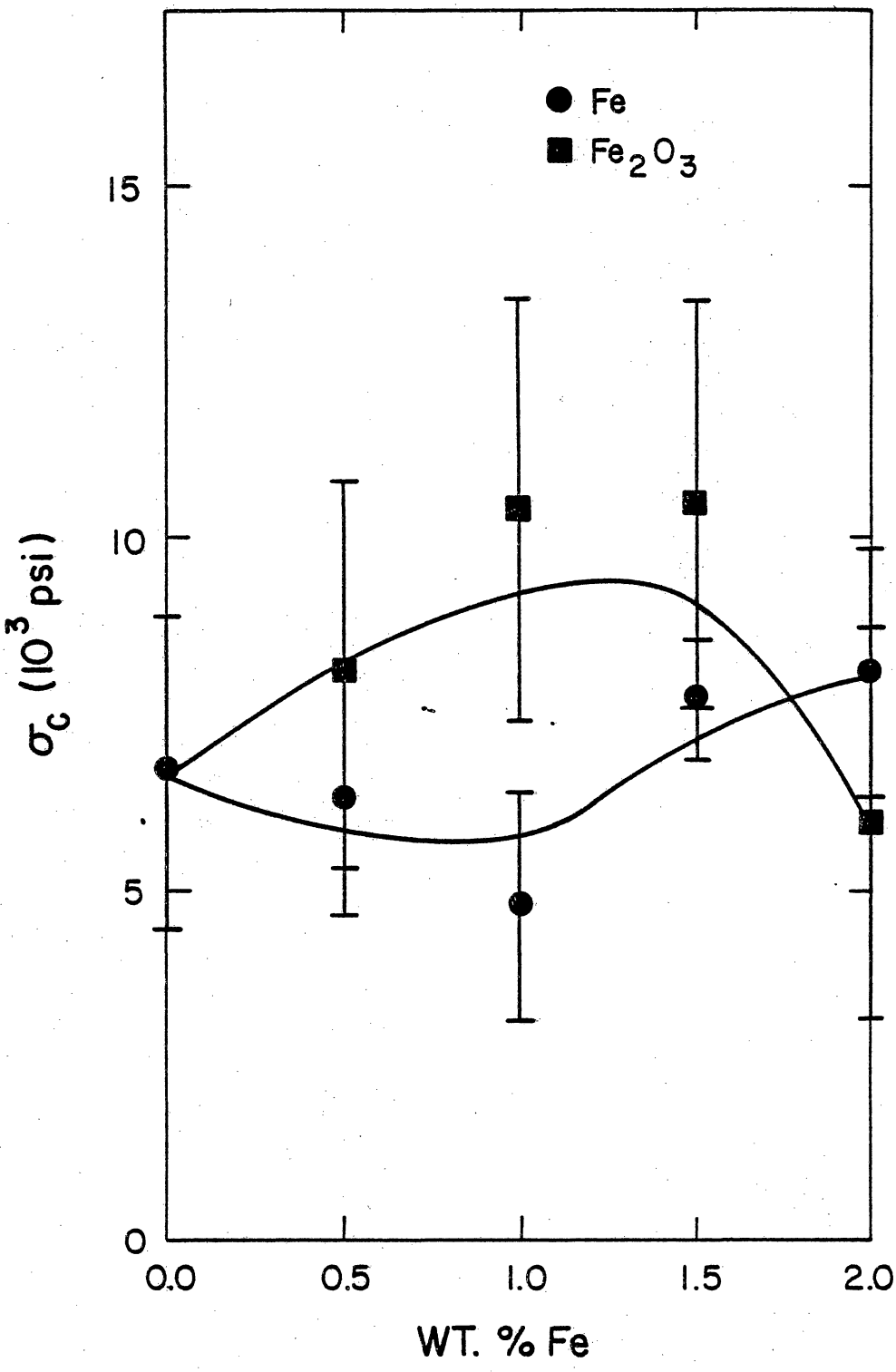

Figure 38. Compressive Strength of 90+ Wt.% Alumina Ramming Mix Exposed to 80% CO-20% H_2O.

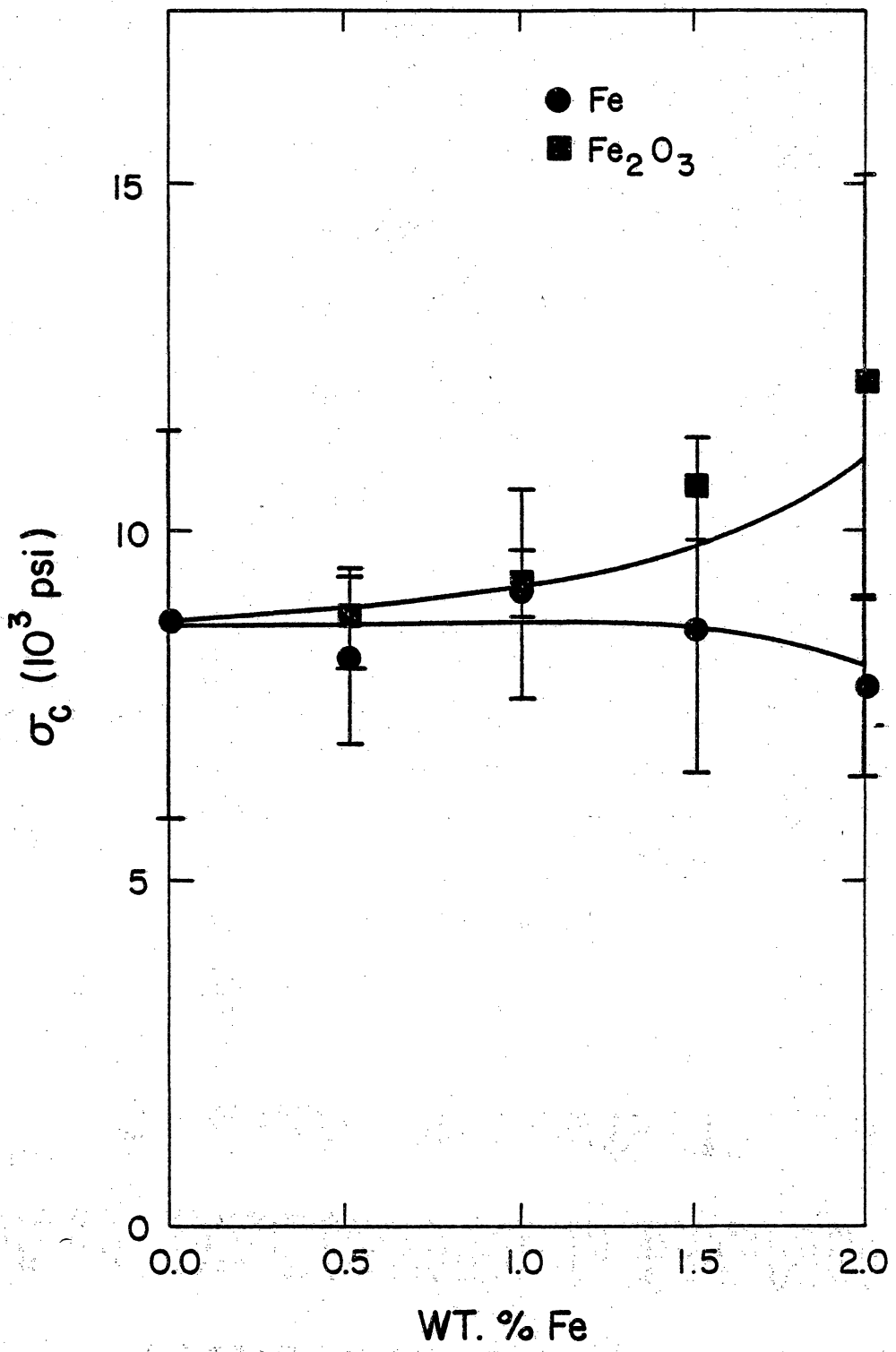

Figure 39. Compressive Strength of 90+ Wt.% Alumina Castable Exposed to 60% CO-40% H_2O.

4,775 psi after exposure. When doped with up to 1.5 wt.% metallic iron, the refractory retained at least 90% of its undoped strength, however, it retained only 66% of this strength when doped with 2.0 wt.% metallic iron, as shown in Figure 40. The castable retained 80 to 89% of its undoped strength when doped with iron oxide.

c. 90+ Wt.% Alumina Phosphate-Bonded Ramming Mix

The strength of the undoped 90+ wt.% alumina ramming mix was 6,900 psi after being exposed to 60% CO - 40% H_2O. Doping the refractory with 0.5 and 1.5 wt.% metallic iron produced, respectively, strengths of 74 and 71% of the undoped strength. Metallic iron dopant levels of 1.0 and 2.0 wt.% had strengths approximately 25% greater than the undoped strength. When iron oxide was added to the refractory, it exhibited strengths 13 to 67% greater than when undoped, as shown in Figure 41.

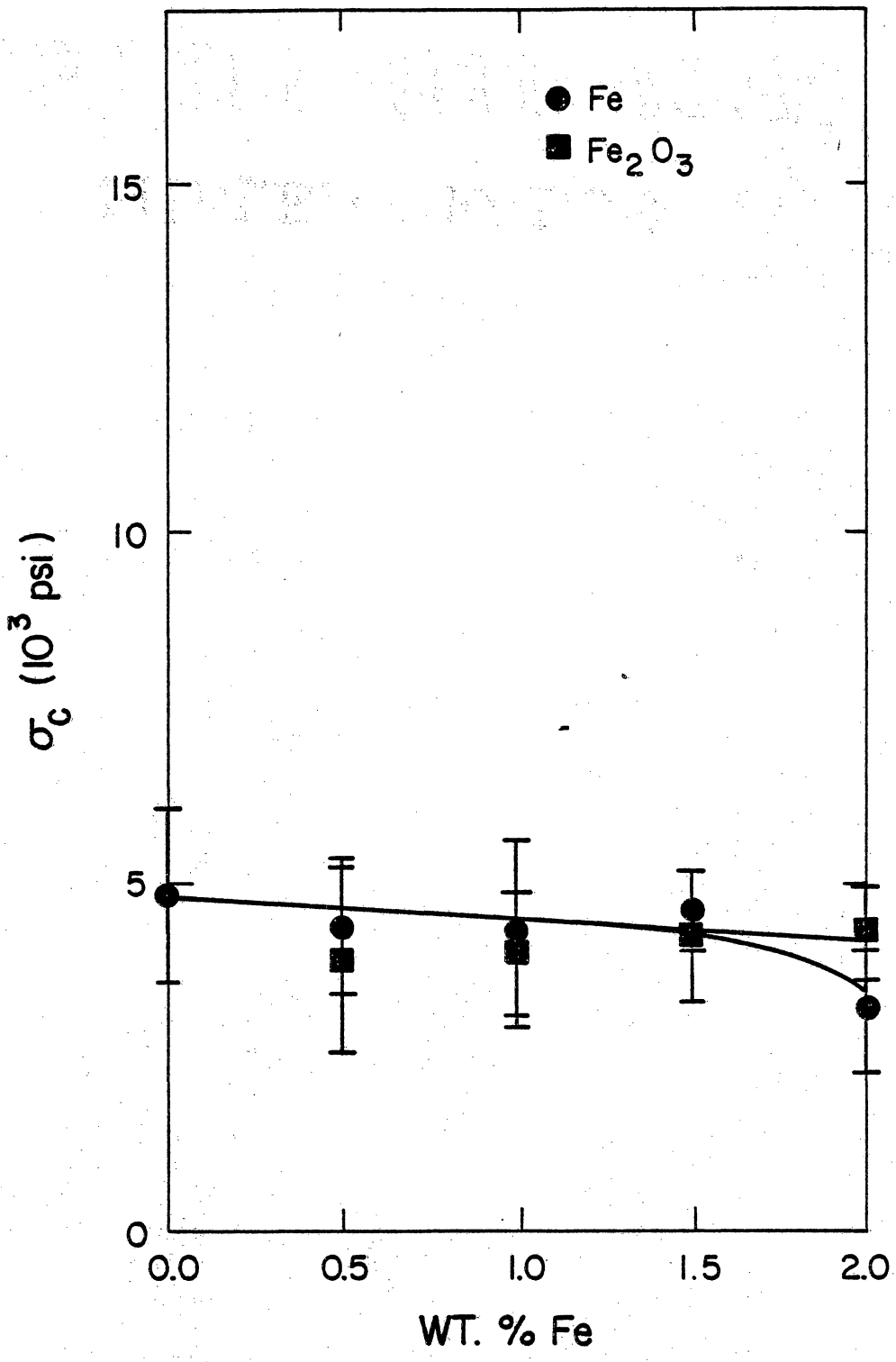

Figure 40. Compressive Strength of 50+ Wt.% Alumina Castable Exposed to 60% CO-40% H_2O.

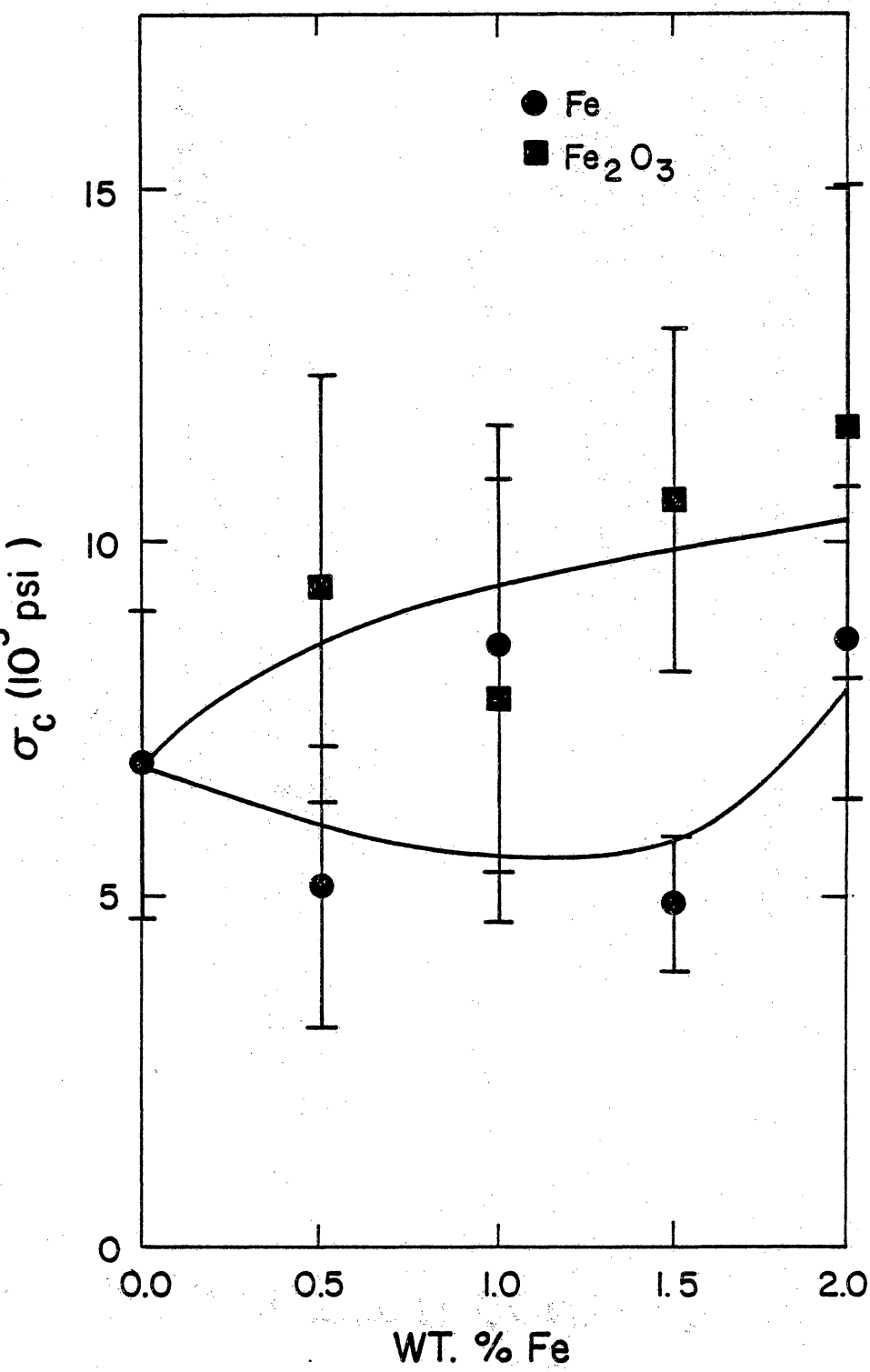

Figure 41. Compressive Strength of 90+ Wt.% Alumina Ramming Mix Exposed to 60% CO-40% H_2O.

V. Discussion

A. Effect of 100 Hr. Exposure to 99.99% CO

1. Comparison of the Three Refractories

a. Spalling

The 90+ wt.% alumina phosphate-bonded ramming mix showed the least amount of spalling of any of the refractories examined. At high metallic iron levels, the ramming mix exhibited no spalling or only small cracks. Similarly doped 90+ wt.% and 50+ wt.% alumina castables experienced advanced stages of spalling or complete disintegration. The resistance of the ramming mix to spalling may be due to phosphorus tieing up the metallic iron, slowing its conversion to iron carbide. Phosphorus may also speed up the conversion of hematite to iron carbide, as evidenced by the cracking and strength losses seen at high dopant levels of hematite-doped samples. No spalling was observed for either of the castables when doped with hematite, however, when eventual conversion to iron carbide, modeled by the metallic iron doping, takes place, the spalling damage was much greater than that for the ramming mix.

b. Compressive Strength

The 90+ wt.% alumina composition had much higher updoped strength

than the 50+ wt.% alumina castable, with the ramming mix being significantly stronger than the 90+ wt.% alumina castable. The ramming mix remained the strongest of the three refractories at all levels of metallic iron doping and at the 0.5 and 1.0 wt.% levels of hematite doping. The 90+ wt.% alumina castable retained some strength, despite severe spalling, with metallic iron doping. The 50+ wt.% alumina castable completely disintegrated at metallic iron levels of 1.0 wt.% and greater, however, at the 0.5 wt.%, it had higher strength than the 90+ wt.% alumina castable. While the ramming mix suffered strength losses at high levels of hematite doping, the castables retained essentially all of their initial strength, with the 90+ wt.% alumina castable actually gaining strength almost to the level of the undoped ramming mix. In an overall comparison of strength, the ramming mix was the most resistant to degradation by CO. While it did undergo strength degradation when doped with hematite, the retained strength of the ramming mix doped with metallic iron was much greater than that for the metallic iron-doped concretes.

2. Dopant Reactions in the Three Refractories

a. 90+ Wt.% Alumina Castable

Casting and pre-firing of metallic iron-doped 90+ wt.% alumina castables cause partial oxidation of the dopant to wüstite (FeO) or magnetite (Fe_3O_4). Prefiring of hematite-doped 90+ wt.% alumina castable produces an unknown yellow substance. It forms upon cooling below 400°C.

During CO exposure, the partially oxidized metallic iron forms iron carbide which is the catalyst for CO decomposition, as seen by the progressive stages of disintegration for the refractory. Hematite and the yellow compound both reduce to magnetite. Evidence supporting formation of this compound has been obtained by exposing 25 gms. of hematite, contained in an alumina firing boat, to CO for 100 hrs. at 500°C at a flow rate of 2 liters per hr. A large amount of carbon was deposited during the test, and black, magnetic crystals, i.e. magnetite, were formed.

b. 50+ Wt.% Alumina Castable

Reactions in the 50+ wt.% alumina castable appears to be the same as in the 90+ wt.% alumina castable.

c. 90+ Wt.% Alumina Phosphate-Bonded Ramming Mix

Curing and prefiring of metallic iron in the ramming mix causes partial oxidation of the iron and/or formation of iron phosphides (Fe_2P,Fe_3P). Hematite appears unaffected by curing or prefiring.

Formation of iron carbide occurs during CO exposure, as evidenced by some spalling. Since the metallic iron-doped samples do not spall nearly as much as similarly doped concretes, possible bonding between iron and phosphorus limits or slows down the formation of the carbide catalyst. The hematite-doped ramming mix turn either grey or black, indicating iron phosphides (Fe_2P,Fe_3P) or blue, characteristic of iron meta-phosphate ($Fe_3(PO_4)_2$) or iron phosphide (Fe_2P). Because cracking

and strength degradation occur at the two highest levels of hematite doping, some iron carbide must also be forming.

B. Basis for Comparing Effects of Additional Gases on CO Disintegration

1. Variations in Undoped Strength of Refractory Samples

The degradation of each refractory when exposed to pure CO forms the baseline for measuring the effects of CO_2, NH_3, H_2, H_2S, and H_2O on CO disintegration. Variations in the undoped strength of all three refractories occurred both within individual exposures to gases, as shown by deviations in Appendix I, and between exposures to the different gas mixtures.

The variation in strength that occurred from one run to the next caused some concern, as there were no signs of either weight change or visible damage to suggest that carbon deposition or CO disintegration was occurring. In a comparison between undoped samples exposed to 99.99% CO and 95% CO - 5% CO_2, strength tests on undoped samples of each refractory that had been prefired, but not exposed to either gas composition, show the same strength variations as were seen for exposed undoped samples. These tests lead to the conclusion that the strength variations are linked to differences in raw materials, preparation techniques, and/or environmental conditions at the time of preparation rather than to exposure effects. The various gaseous environments had the same proportionate effects on the undoped strength of the refractories.

2. Undoped Strength as Baseline for Dopant and Gas Effects

Since there is no visual evidence to suggest that exposure to various gas compositions cause differences in the undoped strength of each refractory, and, since unexposed samples of the refractories, prepared at different times of the year with different consignments of raw material, reflect the same strength deviations, the undoped strength of each refractory in exposure to a particular gas composition will be used as the reference point to characterize both the effects of the iron dopants and the various gas compositions.

Changes from the undoped strength caused by the dopants will be reflected as fractions of undoped strength retained by doped refractories. These strength fractions are summarized in Appendix I, as are the average strengths of the three refractories. The effects of the various gas compositions on CO disintegration can then be characterized by comparing the strength fractions obtained at a particular dopant level in exposures to each of the gas compositions.

3. Consolidation of Dopant Effects

Characterizing the effect of the various gases at each individual dopant level would lead to an unwieldly number of conclusions. This is especially true since, in some cases, a particular gas mixture would modify CO disintegration at all dopant levels, while in other cases it would only modify disintegration at low Fe levels, and in still other cases only at high Fe levels. This type of approach would tend

to complicate the issue rather than resolve it, for seperate conclusions would have to be drawn about the effect of a particular gas at each dopant level. These separate conclusions could be different, if not altogether contradictory, in describing the effect of a particular gas on CO disintegration in each of the three refractories.

A concise statement about the effects of each of the various gas compositions on CO disintegration can be obtained by averaging the strength fractions obtained at all dopant levels for a particular refractory exposed to a specific gas composition. This would show the average effect of the gas in relation to modification of CO disintegration and, overall, would be a more accurate statement. The analysis is done separately from metallic iron and iron oxide dopants, and the results are shown in Table III. The combined strength fractions will be called a strength index, for convenience, with a value of zero representing no retained strength and a value of one indicating the average undoped strength of each refractory in the particular exposure.

4. Spalling Index

The visible condition of each refractory was assessed by arbitrarily assigning the no damage condition a value of 1.00, cracking; 0.75, light spalling (edge and corner): 0.50, heavy spalling (whole face and deeper): 0.25, and complete disintegration: 0.00. These numbers were multiplied by the number of samples exhibiting the particular condition and divided by the total number of samples examined in order to determine the spalling index for the refractory.

TABLE III. STRENGTH INDEXES OF REFRACTORIES

EXPOSED TO VARIOUS GAS COMPOSITIONS

Gas Composition	90+ Wt.% Alumina Castable doped w/ Fe	90+ Wt.% Alumina Castable doped w/ Fe_2O_3	50+ Wt.% Alumina Castable doped w/ Fe	50+ Wt.% Alumina Castable doped w/ Fe_2O_3	90+ Wt.% Alumina Ramming Mix doped w/ Fe	90+ Wt.% Alumina Ramming Mix doped w/ Fe_2O_3
CO	0.336	1.254	0.197	0.994	0.650	0.885
95% CO - 5% CO_2	0.971	1.365	0.287	1.143	1.032	1.160
85% CO - 15% CO_2	1.074	1.014	1.217	1.136	0.656	0.751
80% CO - 20% H_2	1.540	1.721	1.953	2.051	0.929	1.067
60% CO - 40% H_2	1.205	1.179	0.978	1.008	0.976	0.999
80% CO - 20% H_2O	1.418	2.024	1.282	1.362	1.004	1.302
60% CO - 40% H_2O	0.953	1.170	0.854	0.850	0.985	1.424
99.8% CO - 0.2% H_2S	0.892	1.168	0.253	1.076	0.654	0.693
99.2% CO - 0.8% H_2S	0.972	1.064	0.818	1.020	1.487	0.442
99.8% CO - 0.20% NH_3	0.637	0.939	0.508	1.072	0.554	0.802
99.2% CO - 0.8% NH_3	0.855	1.226	0.486	1.363	0.610	0.950

5. Correlation Between Spalling and Strength Loss

Spalling signifies the existence of massive fracture networks in the regions where it occurs. The deeper the spalling zone in a material, the deeper the zone of fracture. Spalling can therefore be a visible indicator of strength degradation in a material. Unless a number can be placed on the degree of spalling, it can only be a qualitative guide to strength degradation. This is why a spalling index was developed for examination of these samples. Because spalling and strength loss are closely related, a relationship between the two should exist. If that relationship shows good correlation, strength degradation could be used as a measure of spalling damage. This is desired, as visual examination is difficult technique for precise reproduction of results.

Comparisons between the strength indexes and spalling indexes for the castables doped with metallic iron and the phosphate-bonded ramming mix doped with metallic iron and iron oxide are shown in Table IV and Figure 42. As seen in the figure, strength degradation and spalling damage follow similar trends. The least squares line has a slope of 1.04, indicating extremely good correlation between the two methods of assessing disintegration damage. Ths intercept point of this line is also near the origin, at a strength index value of 0.042. Scatter tends to increase as the undamaged condition, i.e. the right side of the figure, is approached. This would indicate that other factors influencing the strength of the refractories lose their importance as CO disintegration damage increases, and that visible damage and

TABLE IV. STRENGTH AND SPALLING INDEXES FOR CASTABLES DOPED WITH Fe and 90+ WT.% ALUMINA PHOSPHATE-BONDED RAMMING MIX DOPED WITH Fe AND Fe_2O_3

90+ WT.% ALUMINA CASTABLE W/Fe		50+ WT.% ALUMINA CASTABLE W/Fe		90+ WT.% ALUMINA PHOSPHAST-BONDED RAMMING MIX W/Fe		W/Fe_2O_3	
Strength	Spalling	Strength	Spalling	Strength	Spalling	Strength	Spalling
.336	.362	.197	.238	.554	.641	.442	.422
.637	.812	.253	----	.610	.641	.693	.609
.855	.875	.287	.391	.650	.938	.751	.859
.892	.844	.486	.469	.654	.891	.802	.953
.953	1.000	.508	.719	.656	.578	.855	1.000
.971	.906	.818	.546	.929	.953	.950	1.000
.972	.906	.854	1.000	.976	1.000	.999	1.000
1.074	.906	.997	1.000	.985	1.000	1.067	1.000
1.205	1.000	1.217	.984	1.004	1.000	1.160	.766
1.418	1.000	1.282	1.000	1.032	.844	1.302	1.000
1.540	.844	1.953	.984	1.487	.813	1.424	.984

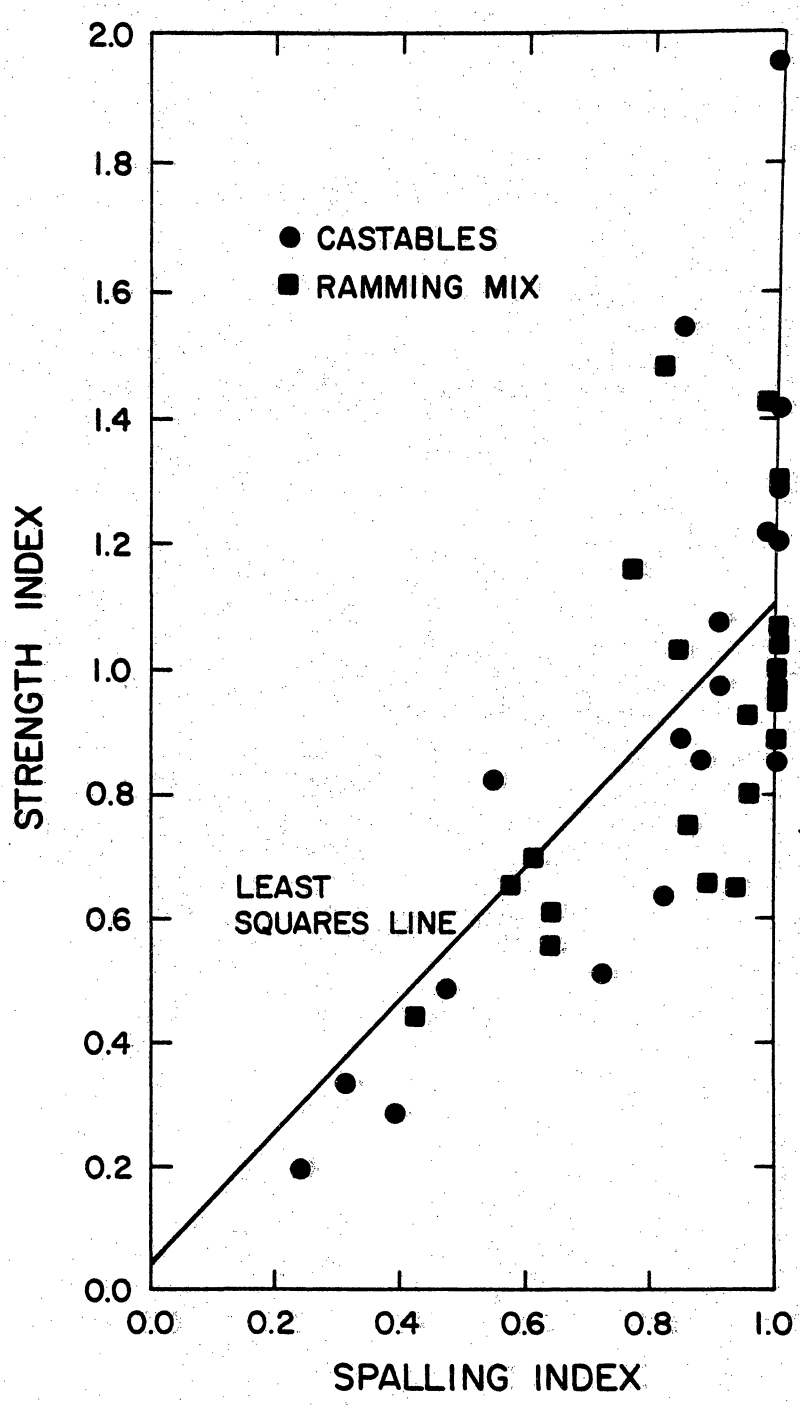

Figure 42. Comparison Between Strength Degradation and Spalling Damage.

strength degradation actually caused by CO disintegration correlate very well.

C. Effect of CO_2 on CO Disintegration

1. Background

Equilibrium conditions at 500°C are attained for the reaction:

$$2CO = CO_2 + C$$

when the ratio of CO to CO_2 is approximately 10^{-5}, as determined in Appendix III. The standard CO disintegration test, as shown in Table V, has a CO to CO_2 ratio that is over nine orders of magnitude larger than was calculated for equilibrium, producing a large driving force for CO decomposition. The addition of small amounts of CO_2 to the reaction gas significantly lowers the CO to CO_2 ratio, and should therefore reduce the driving force of carbon deposition. These ratios are still large in comparison to the equilibrium ratio of the gases, so carbon deposition should not be completely eliminated under either test atmosphere containing CO_2.

2. 90+ Wt.% Alumina Castable

Additions of both 5% and 15% CO_2 to the CO atmosphere were able to suppress CO disintegration in the 90+ wt.% alumina castable in a 100 hr. exposure. The metallic iron-doped refractory retained nearly all of its undoped strength after exposure to the 95% CO - 5% CO_2 gas mixture and was actually stronger than when undoped after exposure to

TABLE V. CO TO CO_2 RATIOS FOR TEST GASES

Gas Composition	CO to CO_2 Ratio	Ratio/Equil. Ratio
Equilibrium	8.22×10^{-6}	
99.99% CO	1.00×10^{4}	1.21×10^{9}
95% CO - 5% CO_2	1.90×10^{-1}	2.31×10^{6}
85% CO - 15% CO_2	5.67×10^{0}	6.90×10^{5}

85% CO - 15% CO_2. This is in sharp contrast to the strength behavior of the castable following exposure to CO only, as shown in Figure 43. When doped with iron oxide, the strength of the castable was not degraded by CO or either of the CO-CO_2 mixtures.

These results suggest that the potential for refractory damage by CO disintegration will decrease as both the amount of CO in the atmosphere and the CO to CO_2 ratio are reduced. This is not to say that CO disintegration will not occur. The experiments with only CO show that disintegration will occur, and in the presence of as little as 0.5 wt.% iron. The experiments with CO-CO_2 mixtures show that the time required to cause disintegration is prolonged by reducing the CO content and CO to CO_2 ratio in the atmosphere. Disintegration is prolonged further if the iron impurities are present in the form of Fe_2O_3 rather than pure Fe, as no disintegration damage is caused even under pure CO, although reduction of the Fe_2O_3 to Fe_3O_4 does occur.

3. 50+ Wt.% Alumina Castable

Addition of 50% CO_2 to the CO resulted in almost no change in the amount of CO disintegration damage that occurred in the 50+ wt.% alumina castable, however, in the exposure to 85% CO-15% CO_2, disintegration damage was totally suppressed. As shown in Figure 44, the strength index of the metallic-iron doped refractory increased only slightly from the CO to the 95% CO-5% CO_2 exposure, whereas it surpassed the strength level of the undoped refractory (1.0 on the scale) under the 85% CO-15% CO_2 atmosphere. It is interesting that reducing

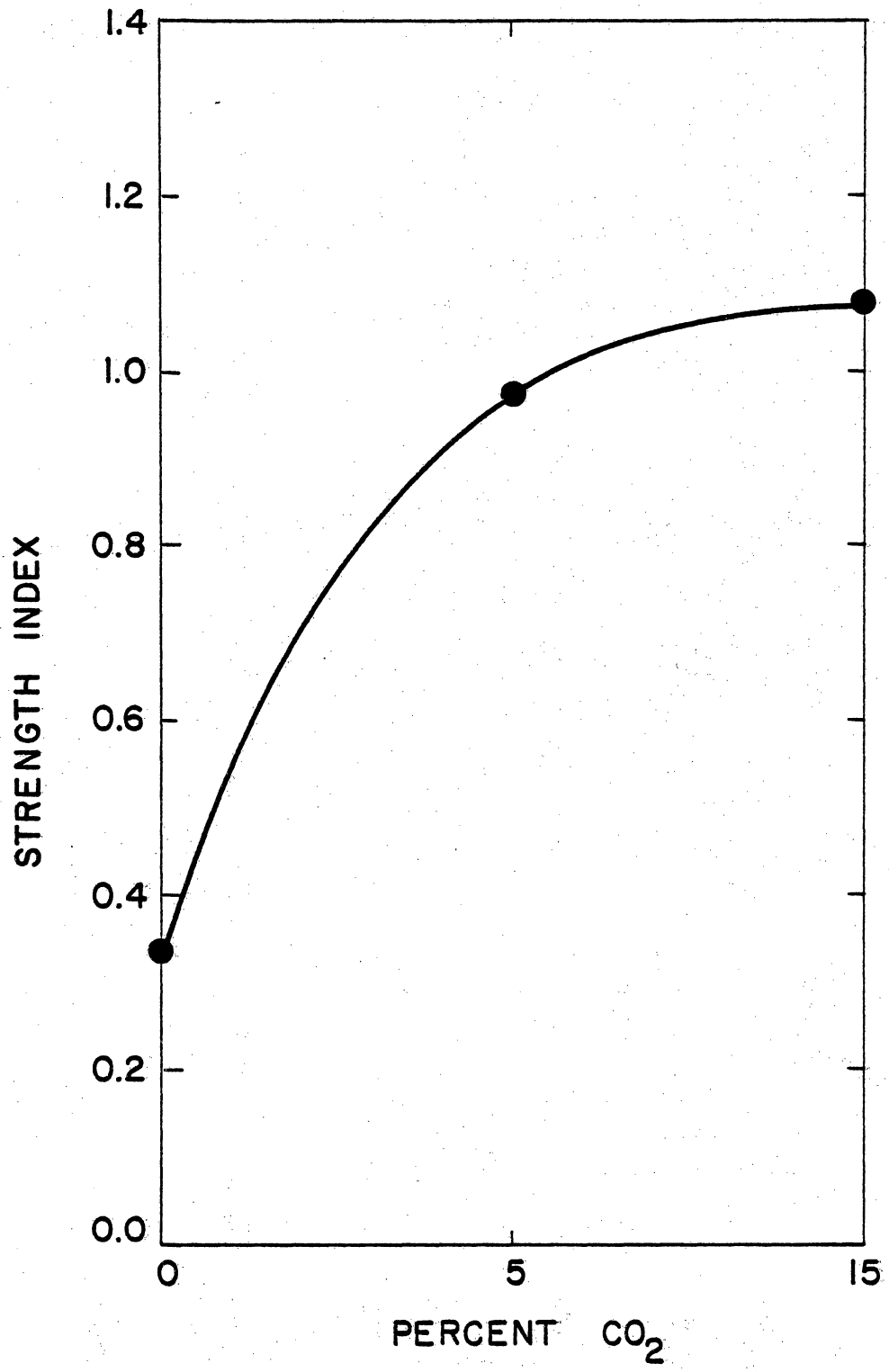

Figure 43. Effect of CO_2 on Strength of Fe-doped 90+ Wt.% Alumina Castable.

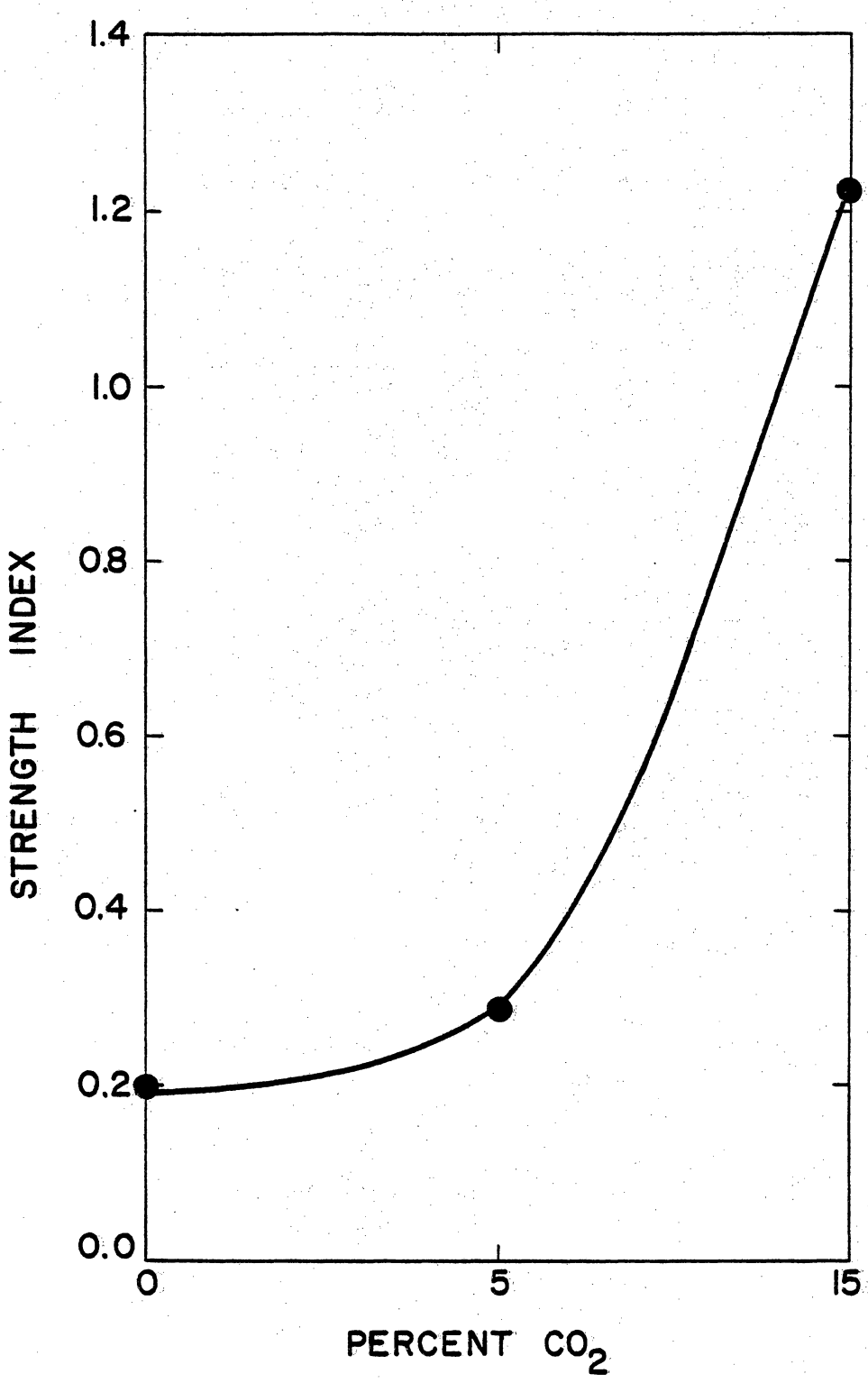

Figure 44. Effect of CO_2 on Strength of Fe-doped 50+ Wt.% Alumina Castable.

CO to CO_2 ratio by nearly three orders of magnitude (from CO to 95% CO-5% CO_2) produced only a small decrease in CO disintegration damage, whereas a further reduction of less than one order of magnitude in the ratio (from 95% CO-15% CO_2) suppressed disintegration. It is possible that the second change in the CO to CO_2 ratio was just enough to suppress formation of the iron carbide catalyst. As with the 90+ wt.% alumina castable, there was no CO disintegration damage in iron oxide-doped samples of the 50+ wt.% alumina castable in exposures to CO or to either CO-CO_2 gas mixture.

4. 90+ Wt.% Alumina Phosphate-Bonded Ramming Mix

Progressive decreasing of the CO to CO_2 ratio does not appear to reduce CO disintegration in the phosphate-bonded refractory. As shown in Figure 45, addition of 5% CO_2 to CO raised the strength index of the metallic iron-doped ramming mix above 1.0, suppressing the effects of CO disintegration. The addition of 15% CO_2 to CO, however, resulted in a strength index nearly the same as for pure CO.

This same type of behavior was observed for iron oxide-doped samples of the ramming mix, as shown in Figure 46. The suppression of spalling damage at the 5% level of CO_2 and the return of that damage at the 15% CO_2 level indicates that the phosphates in the ramming mix may be reacting with the CO_2 as well as CO at the higher CO_2 concentration. Further reductions in the CO to CO_2 ratio, as found in gasifier atmospheres, may again suppress CO disintegration. Also, if CO_2 concentrations may be low enough that disintegration will be suppressed. Ex-

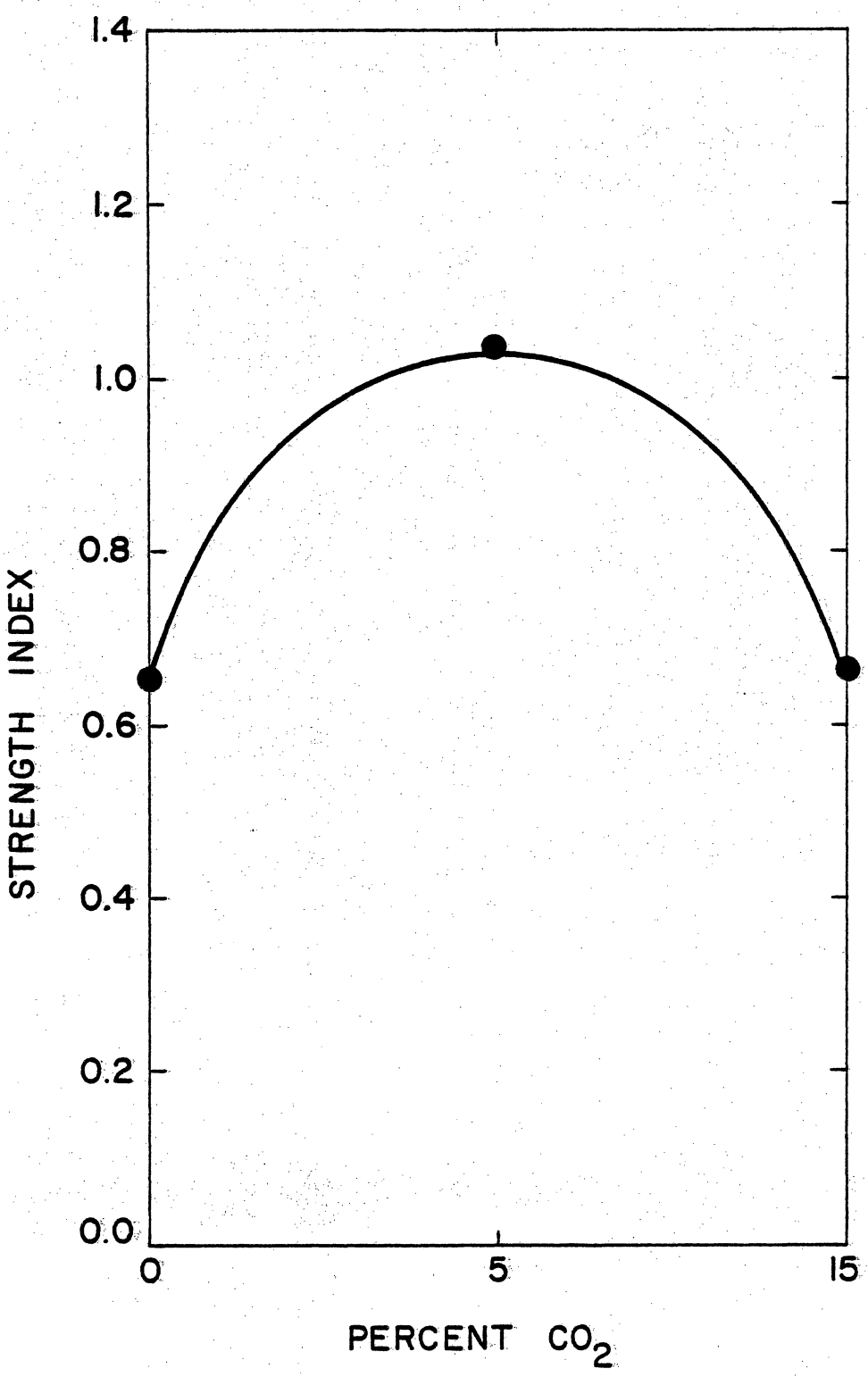

Figure 45. Effect of CO_2 on Strength of Fe-doped 90+ Wt.% Alumina Ramming Mix.

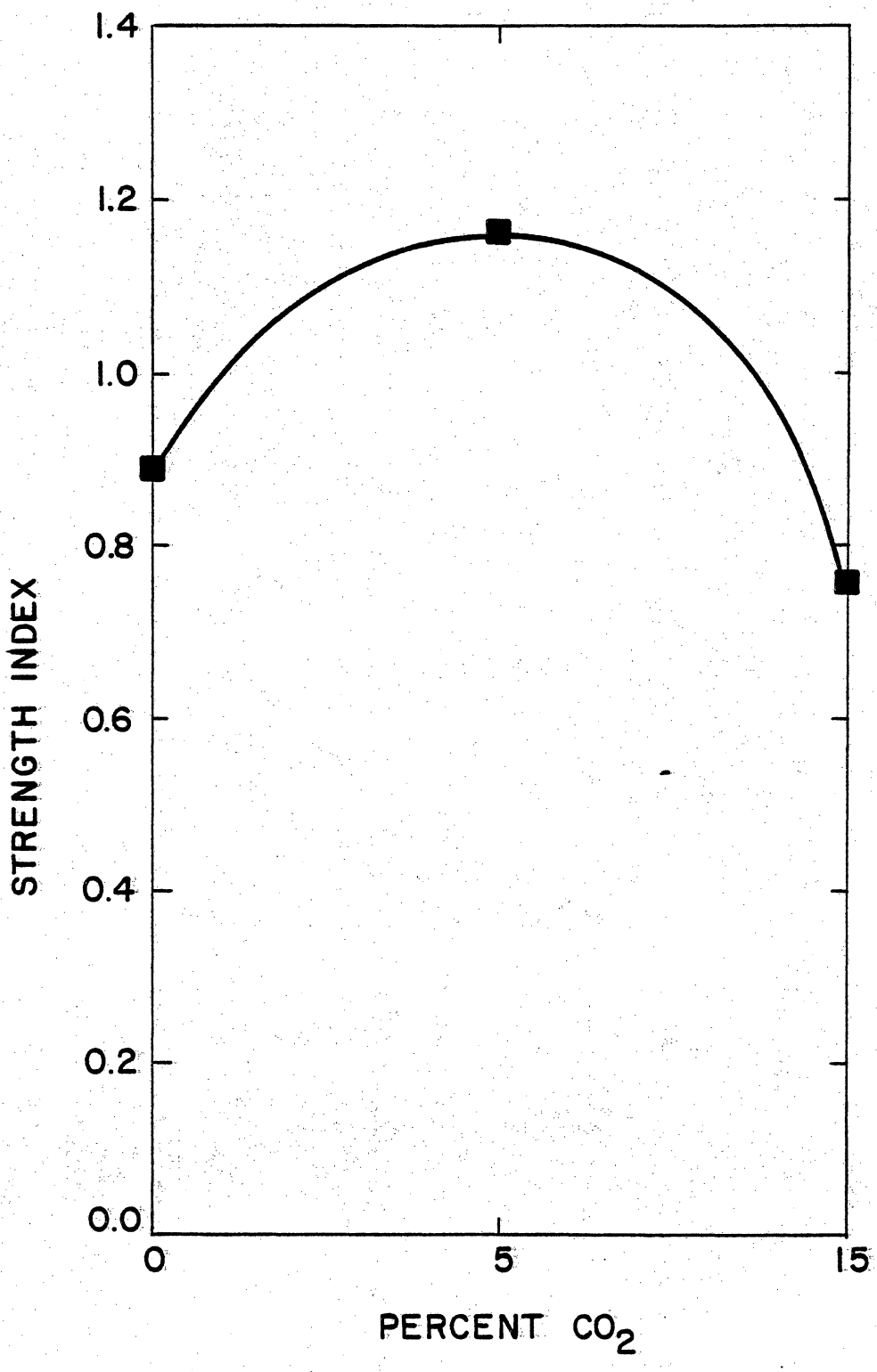

Figure 46. Effect of CO_2 on Strength of Fe_2O_3-doped 90+ Wt.% Alumina Ramming Mix.

posures to DOE gasifier atmospheres should provide answers to this problem.

D. Effect of NH_3 on CO Disintegration

1. Background

Berry, Ames, and Snow[9] observed that small amounts of NH_3 negated the effects of the iron carbide catalyst for CO decomposition. Based on this observation, the addition of 0.2% and 0.8% NH_3 to CO should produce some enhancement of strength indexes of the three refractories.

2. 90+ Wt.% Alumina Castable

Additions of 0.2% and 0.8% NH_3 to CO produced progressive suppression of CO disintegration in the 90+ wt.% alumina castable. A steady increase in the strength index of the metallic iron-doped refractory was observed as the refractory was exposed to increasing amounts of NH_3, as shown in Figure 47, however, CO disintegration was not fully suppressed. The strength index would have to be raised to approximately a level of one on the scale for this to occur.

No CO disintegration was observed in the iron oxide-doped castable in exposures to CO or CO_2 and either amount of NH_3, however, the strength index of the iron oxide-doped material fell significantly below 1.0 for exposure to 99.8 CO-0.2 NH_3, as shown in Table III. Examination of Table X of Appendix 1 shows that this drop of strength index is caused primarily by samples of the refractory doped with 0.5 Fe wt.%

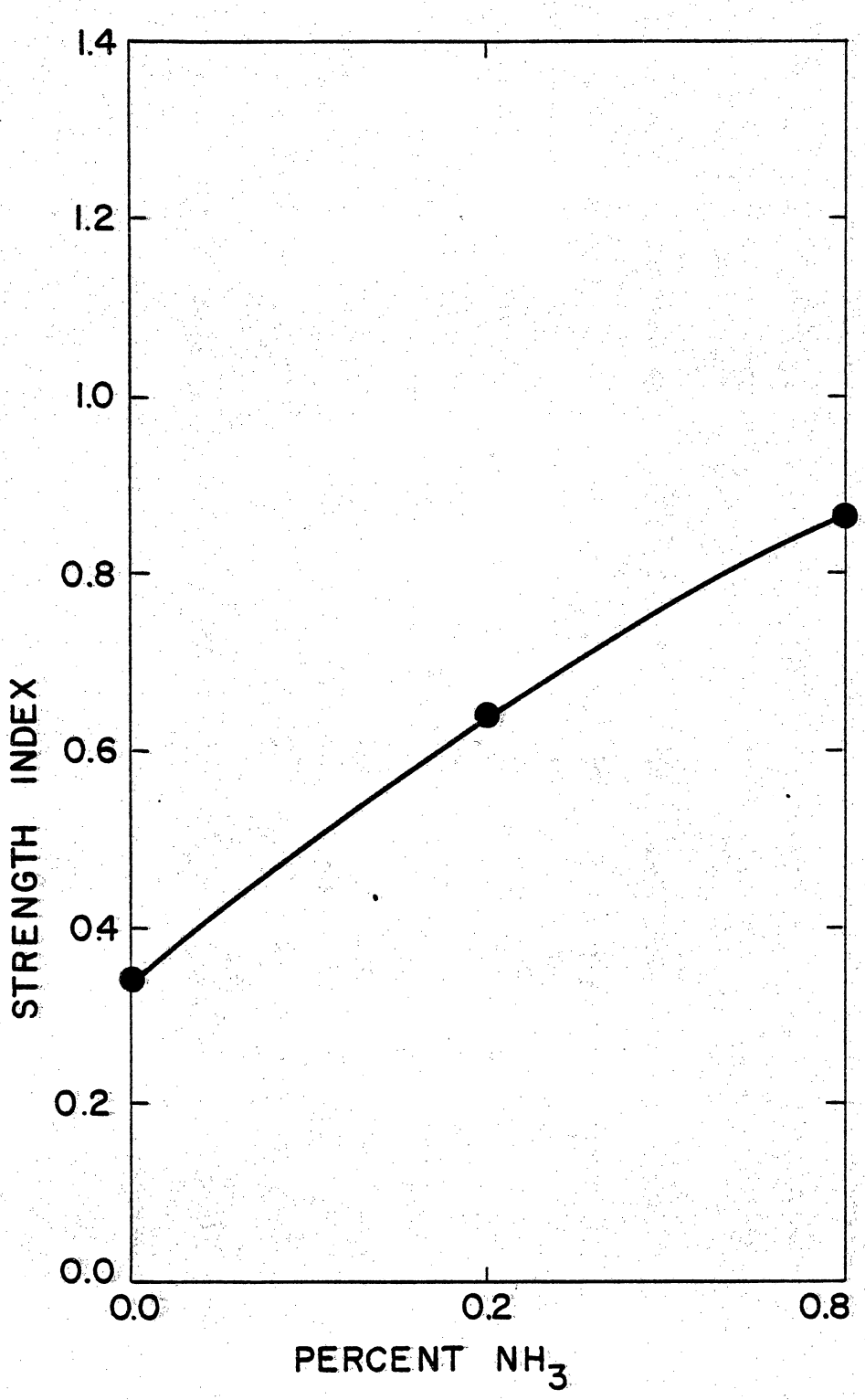

Figure 47. Effect on NH_3 on Strength of Fe-doped 90+ Wt.% Alumina Castable.

iron oxide. There is no apparent spalling of any of these samples, so CO disintegration is not likely to be responsible for the strength decrease that was observed.

3. 50+ Wt.% Alumina Castable

Adding 0.2% NH_3 to CO caused limited improvement in the resistance of the 50+ wt.% alumina castable to CO disintegration. Adding 0.8% NH_3 did not further improve the CO disintegration resistance of the refractory. The strength index of the metallic iron-doped castable increased from 0.19, when exposed to CO, to 0.51 when exposed to 99.8 CO - 0.2 NH_3, as shown in Figure 48. Exposure to the 99.2 CO-0.8 NH_3 gas generated a strength index of 0.49. There was no CO disintegration in iron oxide-doped samples of the refractory under exposures to the gases containing NH_3.

4. 90+ Wt.% Alumina Phosphate-Bonded Ramming Mix

The presence of NH_3 in CO does not retard CO disintegration of the phosphate-bonded refractory. As shown in Figure 49, there was essentially no change in the strength index of the metallic iron-doped ramming mix when either 0.2% or 0.8% NH_3 was added to CO. In the case of the iron oxide-doped ramming mix, 0.8% NH_3 did raise the strength index to nearly 1.0, shown in Figure 50, however, at long exposure times the behavior of the metallic iron-doped refractory will be dominant.

E. Effect of H_2 on CO Disintegration

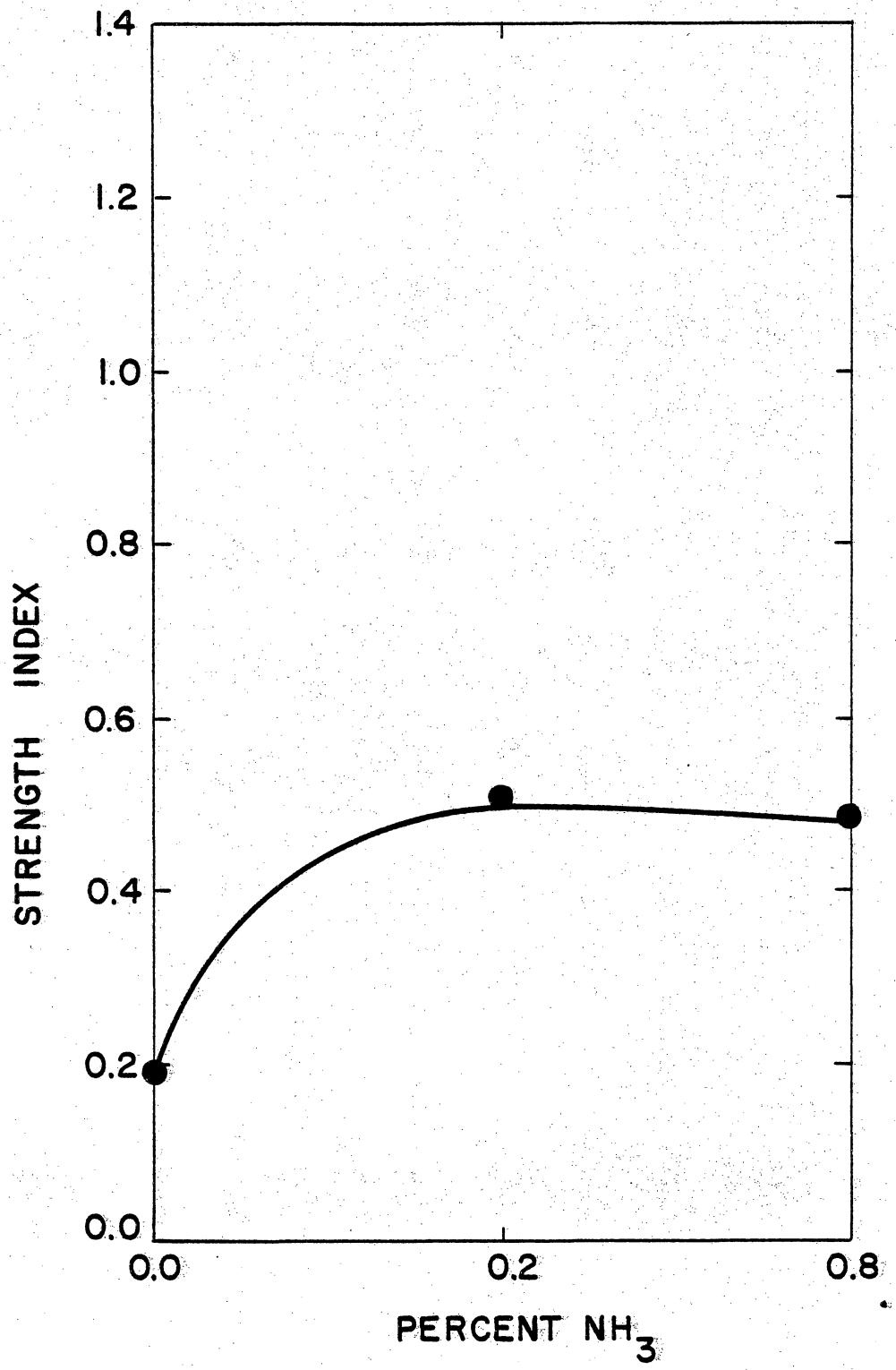

Figure 48. Effect of NH_3 on Strength of Fe-doped 50+ Wt.% Alumina Castable.

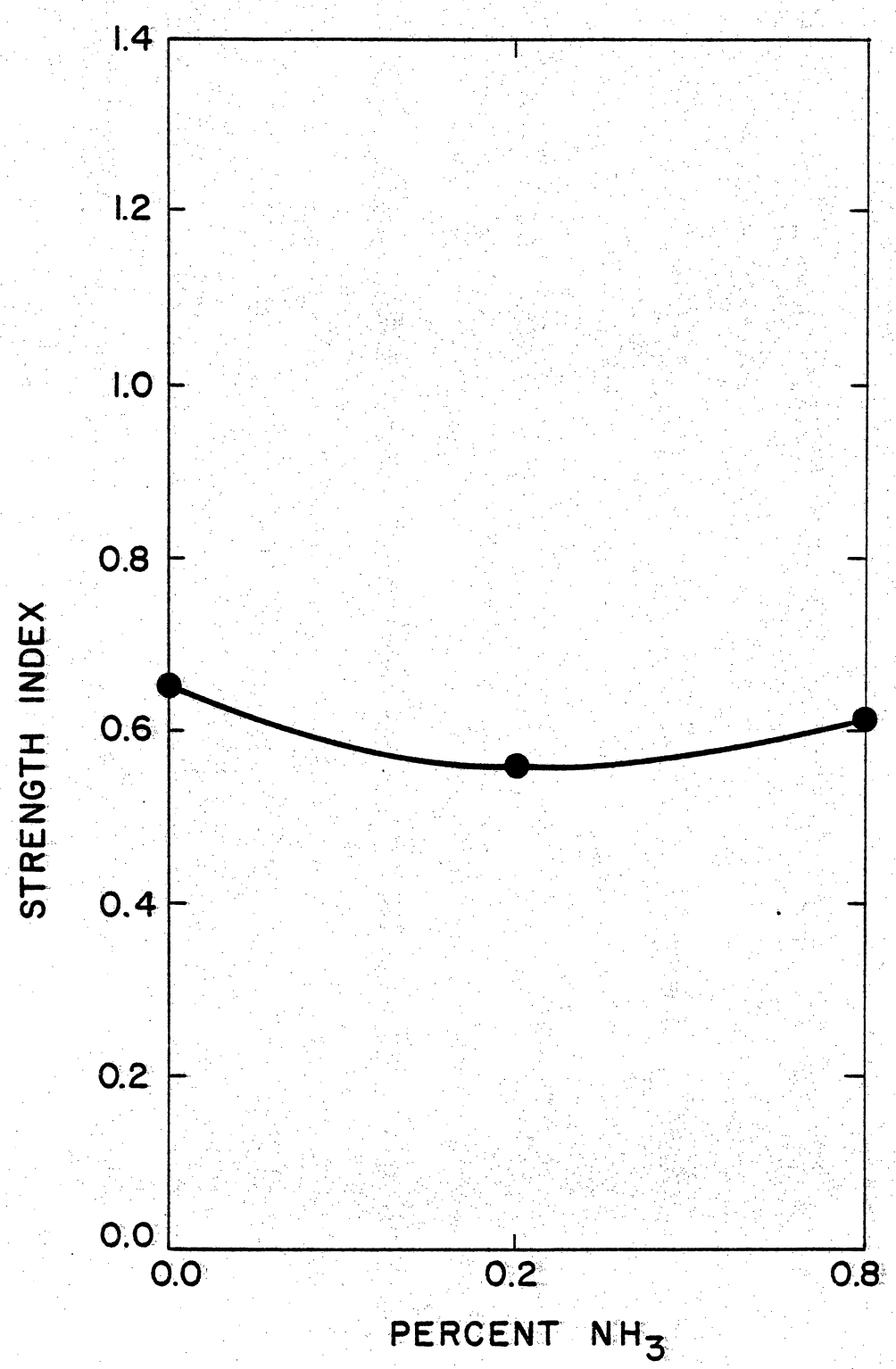

Figure 49. Effect of NH_3 on Strength of Fe-doped 90+ Wt.% Alumina Ramming Mix

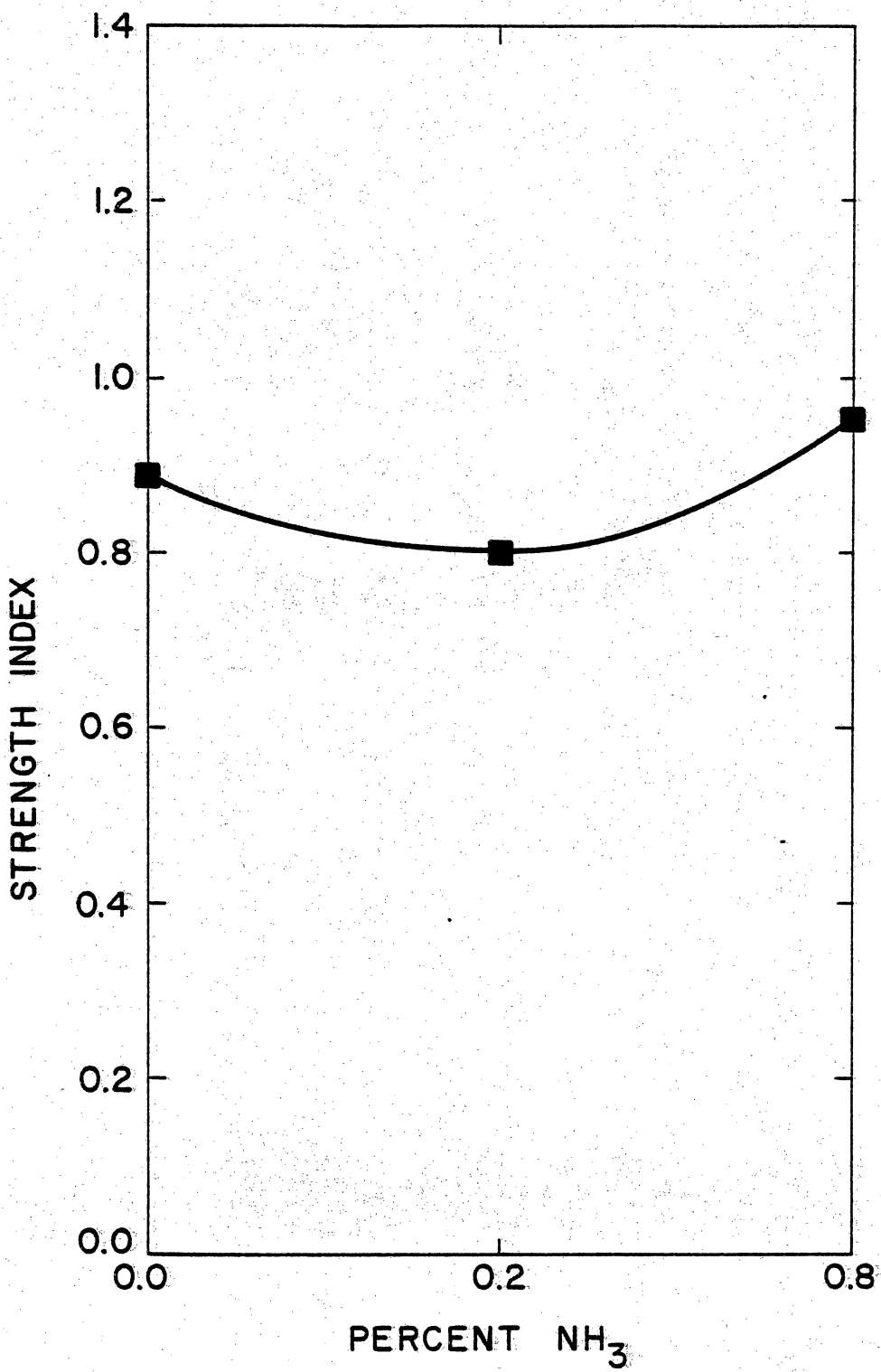

Figure 50. Effect of NH_3 on Strength of Fe_2O_3-doped 90+ Wt.% Alumina Ramming Mix

1. Background

Berry, Ames, and Snow[9] included an analysis of the effects of H_2 in their 1956 study of CO decomposition. This analysis showed that carbon deposition was greater for a test gas containing 4% H_2 than for one containing only CO.

2. 90+ Wt.% Alumina Castable

The addition of 20% H_2 caused suppression of CO disintegration damage in the 90+ wt.% alumina castable at all but the 2.0 wt.% level of metallic iron dopant. Even though three of the four samples at this level had heavy visible spalling, they retained over 90% of this strength of the undoped refractory. Overall, the metallic iron-doped samples exhibited an increase over the undoped strength of more than 50%, as shown in Figure 51. With a 40% H_2 atmosphere, disintegration was suppressed at all levels of metallic iron doping, and, the strength index was still significantly greater than the undoped strength level of 1.0. Iron oxide-doped samples showed no signs of disintegration and were also stronger than the undoped castable.

The suppression of CO disintegration of H_2 is directly opposite of the effect shown by Berry, Ames, and Snow[9]. The reason for this disagreement must be due to the reduced CO content of the atmosphere. This explanation agrees with results obtained for the tests with CO and CO_2. The tests with H_2 show that simply reducing the CO content of the atmosphere and not just the CO/CO_2 ratio greatly retard the onset of disintegration in the 90+ wt.% alumina castable. In addition, the H_2

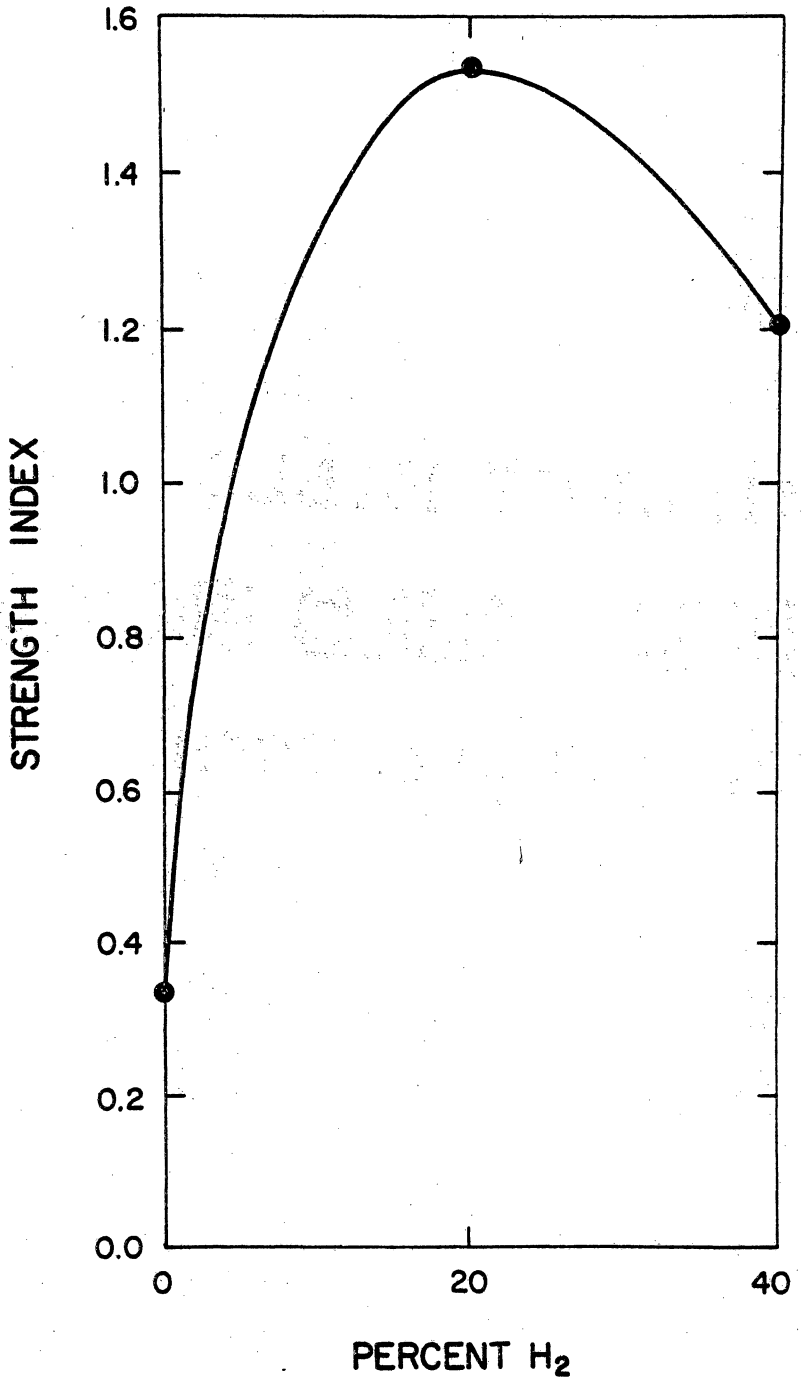

Figure 51. Effect of H_2 on Strength of Fe-doped 90+ Wt.% Alumina castable.

appears to significantly increase the strength of the doped refractory. Strength of the undoped refractory was essentially unchanged.

3. 50+ Wt.% Alumina Castable

As with the 90+ wt.% alumina castable, H_2 suppressed CO disintegration in the 50+ wt.% alumina. No signs of CO disintegration were observed for the metallic iron or iron oxide-doped 50+ wt.% alumina castable in exposures to either H_2-containing test gas. The strength index of the Fe-doped refractory rose to nearly twice the undoped strength level for the 80% CO - 20% H_2 atmosphere, as shown in Figure 52, and then returned to nearly the same as the undoped strength for the 60% CO - 40% H_2 atmosphere. In both cases, the strength index of the iron oxide-doped refractory was within 0.10 of the metallic iron-doped strength index. As with the 90+ wt.% alumina castable, strength of the undoped refractory did not appear to be affected.

4. 90+ Wt.% Alumina Phosphate-Bonded Ramming Mix

CO disintegration was also suppressed in the 90+ wt.% alumina phosphate-bonded ramming mix by H_2. Additions of 20% and 40% H_2 to the atmosphere resulted in strength indexes of over 90% of the undoped strength level of the metallic iron-doped refractory, as shown in Figure 53. The strength index of the iron oxide-doped refractory was at least as great as the undoped level, as shown in Figure 54. Unlike for the castable compositions, the strength of the ramming mix containing iron impurities was not raised significantly above its undoped

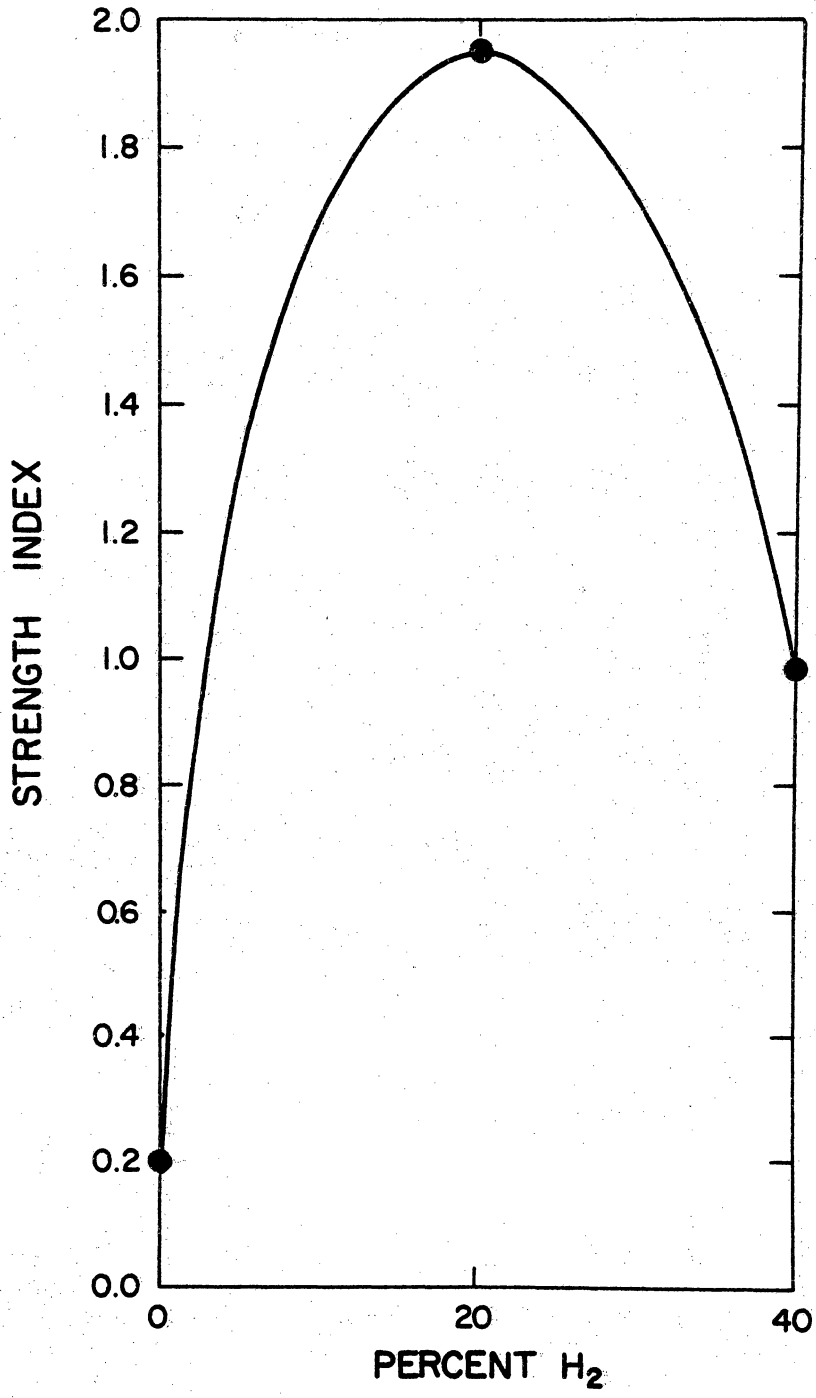

Figure 52. Effect of H_2 on Strength of Fe-doped 50+ Wt.% Alumina Castable.

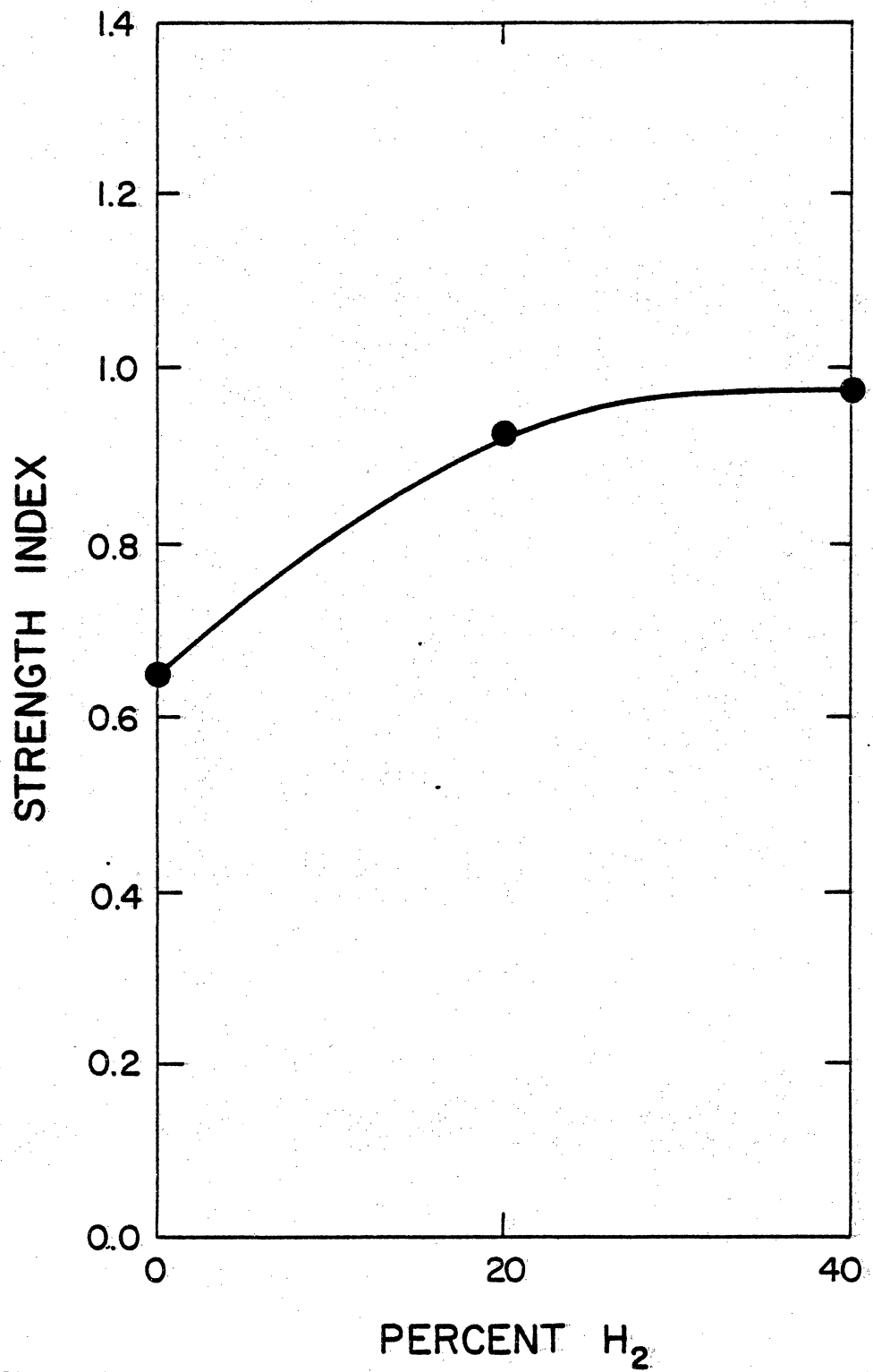

Figure 53. Effect of H_2 on Strength of Fe-doped 90+ Wt.% Alumina Ramming Mix.

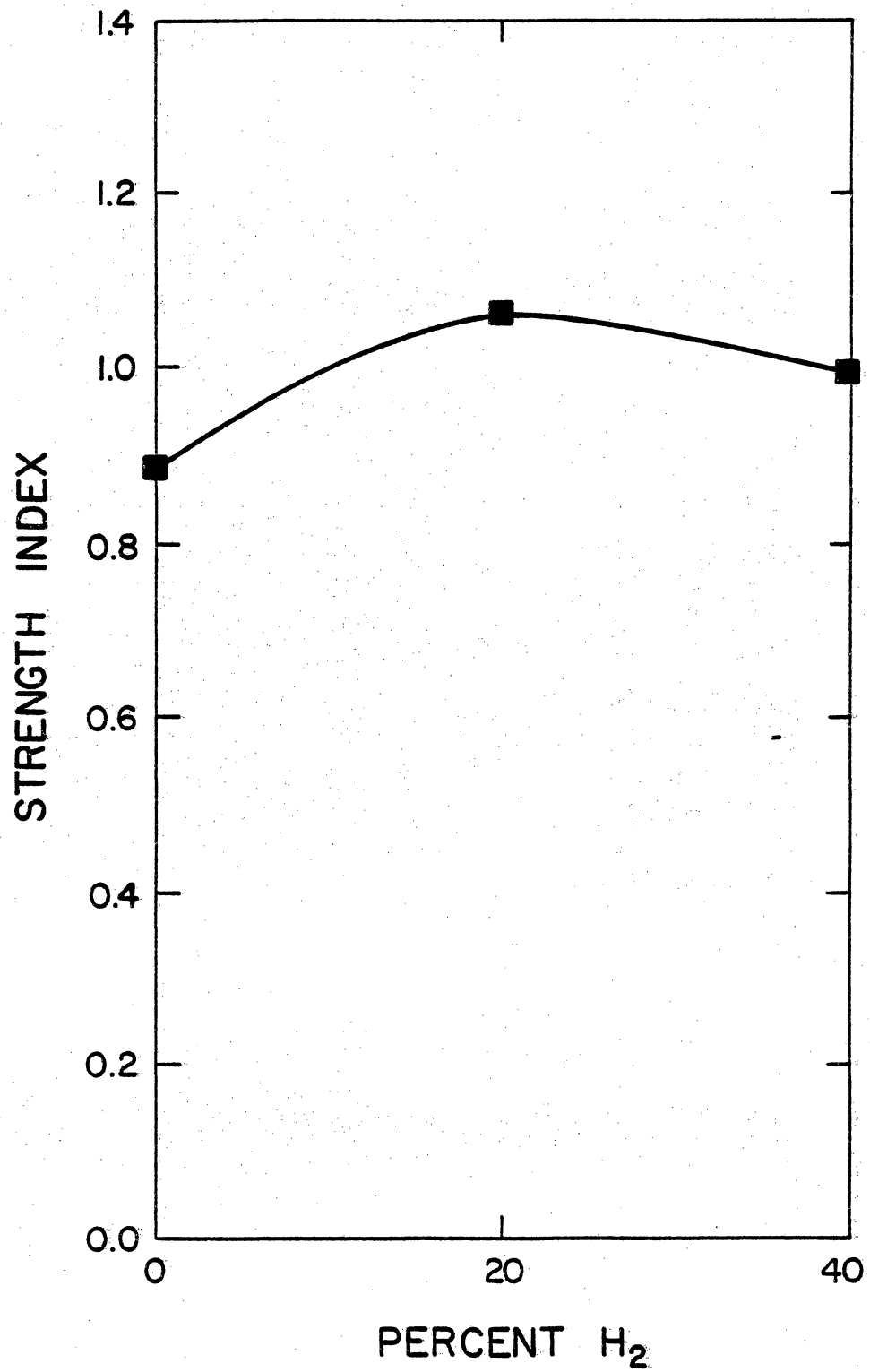

Figure 54. Effect of H_2 on Strength of Fe_2O_3-doped 90+ Wt.% Alumina Ramming Mix.

strength under the influence of H_2.

F. Effect of H_2S on CO Disintegration

1. Background

Schneck[4] reported that the introduction of 0.7% H_2S to blast furnace atmospheres tended to suppress CO disintegration of the fireclay brick linings. Kappmeyer and Hubble[44], and Berry, Ames, and Snow[9] observed that both gaseous and solid forms of sulfur retarded CO decomposition.

2. 90+ Wt.% Alumina Castable

The presence of as little as 0.2% H_2S in the atmosphere appears to significantly retard CO disintegration in the 90+ wt.% alumina castable. The strength index of the metallic iron-doped refractory rose to nearly 90% of the undoped refractory strength with 0.2% H_2S as shown in Figure 55, and to over 95% of the undoped strength with 0.8% H_2S. The iron oxide-doped refractory appeared unaffected by CO disintegration when exposed to the H_2S containing atmospheres and was stronger than the undoped refractory.

3. 50+ Wt.% Alumina Castable

The suppression of CO disintegration by H_2S was not as great for the 50+ wt.% alumina castable as it was for the 90+ wt.% alumina castable. The addition of 0.2% H_2S had little affect on the strength index of the refractory, as shown in Figure 56. When 0.8% H_2S was in the

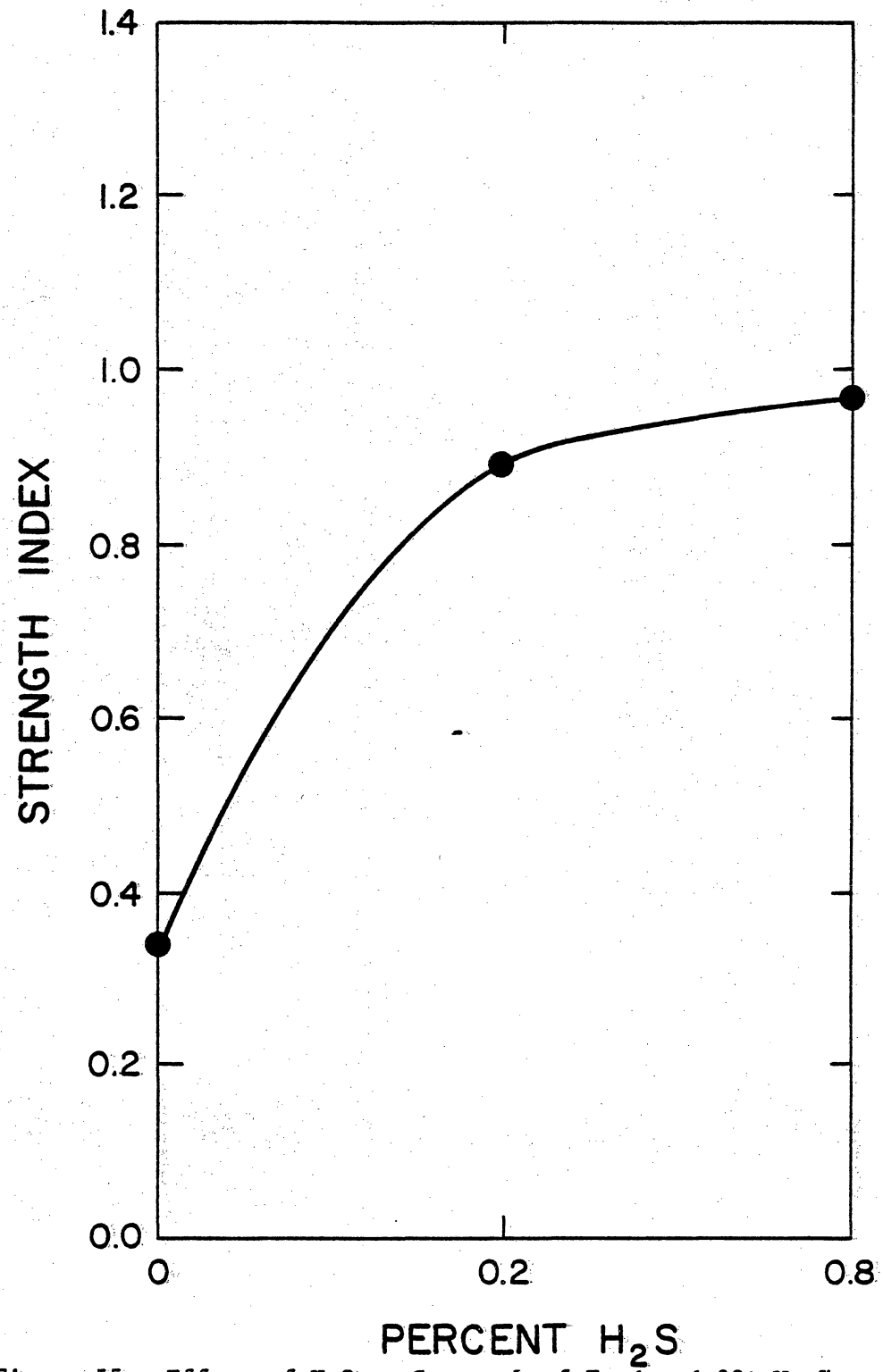

Figure 55. Effect of H_2S on Strength of Fe-doped 90+ Wt.% Alumina Castable.

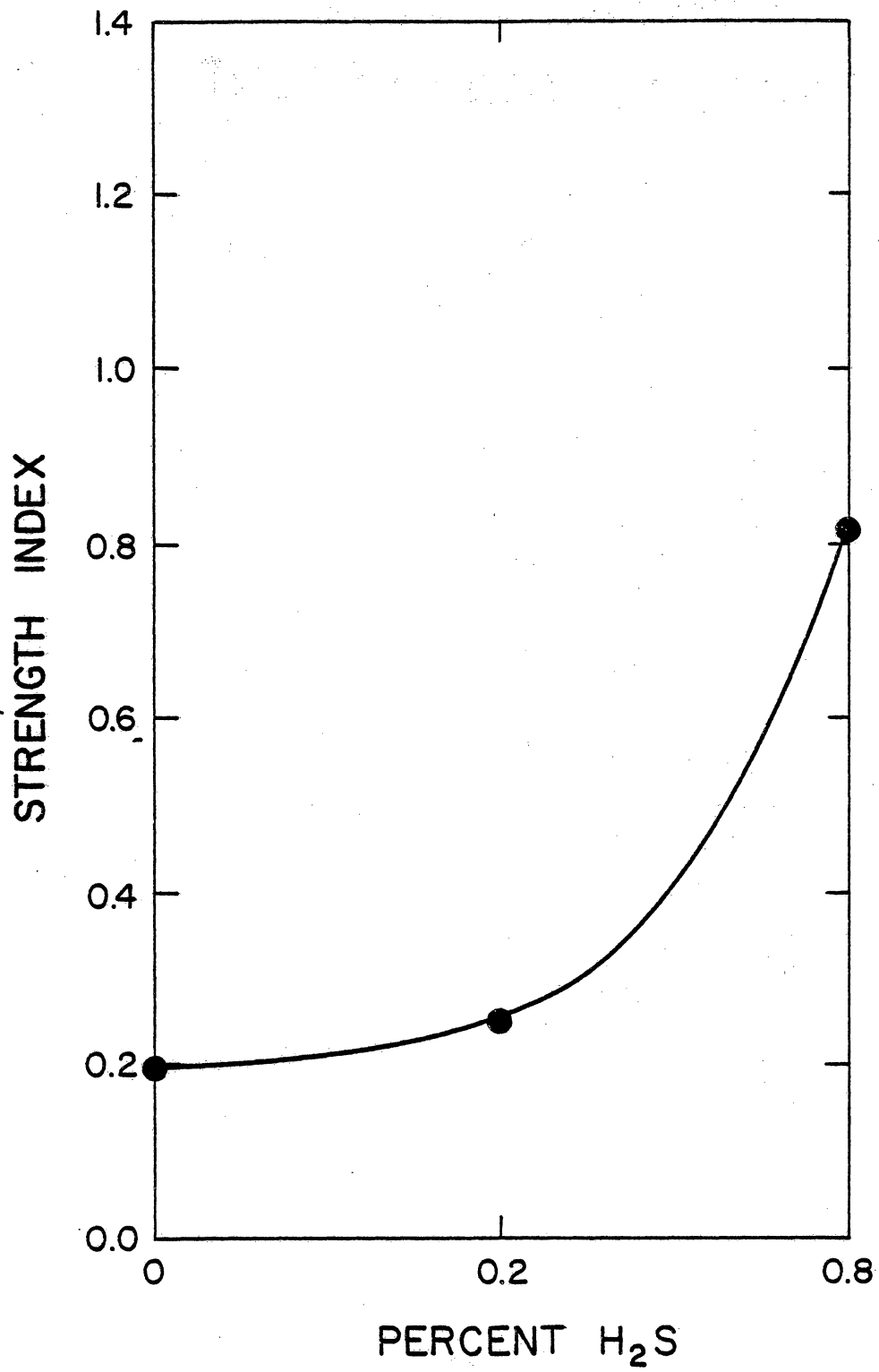

Figure 56. Effect of H_2S on Strength of Fe-doped 50+ Wt.% Alumina Castable.

test gas, the strength index rose to a little over 80% of the undoped strength of the castable. Again, the iron-doped refractory was undamaged by CO, although reduction of the iron oxide was taking place.

4. 90+ Wt.% Alumina Phosphate-Bonded Ramming Mix

The addition of 0.8% H_2S to CO suppressed disintegration in the metallic iron-doped 90+ wt.% alumina phosphate-bonded ramming mix and raised its strength index almost 50% above the undoped strength level. No suppression of disintegration damage occurred when the atmosphere contained 0.2% H_2S, as shown in Figure 57.

When the phosphate-bOnded refractory was doped with iron oxide, degradation of the refractory increased rather than decreased as H_2S was added to the atmosphere. This effect is shown in Figure 58.

The difference between the effects of H_2S on the metallic iron and iron oxide-doped ramming mix could be linked to the way in which phosphorus appears to attach itself to the iron. As shown earlier in the discussion, iron phosphide (Fe_2P, Fe_3P) tended to form with the metallic iron dopant, whereas, an iron phosphate ($Fe_3(PO_4)_2$) may have been formed with the iron oxide dopant. The iron oxide may also have simply reduced to a lower oxidation state, which tended to decompose to a carbide faster in the combined presence of H_2S and phosphorus.

G. Effect of H_2O on CO Disintegration

1. Background

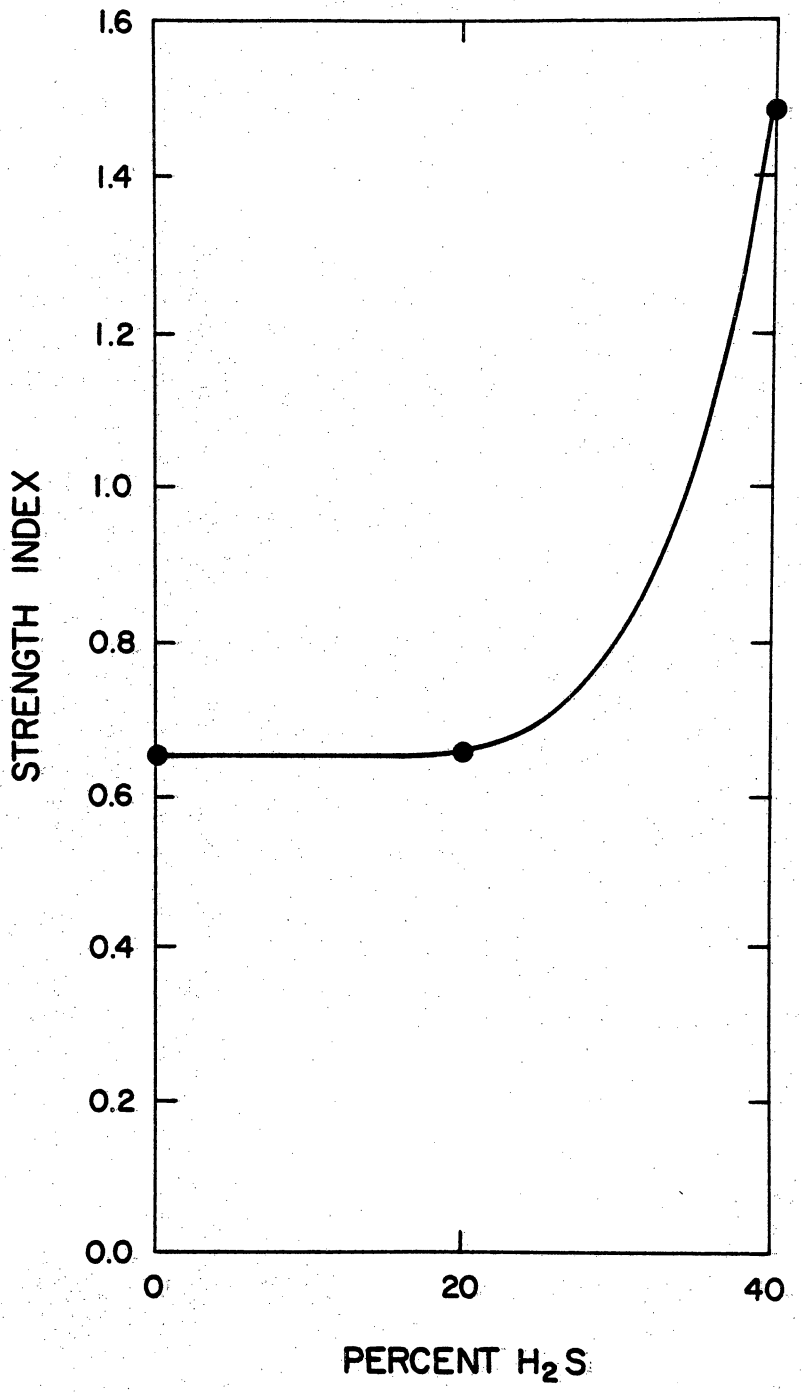

Figure 57. Effect of H_2S on Strength of Fe-doped 90+ Wt.% Alumina Ramming Mix.

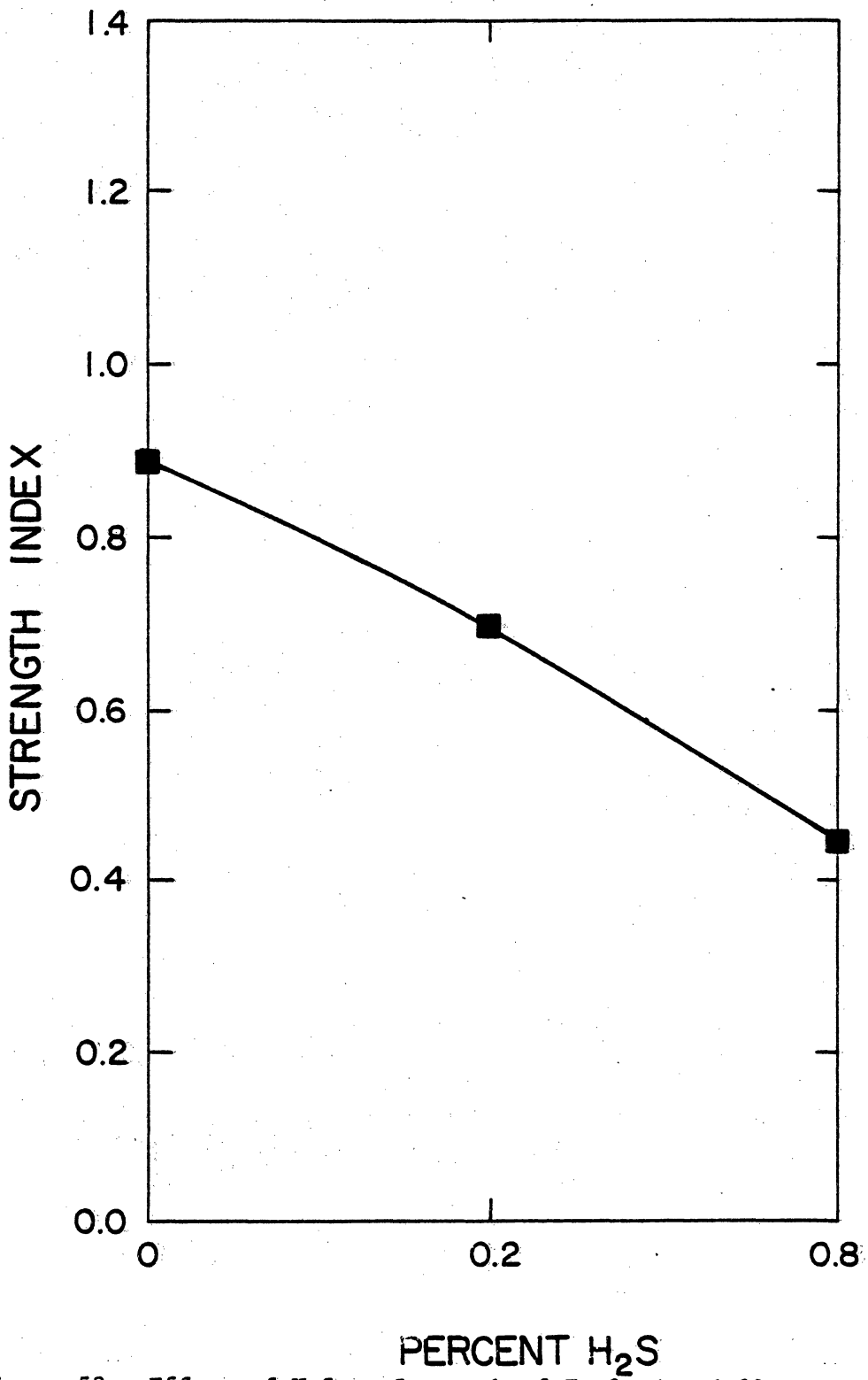

Figure 58. Effect of H_2S on Strength of Fe_2O_3-doped 90+ Wt.% Alumina Ramming Mix.

Like H_2, H_2O was found by Berry, Ames, and Snow[9] to accelerate CO decomposition. A gas containing 3% H_2O deposited more carbon on an iron carbide catalyst than one containing only CO.

2. 90+ Wt.% Alumina Castable

CO disintegration was significantly retarded in the 90+ wt.% alumina castable when it was exposed to the 20% and 40% H_2O atmospheres. As shown in Figure 59, the metallic iron-doped refractory retained over 90% of its undoped strength in the 40% H_2O exposure and was more than 40% stronger than when undoped in the 20% H_2O exposure. Strength of the iron oxide-doped refractory was enhanced to twice the undoped strength by exposure to the 20% H_2O atmosphere, as noted in Table III.

The effect of H_2O in these tests closely parallels the effect of H_2. As with H_2, H_2O was expected to accelerate CO disintegration. Reducing the CO concentration to 80% or less of the atmosphere appears to offset these accelerating effects.

3. 50+ Wt.% Alumina Castable

The effect of H_2O on the 50+ wt.% alumina castable is similar to its effect on the 90+ wt.% alumina castable. The strength index of the metallic iron-doped castable rises to more than 120% of its undoped strength with 20% H_2O in the atmosphere, as shown in Figure 60, then drops to 85% of the undoped strength with 40% H_2O. Strength of the iron oxide-doped refractory was nearly the same as for the metallic iron-doped refractory in each H_2O-containing atmosphere, as shown in

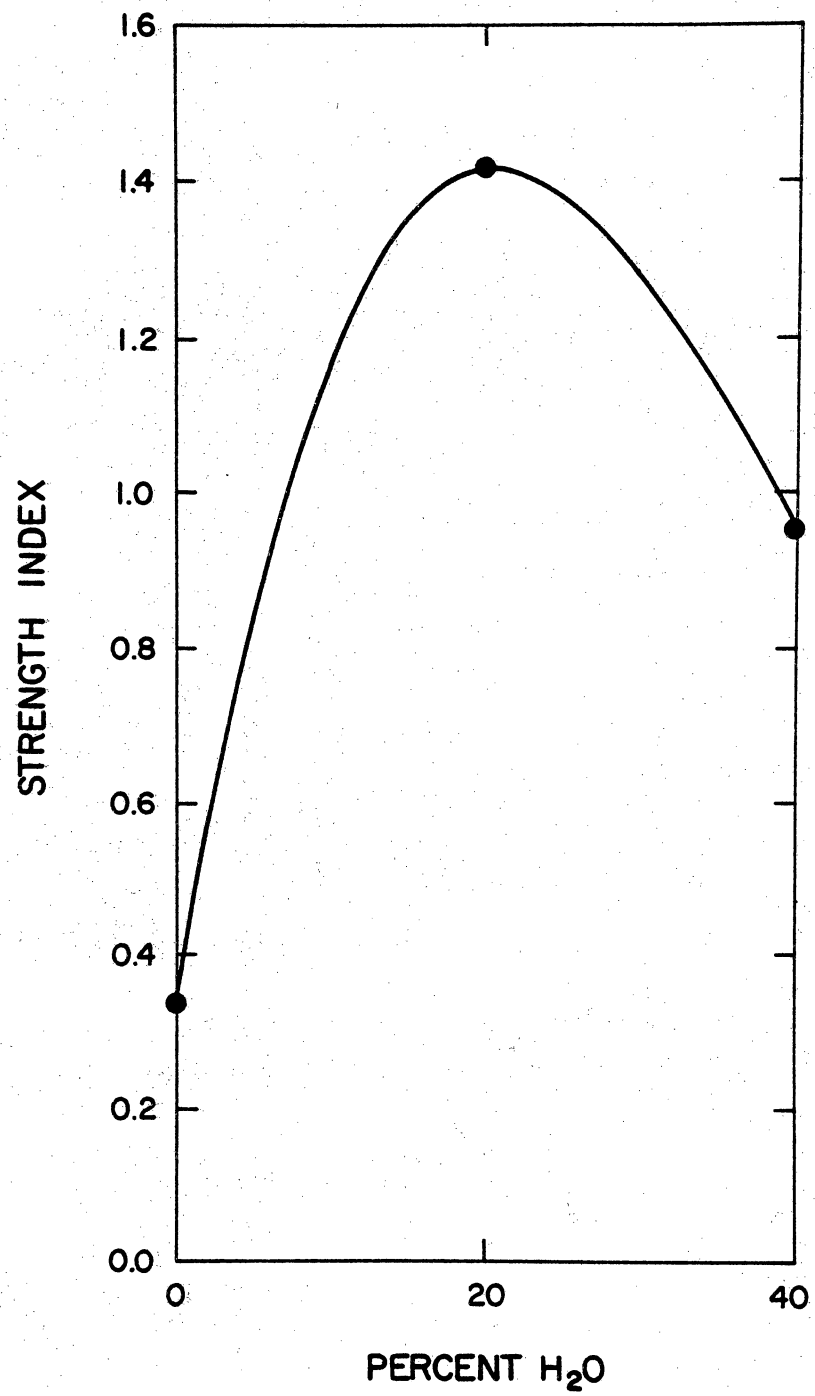

Figure 59. Effect of H_2O on Strength of Fe-doped 90+ Wt.% Alumina Castable.

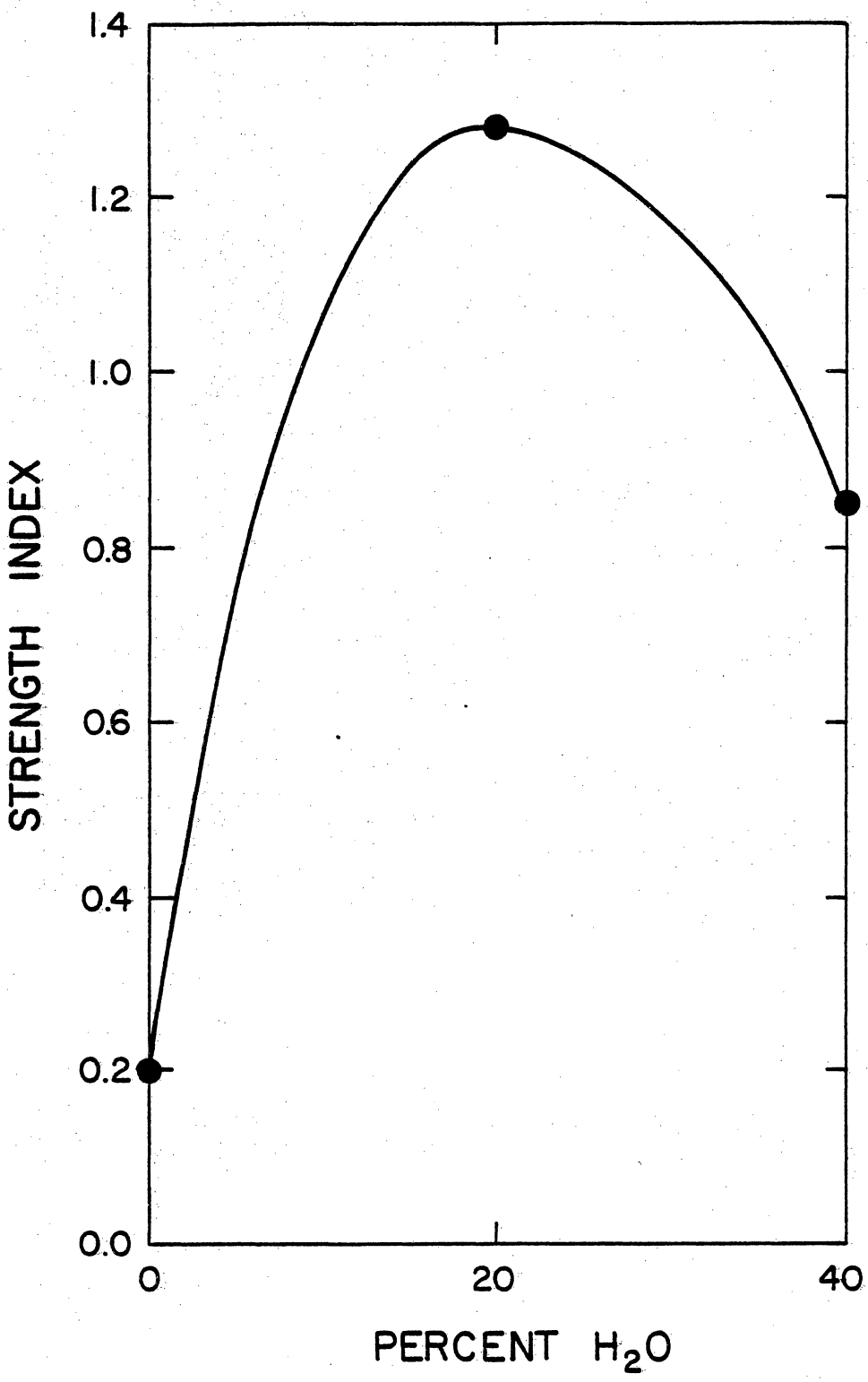

Figure 60. Effect of H_2O on Strength of Fe-doped 50+ Wt.% Alumina Castable.

Table III.

4. 90+ Wt.% Alumina Phosphate-Bonded Ramming Mix

CO disintegration was suppressed by both H_2O atmospheres in the 90+ wt.% alumina phosphate-bonded refractory as well as in the castables. The strength of the metallic iron-doped ramming mix was nearly the same as its undoped strength for both the 20% and 40% H_2O test gases, as shown in Figure 61. The iron oxide-doped refractory had even greater strength enhancement, as shown in Figure 62.

H. Comparison of Gas Effects

1. 90+ Wt.% Alumina Castable

H_2 and H_2O have similar effects on the 90+ wt.% alumina castable, as seen by comparing Figure 51 to Figure 59. The addition of 20% of either of these gases, separately, to CO appears to strengthen the metallic iron and iron oxide-doped castables considerably. Although heavy spalling occurred on samples doped with 2.0 wt.% Fe in the 20% H_2 atmosphere, samples doped with 1.0 wt.% and 1.5 wt.% Fe had the highest average strengths on record for this castable except when doped with Fe_2O_3. The extra strengthening effects of H_2 and H_2O disappear when they compose 40% of the atmosphere.

The effects of H_2S and NH_3 are generally similar. As more of each gas is added, there is less disintegration damage. H_2S is more effective than NH_3, especially at the 0.2% level. CO_2 additions of 5% and 15% generate effects that appear almost the same as those plotted for

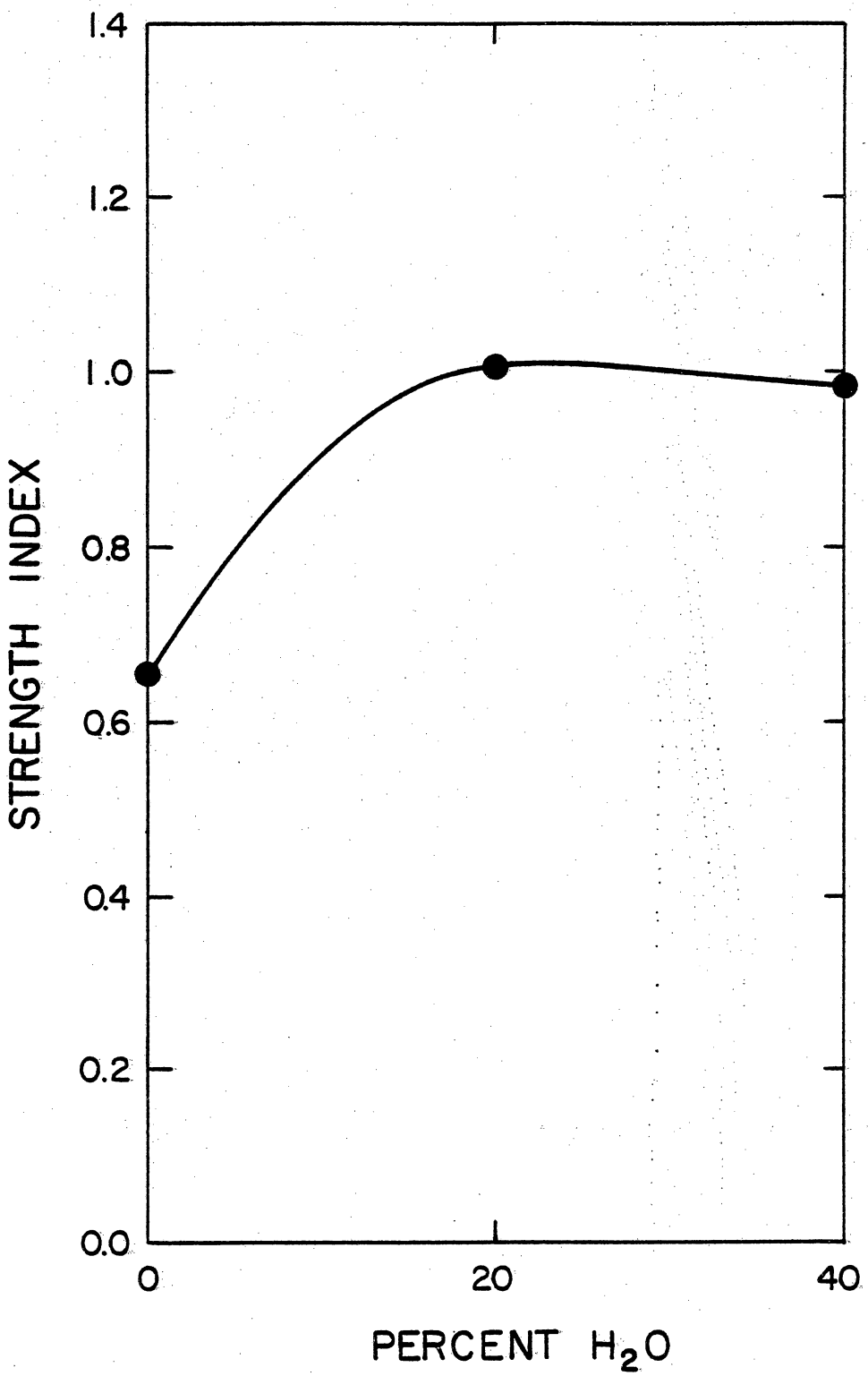

Figure 61. Effect of H_2O on Strength of Fe-doped 90+ Wt.% Alumina Ramming Mix.

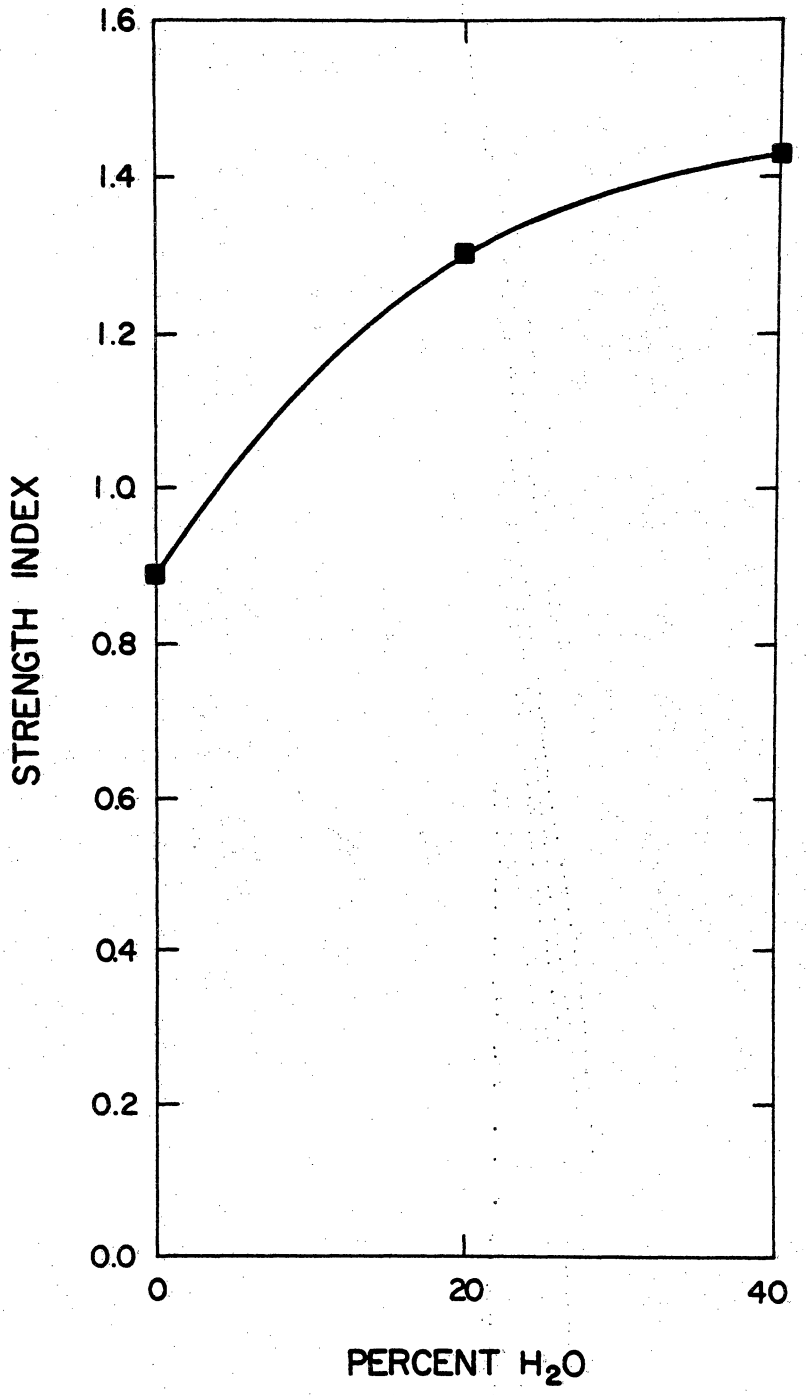

Figure 62. Effect of H_2O on Strength of Fe_2O_3-doped 90+ Wt.% Alumina Ramming Mix.

H_2S in Figure 55, except that the strength indexes are 0.05 to 0.10 greater for the CO_2.

2. 50+ Wt.% Alumina Castable

As with the 90+ wt.% alumina castable, the effects of H_2 and H_2O are quite similar for the 50+ wt.% alumina castable. H_2 (at the 20% level again) causes the most strength enhancement of the refractory. Curves of H_2S and CO_2 are similar in appearance. Both gases tend to be ineffective retardants at their lower level (0.2% for H_2S, 5% for CO_2) and then more effective at their higher level. NH_3 is more effective at retarding CO disintegration at the 0.2% level than H_2S, but is much less effective at the 0.8% level. H_2S at the 0.8% level, along with H_2 and H_2O at the 40% level, causes the metallic iron-doped castable to retain an average of 80% of its undoped strength.

3. 90+ Wt.% Alumina Phosphate-Bonded Ramming Mix

H_2, H_2O and 5% CO_2 effectively retard CO disintegration in both metallic iron and iron oxide-doped 90+ wt.% alumina phosphate-bonded refractory, however, the effectiveness of CO_2 disappears at its 15% level. H_2 does not have the strengthening effect seen for the castables and H_2O only strengthens the ramming mix when it is doped with iron oxide, as shown in Figure 62. The 0.8% level of NH_3 suppresses CO disintegration in the iron oxide-doped ramming mix, but not the metallic iron-doped. The 0.8% level of H_2S suppresses CO disintegration and significantly strengthens the metallic iron-doped refractory,

however, both the 0.2% and 0.8% levels of this gas accelerate disintegration of the iron oxide-doped refractory.

VI. Conclusions

A. Effect of Various Gases on CO Disintegration

1. 0.5 Wt.% and more Fe caused CO disintegration in all three monolithic refractories.

2. CO_2, NH_3, H_2, H_2S, and H_2O all retard CO disintegration to a greater or lesser extent in both castables.

3. H_2 and H_2O retard CO disintegration in the phosphate-bonded ramming mix, whereas the retarding effect of CO_2 is questionable, and of NH_3 is non-existent. H_2S actually accelerates rather than retards disintegration.

4. The retarding effects of 20% and more H_2 and H_2O in CO is in contrast to earlier observations in which less than 5% of each gas in CO accelerated carbon deposition.

B. Effect of Iron-Impurity Particle Size on CO Disintegration of 90 + Wt.% Alumina Castable (Appendix IV)

1. The size of the iron-impurity definitely can affect CO disintegration behavior.

2. Particles in a narrow size range, neither a maximum nor a minimum, can yield maximum service life of the refractory.

3. Fracture behavior around large particles is different from fracture behavior around smaller particles.

4. Refractories with a different composition, and/or different grog size distribution will probably have different optimum resistance impurity size range.

C. Effect of Pressure on CO Disintegration (Appendix V)

1. Elevated pressure greatly accelerates CO disintegration in all three monolithic refractories.

2. Pressure does not affect reduction of iron oxide.

3. High pressure causes carbon deposition in undoped castables.

4. As little as 0.05% Fe can lead to drastically reduced service life of refractory.

D. Correlation Between Present Study and Other Investigations

The effects of CO_2, NH_3, H_2, H_2S, and H_2O on CO disintegration observed in this study are similar to the effects noted in other studies with the expection of

The retarding effects of H_2 and H_2O for all three refractories examined and the accelerating effect of H_2S for the 90+ wt.% alumina phosphate-bonded ramming mix.

VII. Summary

Three monolithic refractories (a 90+ wt.% alumina castable, a 50+ wt.% alumina castable, and a 90+ wt.% alumina phosphate-bonded ramming mix) doped with up to 2.0 Fe wt.% metallic iron and iron oxide were exposed to CO at atmospheric pressure and 600 psi and to various mixtures of CO_2, NH_3, H_2, H_2S, or H_2O with CO at atmospheric pressure in tests lasting 100 hr. at 500 deg. C. The 90+ wt.% alumina castable was also doped with 2.0 Fe wt.% sintered Fe_2O_3 in four distinctly different particle size ranges and exposed to CO for 100 hr. at 500 deg. C, atmospheric pressure. All samples were examined for spalling after exposures and tested for compressive strength.

The presence of 0.5 wt.% and more metallic iron caused strength losses in all three refractories. Doping either castables with hematite did not cause significant strength degradation after 100 hr. exposure to CO. The ramming mix experienced strength losses when doped with 1.5 and 2.0 Fe wt.% hematite.

Raising the gas pressure accelerated CO disintegration in all three refractories. Fe-doped samples that had only minor amounts of deterioration at atmospheric pressure completely disintegrated at 600 psi. Undoped samples of both castables also had visible amounts of carbon deposition, accompanied by slight spalling in the 50+ wt.% alumina castable, at the higher pressure. Disintegration of the undoped 90+ wt.% alumina phosphate-bonded refractory was not accelerated

by the 100 hr. exposure to CO at 600 psi. Degradation of the Fe_2O_3-doped castables was not accelerated by high pressure, indicating that the reduction of the Fe_2O_3 impurity is not affected by elevated pressure. Spalling was seen in the phosphate-bonded refractory doped with 1.0 Fe wt.% Fe_2O_3, which had remained unaffected by CO at atmospheric pressure, indicating that the accelerating effect of pressure on the Fe_2O_3-doped ramming mix is not as great as it is for Fe-doped refractories.

At atmospheric pressure, all additions of CO_2, H_2, H_2S and H_2O were very effective in retarding CO disintegration in the 90+ wt.% alumina castable. When the refractory was doped with either metallic iron or iron oxide, 20% H_2 or H_2O mixed with CO also strengthened the refractory considerably. NH_3 also retarded CO disintegration, but, it was less effective than the other gases.

H_2 and H_2O had similar effects on the 50+ wt.% alumina castable as on the 90+ wt.% alumina castable. The smaller additions of CO_2 and H_2S to CO did not retard CO disintegration, however, the larger additions of these gases did suppress disintegration. Both levels of NH_3 suppressed CO disintegration only slightly.

H_2, H_2O and 5% CO effectively retarded CO disintegration in the 90+ wt.% alumina phosphate bonded ramming mix. NH_3 slightly suppressed disintegration in the iron oxide-doped refractory, but not in the metallic iron-doped. Disintegration was suppressed in the metallic iron-doped ramming mix with the larger addition of H_2S, however, both additions of this gas significantly accelerated deterioration of the iron-oxide doped ramming mix.

The average particle size of sintered iron oxide addition also appears to have a considerable influence on the CO resistance of the 90+ wt.% alumina castable, especially in relation to long-term exposures to dilute CO atmospheres. After a 100 hr. exposure to CO at atmospheric pressure, it was found that the samples with inclusions in the 35-80 mesh range were stronger than those with larger or smaller inclusion particle sizes. It was also observed that larger particle sizes cause more failure to the refractory than smaller particle sizes. Apparently large particles cause a few large cracks that are very destructive whereas small particles cause many small cracks which are not nearly as destructive with respect to strength.

VIII. Bibliography

1. Howard-Smith, I., and Werner, G. J., Coal Conversion Technology, Park Ridge, J. J., Noyes Data Corporation (1976).

2. Second Annual Symposium on Coal Gasification, Liquefaction, And Utilization, August 5-7, University of Pittsburgh, Pa. (1975).

3. Third Annual Conference on Materials For Coal Conversion and Utilization, October 10-12, USNBS, Gaithersburg, Md. (1978).

4. Pattinson, J. J., Iron and Steel Inst., 1, 85 (1876).

5. Stammer, K., Pogg. Ann., 82, 136 (1851).

6. Deville, H., Comp. Rondue., 59, 873-876 (1864).

7. Bell, H., J. Chem. Soc., 22, 203-254 (1869).

8. Davis, W. R., Slawson, R. J., and Rigby, G. R., Nature, 171, 756 (1953).

9. Berry, T. F., Ames, R. N., and Snow, R. B., J. Am. Ceram. Soc., 39 (9) 308-318 (1956).

10. Batta, G., and Scheepers, L., Proc. XIth Int. Congr. of Pure and Applied Chem., 5, 407-416 (1947).

11. Clews, F. H., Richardson, H. M., Dobbins, N. E., and Rigby, G. R., Trans. Brit. Ceram. Soc., 42, 105-110 (1943).

12. Scheepers, L., Congr. Chim. Ind., 15th Congr., Brussels, 2, 1003-1011 (1935).

13. Hubbard, D. E. and Rees, W. J., Trans. Brit. Ceram. Soc., 28 (6) 277-309 (1929).

14. Baukloh, W., and Schilling, H. J., Tonind-Ztg., 64 (55) 397-399; (56) 406-408 (1940).

15. Hibbot, H. W., and Rees, W. J., Trans. Brit. Ceram. Soc., 32, 253-269 (1933).

16. Frad, W. A., Dissertation, Univ. Missouri (1954); Dissertation Abstr., 15, 94-95 (1955).

17. Shea, J. A., Am. Ceram. Soc. Bull., 28 (7) 253-259 (1950); Steel, 127 (Nov. 27) 74, 77-78 (1950); Iron Steel Eng., 27 (12) 116-119 (1950); Blast Furnace Steel Plant, 39 (3) 333-336 (1951); U.S. Pat. 2,725,225; 2,725,226; 2,725,227; and 2,724,887.

18. Furnas, C. C., J. Am. Ceram. Soc., 19 (6) 177-186 (1936).

19. Carnes, K. C., Glass Ind., 21 (12) 522, 535 (1940).

20. Nadachowski, F., Prace Inst. Ministerstwa Hutnic, 6 (4) 170-175 (1954).

21. Lovell, G. H. B., E. African Govt. Met. Lab. Bull., 7 (1951).

22. Lozinskii, N. M., and Ter-Mikaelyantz, E. I., Ogneupory, 2 (12) 18-20 (1934).

23. Boudouard, O., Ann. Chim. Phys., 24 (5) 85 (1901).

24. Diepschlag, E., and Fiest, K., Feurfest, 4 (9) 133-136 (1928); Blast Furnace Steel Plant, 17 (2) 280-282 (1929).

25. Shapland, J. T., and Livovich, A. F., Am. Ceram. Soc. Bull., 43 (7) 510-513 (1964).

26. Gitzen, W. H., Heilich, R. P., and Rohr, F. I., Am. Ceram. Soc. Bull., 43 (7) 518-523 (1964).

27. Towers, H., Iron and Steel (London), 28, 129-134 (1955).

28. Stein, J. G. and Co., Ltd., Refractories Bull., No. 12 (Dec) (1932).

29. Babkin, M. P., and Golovatii, R. N., Ogneupory, 3 (8) 582-587 (1935).

30. Hartman, F. (Kohle-und Eisenforschung G.m.b.H.) Ger. Pat. 659, 722, Apr. 1938; VI/806.12.10.

31. Holmquist, P. J., Jerukontorets Ann., 118, 519-530 (1934).

32. Lindgren, R. A., Brick and Clay Record, 91, 38, 40, 42 (1937).

33. Baukloh, W., and Hellbrüge, J., Arch. Eisenhüttenw, 15, 163-166 (1941).

34. Booley, F., Gas World (Coking Section), 29 (347) 2-3 (1942).

35. Golovatii, R. N., and Smolyantzkii, I. A., Ogneupory, 2 (12) 21-25 (1934).

36. Tadokoro, Y., Chem. Eng. Conf. World Power Conf., B8 (1936).

37. Budnikov, P. P., and Nirenshtein, D. A., Stahl, 7, 48-52 (1934).

38. Clopham, S. D., M. S. Thesis, Ohio State Univ., Columbus, Ohio (1973).

39. Golovatii, R. N., Ogneupory, 4, 686-691 (1936).

40. Kramaranko, A. I., Novosti Tekhniki, No. 54, 15 (1934).

41. Hugill, W., Ellerton, H., and Green, A. T., Trans. Brit. Ceram. Soc., 32 (12) 533-550 (1933); 37 (1) 6-16 (1938).

42. Swarup, D., and Sataravala, R. P., Trans. Indian Ceram. Soc., 2 (1) 15-31 (1943).

43. Davis, W. R., and Rigby, J. R., Trans. Brit. Ceram. Soc., 53 (8) 511-523 (1954).

44. Kappmeyer, K. K., and Hubble, D. H., Am. Ceram. Soc. Bull., 51 (7) 568-573 (1972).

45. Chufarov, G. I., and Antonova, M. F., Izvest. Akad. Nauk S.S.S. R. Otdel Tekh Nauk, 1947 (4) 381-389.

46. Schenk, H., Majdic, A., Graf, D., Raebel, G., and Bonner, H., Arch. Eisenhüttenw, 39 (2) 101-107 (1968).

47. Bartha, P., Koehne, V., and Kurjat, J., Tonind-Ztg. Keram. Rundschau, 97 (7) 244-247 (1973).

48. Chesters, J. H., Brit. Eng. Report J., 28, 428 (1946).

49. Rigby, G. R., Booth, H., and Green, A. T., Trans. Brit. Ceram. Soc., 37 (3) 75-99 (1938); 38 (7) 418-434 (1939).

50. Am. Soc. Testing Materials, Proc., 50, 207-208 (1950).

51. Am. Soc. Testing Materials, Standards, 1955 (III), 666-667 (1955).

52. Trostel, L. J., Ind. Heating, 17, 1056-1058, 1065 (1951); J. Am. Ceram. Soc., 34 (3) 76-82 (1951).

53. Pukall, K., Sprechsaal, 71 (26) 321-324 (1938).

54. Phelps, S. M., Refractories Inst. Tech. Bull., No. 89 (1952).

55. Rowden, E., and Green, A. T., Trans. Brit. Ceram. Soc., 37 (3) 75-99 (1938); 38 (7) 418-434 (1939).

56. Rowden, E., Trans. Brit. Ceram. Soc., 43 (7) 105-130 (1944); 49, 172-182 (1950).

57. Westman, A. E. R., J. Am. Ceram. Soc., 11 (8) 633-638 (1928).

APPENDIX I

Tabulated Strength and Weight Loss Data for 90+ wt.% Alumina Castable, 50+ wt.% Alumina Castable, and 90+ wt.% Alumina Phosphate-bonded Ramming Mix Exposed to Various Gas Compositions

Table No.	Gas Composition
I-III	CO
IV-VI	95% CO-5% CO_2
VII-IX	85% CO-15% CO_2
X-XII	99.8% CO-0.2% NH_3
XIII-XV	99.2% CO-0.8% NH_3
XVI-XVIII	80% CO-20% H_2
XIX-XXI	60% CO-40% H_2
XXII-XIV	99.8% CO-0.2% H_2S
XXV-XXVII	99.2% CO-0.8% H_2S
XXVIII-XXX	80% CO-20% H_2O
XXXI-XXXIII	60% CO-40% H_2O

TABLE I: STRENGTH AND WEIGHT LOSS DATA FOR 90+ WT.% ALUMINA CASTABLE EXPOSED TO 99.99% CO INGAS

DOPANT	ADDED WT.% Fe	COMPRESSIVE STRENGTH (PSI) $\sigma_c \pm s$	FRACTION OF UNDOPED STRENGTH	RATIO OF WT. AFTER TO WT. BEFORE	NUMBER OF SAMPLES
None	0.0	10,325 ± 1,250		1.000	5
Fe	0.5	5,800 ± 2,725	0.562	0.949	5
Fe	1.0	3,475 ± 2,250	0.337	0.774	5
Fe	1.5	3,350 ± 2,150	0.325	0.529	5
Fe	2.0	2,475 ± 3,350	0.240	0.303	5
Fe_2O_3	0.5	13,300 ± 1,225	1.288	1.000	5
Fe_2O_3	1.0	12,775 ± 950	1.237	1.000	5
Fe_2O_3	1.5	13,075 ± 750	1.266	1.000	5
Fe_2O_3	2.0	12,650 ± 500	1.225	1.000	5

TABLE II: STRENGTH AND WEIGHT LOSS DATA FOR 50+ WT.% ALUMINA CASTABLE EXPOSED TO 99.99% CO INGAS

DOPANT/WT. % Fe	ADDED	COMPRESSIVE STRENGTH (PSI) $\sigma_c \pm s$	FRACTION OF UNDOPED STRENGTH	RATIO OF WT. AFTER TO WT. BEFORE	NUMBER OF SAMPLES
None	0.0	6,750 ± 1,450		1.000	5
Fe	0.5	5,125 ± 900	0.759	0.987	5
Fe	1.0	0 ± 0	0	0	5
Fe	1.5	75 ± 200	0.011	0.024	5
Fe	2.0	125 ± 275	0.019	0.050	5
Fe_2O_3	0.5	6,300 ± 1,175	0.933	1.000	5
Fe_2O_3	1.0	5,575 ± 1,075	0.827	1.000	5
Fe_2O_3	1.5	7,675 ± 375	1.137	1.000	5
Fe_2O_3	2.0	7,275 ± 975	1.078	1.000	5

TABLE III: STRENGTH AND WEIGHT LOSS DATA FOR 90+ WT.% ALUMINA RAMMING MIX EXPOSED TO 99.99% CO INGAS

DOPANT	ADDED WT.% Fe	COMPRESSIVE STRENGTH (PSI) σ_c ± s	FRACTION OF UNDOPED STRENGTH	RATIO OF WT. AFTER TO WT. BEFORE	NUMBER OF SAMPLES
None	0.0	13,750 ± 2,475		0.985	4
Fe	0.5	9,875 ± 3,175	0.718	0.977	4
Fe	1.0	9,600 ± 1,325	0.698	0.980	4
Fe	1.5	6,475 ± 2,175	0.471	0.965	4
Fe	2.0	9,775 ± 1,650	0.711	0.972	4
Fe_2O_3	0.5	13,000 ± 2,650	0.945	0.950	4
Fe_2O_3	1.0	14,675 ± 2,100	1.067	0.970	4
Fe_2O_3	1.5	11,625 ± 1,950	0.845	0.965	4
Fe_2O_3	2.0	9,375 ± 1,900	0.682	0.955	4

TABLE IV: STRENGTH AND WEIGHT LOSS DATA FOR 90+ WT.% ALUMINA CASTABLE EXPOSED TO 95% CO - 5% CO_2 INGAS

DOPANT	ADDED WT.% Fe	COMPRESSIVE STRENGTH (PSI) $\sigma_c \pm s$	FRACTION OF UNDOPED STRENGTH	RATIO OF WT. AFTER TO WT. BEFORE	NUMBER OF SAMPLES
None	0.0	5,800 ± 2,750		1.001	4
Fe	0.5	7,600 ± 925	1.310	0.999	4
Fe	1.0	5,925 ± 900	1.022	0.954	4
Fe	1.5	4,650 ± 3,550	0.802	0.736	4
Fe	2.0	4,350 ± 3,925	0.750	0.714	4
Fe_2O_3	0.5	8,875 ± 300	1.530	0.999	4
Fe_2O_3	1.0	7,600 ± 1,300	1.310	0.987	4
Fe_2O_3	1.5	7,000 ± 750	1.207	1.000	4
Fe_2O_3	2.0	8,200 ± 3,275	1.414	1.000	4

TABLE V: STRENGTH AND WEIGHT LOSS DATA FOR 50+ WT.% ALUMINA CASTABLE EXPOSED TO 95% CO - 5% CO_2 INGAS

DOPANT	ADDED WT.% Fe	COMPRESSIVE STRENGTH (PSI) $\sigma_c \pm s$	FRACTION OF UNDOPED STRENGTH	RATIO OF WT. AFTER TO WT. BEFORE	NUMBER OF SAMPLES
None	0.0	4,450 ± 1,075		1.000	4
Fe	0.5	3,150 ± 2,150	0.708	0.729	4
Fe	1.0	0 ± 0	0	0	4
Fe	1.5	0 ± 0	0	0	4
Fe	2.0	1,950 ± 2,575	0.438	0.493	4
Fe_2O_3	0.5	6,175 ± 1,450	1.388	1.000	4
Fe_2O_3	1.0	4,700 ± 1,500	1.056	1.000	4
Fe_2O_3	1.5	5,750 ± 2,325	1.292	1.001	4
Fe_2O_3	2.0	3,725 ± 1,550	.837	1.003	4

TABLE VI: STRENGTH AND WEIGHT LOSS DATA FOR 90+ WT.% ALUMINA RAMMING MIX EXPOSED TO 95% CO - 5% CO_2 INGAS

DOPANT	ADDED WT.% Fe	COMPRESSIVE STRENGTH (PSI) $\sigma_c \pm s$	FRACTION OF UNDOPED STRENGTH	RATIO OF WT. AFTER TO WT. BEFORE	NUMBER OF SAMPLES
None	0.0	8,075 ± 2,675		1.000	4
Fe	0.5	8,650 ± 3,575	1.071	1.000	4
Fe	1.0	7,650 ± 5,875	0.947	1.004	4
Fe	1.5	8,975 ± 3,875	1.111	0.999	3
Fe	2.0	8,050 ± 3,700	0.997	0.987	4
Fe_2O_3	0.5	11,300 ± 300	1.399	0.999	4
Fe_2O_3	1.0	11,900 ± 3,000	1.474	1.000	4
Fe_2O_3	1.5	11,800 ± 4,425	1.461	0.999	4
Fe_2O_3	2.0	2,475 ± 4,950	0.307	0.748	4

TABLE VII: STRENGTH AND WEIGHT LOSS DATA FOR 90+ WT.% ALUMINA CASTABLE EXPOSED TO 85% CO - 15% CO_2 INGAS

DOPANT	ADDED WT.% Fe	COMPRESSIVE STRENGTH (PSI) $\sigma_c \pm s$	FRACTION OF UNDOPED STRENGTH	RATIO OF WT. AFTER TO WT. BEFORE	NUMBER OF SAMPLES
None	0.0	7,025 ± 1,100		1.000	4
Fe	0.5	8,750 ± 600	1.246	0.935	4
Fe	1.0	8,000 ± 2,000	1.139	0.999	4
Fe	1.5	6,125 ± 1,675	0.872	0.963	4
Fe	2.0	7,300 ± 1,725	1.039	1.002	4
Fe_2O_3	0.5	7,050 ± 600	1.004	1.006	4
Fe_2O_3	1.0	6,225 ± 1,875	0.886	1.008	4
Fe_2O_3	1.5	6,650 ± 925	0.947	1.008	4
Fe_2O_3	2.0	8,600 ± 550	1.224	1.008	4

TABLE VIII: STRENGTH AND WEIGHT LOSS DATA FOR 50+ WT.% ALUMINA CASTABLE EXPOSED TO 85% CO - 15% CO_2 INGAS

DOPANT	ADDED WT.% Fe	COMPRESSIVE STRENGTH (PSI) $\sigma_c \pm s$	FRACTION OF UNDOPED STRENGTH	RATIO OF WT. AFTER TO WT. BEFORE	NUMBER OF SAMPLES
None	0.0	4,425 ± 725		1.011	4
Fe	0.5	5,350 ± 525	1.209	1.008	4
Fe	1.0	5,150 ± 1,000	1.164	1.006	4
Fe	1.5	4,925 ± 1,525	1.113	1.009	4
Fe	2.0	6,125 ± 1,550	1.384	1.008	4
Fe_2O_3	0.5	4,825 ± 550	1.090	1.011	4
Fe_2O_3	1.0	4,650 ± 175	1.051	1.010	4
Fe_2O_3	1.5	5,125 ± 800	1.158	1.010	4
Fe_2O_3	2.0	5,500 ± 825	1.243	1.009	4

TABLE IX: STRENGTH AND WEIGHT LOSS DATA FOR 90+ WT.% ALUMINA RAMMING MIX EXPOSED TO 85% CO - 15% CO_2 INGAS

DOPANT	ADDED WT.% Fe	COMPRESSIVE STRENGTH (PSI) $\sigma_c \pm s$	FRACTION OF UNDOPED STRENGTH	RATIO OF WT. AFTER TO WT. BEFORE	NUMBER OF SAMPLES
None	0.0	11,625 ± 2,150		1.007	4
Fe	0.5	10,625 ± 1,400	0.914	1.008	4
Fe	1.0	8,375 ± 3,325	0.720	0.900	4
Fe	1.5	4,750 ± 700	0.409	0.561	4
Fe	2.0	6,750 ± 2,750	0.581	0.855	3
Fe_2O_3	0.5	11,750 ± 3,450	1.011	1.007	4
Fe_2O_3	1.0	10,500 ± 4,725	0.903	1.002	4
Fe_2O_3	1.5	6,075 ± 2,475	0.523	0.702	4
Fe_2O_3	2.0	4,975 ± 4,300	0.428	0.755	3

TABLE X: STRENGTH AND WEIGHT LOSS DATA FOR 90+ WT.% ALUMINA CASTABLE EXPOSED TO 99.8% CO - 0.2% NH_3 INGAS

ADDED DOPANT/WT.% Fe		COMPRESSIVE STRENGTH (PSI) $\sigma_c \pm s$	FRACTION OF UNDOPED STRENGTH	RATIO OF WT. AFTER TO WT. BEFORE	NUMBER OF SAMPLES
None	0.0	6,100 ± 1,100		1.007	4
Fe	0.5	5,275 ± 3,725	0.865	0.999	4
Fe	1.0	4,750 ± 1,150	0.779	0.982	4
Fe	1.5	2,300 ± 2,125	0.377	0.641	4
Fe	2.0	3,200 ± 2,125	0.525	0.850	4
Fe_2O_3	0.5	4,075 ± 550	0.668	0.999	4
Fe_2O_3	1.0	5,859 ± 1,750	0.959	0.999	4
Fe_2O_3	1.5	6,175 ± 925	1.012	0.999	4
Fe_2O_3	2.0	6,800 ± 3,175	1.115	0.999	4

TABLE XI: STRENGTH AND WEIGHT LOSS DATA FOR 50+ WT.% ALUMINA CASTABLE EXPOSED TO 99.8% CO - 0.2% NH_3 INGAS

DOPANT	ADDED WT.% Fe	COMPRESSIVE STRENGTH (PSI) $\sigma_c \pm s$	FRACTION OF UNDOPED STRENGTH	RATIO OF WT. AFTER TO WT. BEFORE	NUMBER OF SAMPLES
None	0.0	4,875 ± 1,250		0.999	4
Fe	0.5	4,650 ± 875	0.954	1.000	4
Fe	1.0	3,800 ± 1,250	0.779	0.999	4
Fe	1.5	1,350 ± 1,600	0.277	0.403	4
Fe	2.0	100 ± 225	0.021	0.099	4
Fe_2O_3	0.5	5,250 ± 650	1.077	0.999	4
Fe_2O_3	1.0	4,775 ± 475	0.979	0.999	4
Fe_2O_3	1.5	4,125 ± 850	1.051	1.003	4
Fe_2O_3	2.0	5,750 ± 850	1.179	1.004	4

TABLE XII: STRENGTH AND WEIGHT LOSS DATA FOR 90+ WT.% ALUMINA RAMMING MIX EXPOSED TO 99.8% CO - 0.2% NH_3 INGAS

DOPANT	ADDED WT.% Fe	COMPRESSIVE STRENGTH (PSI) $\sigma_c \pm s$	FRACTION OF UNDOPED STRENGTH	RATIO OF WT. AFTER TO WT. BEFORE	NUMBER OF SAMPLES
None	0.0	14,950 ± 1,825		0.988	4
Fe	0.5	11,500 ± 2,275	0.769	0.999	4
Fe	1.0	5,250 ± 1,850	0.351	0.630	4
Fe	1.5	9,150 ± 4,300	0.612	0.864	4
Fe	2.0	7,225 ± 3,650	0.483	0.914	4
Fe_2O_3	0.5	14,650 ± 3,600	0.980	0.999	4
Fe_2O_3	1.0	13,400 ± 1,775	0.896	1.000	4
Fe_2O_3	1.5	11,150 ± 4,900	0.746	1.001	4
Fe_2O_3	2.0	8,750 ± 1,800	0.585	1.002	4

TABLE XIII. STRENGTH AND WEIGHT LOSS DATA FOR 90+ WT.% ALUMINA CASTABLE EXPOSED TO 99.2% CO - 0.8% NH_3 INGAS

DOPANT	ADDED WT.% Fe	COMPRESSIVE STRENGTH (PSI) $\sigma_c \pm s$	FRACTION OF UNDOPED STRENGTH	RATIO OF WT. AFTER TO WT. BEFORE	NUMBER OF SAMPLES
None	0.0	6,350 ± 1,500		1.001	4
Fe	0.5	5,750 ± 1,375	0.906	0.958	4
Fe	1.0	4,300 ± 2,725	0.677	0.910	4
Fe	1.5	4,700 ± 1,975	0.740	0.827	4
Fe	2.0	6,975 ± 3,225	1.098	0.946	4
Fe_2O_3	0.5	7,000 ± 1,125	1.102	1.001	4
Fe_2O_3	1.0	5,975 ± 1,125	0.941	1.001	4
Fe_2O_3	1.5	9,225 ± 1,675	1.453	1.001	4
Fe_2O_3	2.0	8,925 ± 2,000	1.406	1.001	4

TABLE XIV. STRENGTH AND WEIGHT LOSS DATA FOR 50+ WT.% ALUMINA CASTABLE EXPOSED TO 99.2% CO - 0.8% NH_3 INGAS

DOPANT	ADDED WT.% Fe	COMPRESSIVE STRENGTH (PSI) σ_c ± s	FRACTION OF UNDOPED STRENGTH	RATIO OF WT. AFTER TO WT. BEFORE	NUMBER OF SAMPLES
None	0.0	3,925 ± 800		1.000	4
Fe	0.5	5,225 ± 1,350	1.331	1.050	4
Fe	1.0	75 ± 150	0.019	0.399	4
Fe	1.5	575 ± 675	0.146	0.307	4
Fe	2.0	1,750 ± 1,025	0.446	0.444	4
Fe_2O_3	0.5	5,950 ± 525	1.516	0.999	4
Fe_2O_3	1.0	4,550 ± 475	1.159	1.000	4
Fe_2O_3	1.5	5,275 ± 525	1.344	1.004	4
Fe_2O_3	2.0	5,625 ± 200	1.433	0.918	4

TABLE XV. STRENGTH AND WEIGHT LOSS DATA FOR 90+ WT.% ALUMINA RAMMING MIX EXPOSED TO 99.2% CO - 0.8% NH_3 INGAS

DOPANT	ADDED WT.% Fe	COMPRESSIVE STRENGTH (PSI) σ_c ± s	FRACTION OF UNDOPED STRENGTH	RATIO OF WT. AFTER TO WT. BEFORE	NUMBER OF SAMPLES
None	0.0	12,150 ± 3,025		1.000	4
Fe	0.5	10,725 ± 1,125	0.883	1.000	4
Fe	1.0	4,750 ± 3,625	0.391	0.723	4
Fe	1.5	6,725 ± 2,525	0.553	0.849	4
Fe	2.0	7,450 ± 2,350	0.613	0.981	4
Fe_2O_3	0.5	12,700 ± 4,275	1.045	0.999	4
Fe_2O_3	1.0	11,350 ± 3,800	0.934	1.000	4
Fe_2O_3	1.5	10,975 ± 1,325	0.903	1.001	4
Fe_2O_3	2.0	11,150 ± 1,525	0.918	1.001	4

TABLE XVI. STRENGTH AND WEIGHT LOSS DATA FOR 90+ Wt.% ALUMINA CASTABLE EXPOSED TO 80% CO - 20% H_2 INGAS

DOPANT	ADDED WT.% Fe	COMPRESSIVE STRENGTH (PSI) $\sigma_c \pm s$	FRACTION OF UNDOPED STRENGTH	RATIO OF WT. AFTER TO WT. BEFORE	NUMBER OF SAMPLES
None	0.0	5,325 ± 900		0.998	4
Fe	0.5	6,000 ± 850	1.126	0.996	4
Fe	1.0	11,125 ± 1,225	2.089	0.997	4
Fe	1.5	10,800 ± 1,150	2.028	0.996	4
Fe	2.0	4,875 ± 1,100	0.915	0.765	4
Fe_2O_3	0.5	9,950 ± 950	1.869	0.998	4
Fe_2O_3	1.0	7,625 ± 575	1.432	0.998	4
Fe_2O_3	1.5	11,050 ± 1,825	2.075	0.997	4
Fe_2O_3	2.0	8,025 ± 3,350	1.507	0.997	4

TABLE XVII. STRENGTH AND WEIGHT LOSS DATA FOR 50% WT.% ALUMINA CASTABLE EXPOSED TO 80% CO - 20% H_2 INGAS

DOPANT	ADDED WT.% Fe	COMPRESSIVE STRENGTH (PSI) $\sigma_c \pm s$	FRACTION OF UNDOPED STRENGTH	RATIO OF WT. AFTER TO WT. BEFORE	NUMBER OF SAMPLES
None	0.0	5,100 ± 600		0.998	4
Fe	0.5	5,750 ± 1,060	1.127	0.996	4
Fe	1.0	10,425 ± 1,325	2.044	0.996	4
Fe	1.5	12,150 ± 2,125	2.382	0.995	4
Fe	2.0	11,525 ± 1,475	2.260	0.969	4
Fe_2O_3	0.5	6,000 ± 1,850	1.176	0.996	4
Fe_2O_3	1.0	11,050 ± 1,300	2.167	0.995	4
Fe_2O_3	1.5	13,175 ± 1,600	2.583	0.995	4
Fe_2O_3	2.0	11,625 ± 2,650	2.279	0.994	4

TABLE XVIII. STRENGTH AND WEIGHT LOSS DATA FOR 90+ WT.% ALUMINA RAMMING MIX EXPOSED TO 80% CO - 20% H_2 INGAS

DOPANT/WT.% Fe	ADDED	COMPRESSIVE STRENGTH (PSI) $\sigma_c \pm s$	FRACTION OF UNDOPED STRENGTH	RATIO OF WT. AFTER TO WT. BEFORE	NUMBER OF SAMPLES
None	0.0	12,000 ± 3,250		0.999	4
Fe	0.5	9,900 ± 1,400	0.825	0.997	4
Fe	1.0	10,775 ± 2,875	0.898	0.996	4
Fe	1.5	11,400 ± 750	0.950	0.959	4
Fe	2.0	12,500 ± 2,100	1.042	0.968	4
Fe_2O_3	0.5	15,100 ± 2,500	1.258	0.998	4
Fe_2O_3	1.0	15,925 ± 1,300	1.327	0.995	4
Fe_2O_3	1.5	11,925 ± 2,375	0.994	0.994	4
Fe_2O_3	2.0	8,250 ± 750	0.688	0.996	4

TABLE XIX. STRENGTH AND WEIGHT LOSS DATA FOR 90+ WT.% ALUMINA CASTABLE EXPOSED TO 60% CO - 40% H_2 INGAS

DOPANT	ADDED WT.% Fe	COMPRESSIVE STRENGTH (PSI) $\sigma_c \pm s$	FRACTION OF UNDOPED STRENGTH	RATIO OF WT. AFTER TO WT. BEFORE	NUMBER OF SAMPLES
None	0.0	6,975 ± 875		1.000	4
Fe	0.5	6,775 ± 550	0.971	0.968	4
Fe	1.0	9,775 ± 425	1.401	1.031	4
Fe	1.5	8,075 ± 925	1.158	0.897	4
Fe	2.0	9,000 ± 1,325	1.290	0.997	4
Fe_2O_3	0.5	7,875 ± 1,275	1.129	0.999	4
Fe_2O_3	1.0	8,050 ± 1,750	1.154	0.999	4
Fe_2O_3	1.5	8,775 ± 2,200	1.258	0.999	3
Fe_2O_3	2.0	8,200 ± 2,400	1.176	0.998	4

TABLE XX. STRENGTH AND WEIGHT LOSS DATA FOR 50+ WT.% ALUMINA CASTABLE EXPOSED TO 60% CO - 40% H_2 INGAS

DOPANT/WT.% Fe	ADDED	COMPRESSIVE STRENGTH (PSI) σ_c ± s	FRACTION OF UNDOPED STRENGTH	RATIO OF WT. AFTER TO WT. BEFORE	NUMBER OF SAMPLES
None	0.0	5,125 ± 650		0.997	4
Fe	0.5	4,075 ± 775	0.795	0.997	4
Fe	1.0	5,725 ± 850	1.117	0.996	4
Fe	1.5	5,150 ± 400	1.005	0.996	4
Fe	2.0	5,100 ± 1,125	0.995	0.996	4
Fe_2O_3	0.5	4,875 ± 1,075	0.951	0.998	4
Fe_2O_3	1.0	5,275 ± 375	1.029	0.997	4
Fe_2O_3	1.5	4,250 ± 875	0.829	0.997	4
Fe_2O_3	2.0	6,275 ± 800	1.224	0.997	4

TABLE XXI. STRENGTH AND WEIGHT LOSS DATA FOR 90+ WT/% ALUMINA RAMMING MIX EXPOSED TO 60% CO - 40% H_2 INGAS

DOPANT	ADDED WT.% Fe	COMPRESSIVE STRENGTH (PSI) σ_c ± s	FRACTION OF UNDOPED STRENGTH	RATIO OF WT. AFTER TO WT. BEFORE	NUMBER OF SAMPLES
None	0.0	10,450 ± 3,375		0.999	4
Fe	0.5	8,650 ± 2,475	0.828	0.997	4
Fe	1.0	10,300 ± 1,900	0.986	0.996	4
Fe	1.5	10,925 ± 2,275	1.045	0.996	4
Fe	2.0	10,925 ± 1,225	1.045	0.996	4
Fe_2O_3	0.5	10,675 ± 1,725	1.022	0.997	4
Fe_2O_3	1.0	9,625 ± 1,900	0.921	0.996	4
Fe_2O_3	1.5	11,050 ± 950	1.057	0.996	4
Fe_2O_3	2.0	10,400 ± 3,375	0.995	0.995	4

TABLE XXII. STRENGTH AND WEIGHT LOSS DATA FOR 90+ WT.% ALUMINA CASTABLE EXPOSED TO 99.8% CO - 0.2% H_2S INGAS

DOPANT	ADDED WT.% Fe	COMPRESSIVE STRENGTH (PSI) $\sigma_c \pm s$	FRACTION OF UNDOPED STRENGTH	RATIO OF WT. AFTER TO WT. BEFORE	NUMBER OF SAMPLES
None	0.0	7,200 ± 1,250		0.999	4
Fe	0.5	7,000 ± 2,750	0.972	0.999	4
Fe	1.0	5,375 ± 3,000	0.747	0.999	4
Fe	1.5	7,000 ± 2,350	0.972	0.988	4
Fe	2.0	6,300 ± 3,525	0.875	0.968	4
Fe_2O_3	0.5	8,550 ± 400	1.188	0.999	4
Fe_2O_3	1.0	8,575 ± 1,250	1.191	1.000	4
Fe_2O_3	1.5	7,775 ± 600	1.080	1.000	4
Fe_2O_3	2.0	8,725 ± 1,225	1.212	1.000	4

TABLE XXIII. STRENGTH AND WEIGHT LOSS DATA FOR 50+ WT.% ALUMINA CASTABLE EXPOSED TO 99.8% CO - 0.2% H_2S INGAS

DOPANT	ADDED WT.% Fe	COMPRESSIVE STRENGTH (PSI) $\sigma_c \pm s$	FRACTION OF UNDOPED STRENGTH	RATIO OF WT. AFTER TO WT. BEFORE	NUMBER OF SAMPLES
None	0.0	4,375 ± 1,050		0.999	4
Fe	0.5	1,575 ± 475	0.360	0.996	4
Fe	1.0	0 ± 0	0	0.515	4
Fe	1.5	0 ± 0	0	0.239	4
Fe	2.0	2,850 ± 2,650	0.651	0.692	4
Fe_2O_3	0.5	4,925 ± 775	1.131	0.999	4
Fe_2O_3	1.0	4,950 ± 875	1.131	0.999	4
Fe_2O_3	1.5	4,650 ± 1,650	1.063	0.999	4
Fe_2O_3	2.0	4,275 ± 725	0.977	0.998	4

TABLE XXIV. STRENGTH AND WEIGHT LOSS DATA FOR 90+ WT.% ALUMINA RAMMING MIX EXPOSED TO 99.8% CO - 0.2% H_2S INGAS

DOPANT	ADDED WT.% Fe	COMPRESSIVE STRENGTH (PSI) $\sigma_c \pm s$	FRACTION OF UNDOPED STRENGTH	RATIO OF WT. AFTER TO WT. BEFORE	NUMBER OF SAMPLES
None	0.0	8,250 ± 975		0.999	4
Fe	0.5	6,000 ± 650	0.727	0.990	4
Fe	1.0	5,000 ± 1,150	0.606	0.971	4
Fe	1.5	5,325 ± 1,750	0.645	0.986	4
Fe	2.0	5,250 ± 1,675	0.636	0.987	4
Fe_2O_3	0.5	9,525 ± 2,550	1.155	0.999	4
Fe_2O_3	1.0	9,325 ± 2,050	1.130	0.997	4
Fe_2O_3	1.5	1,725 ± 2,075	0.209	0.644	4
Fe_2O_3	2.0	2,275 ± 2,225	0.276	0.690	4

TABLE XXV. STRENGTH AND WEIGHT LOSS DATA FOR 90+ WT.% ALUMINA CASTABLE EXPOSED TO 99.2% CO - 0.8% H_2S INGAS

DOPANT	ADDED WT.% Fe	COMPRESSIVE STRENGTH (PSI) $\sigma_c \pm s$	FRACTION OF UNDOPED STRENGTH	RATIO OF WT. AFTER TO WT. BEFORE	NUMBER OF SAMPLES
None	0.0	7,475 ± 675		0.998	4
Fe	0.5	8,075 ± 1,350	1.080	0.990	4
Fe	1.0	9,100 ± 475	1.217	0.996	4
Fe	1.5	7,775 ± 2,200	1.040	0.999	4
Fe	2.0	4,125 ± 4,775	0.552	0.683	4
Fe_2O_3	0.5	7,850 ± 2,100	1.050	1.000	4
Fe_2O_3	1.0	8,900 ± 950	1.191	0.999	4
Fe_2O_3	1.5	7,150 ± 550	0.957	0.999	4
Fe_2O_3	2.0	7,925 ± 2,950	1.060	1.000	4

TABLE XXVI. STRENGTH AND WEIGHT LOSS DATA FOR 50+ WT.% ALUMINA CASTABLE EXPOSED TO 99.2% CO - 0.8% H_2S INGAS

DOPANT	ADDED WT.% Fe	COMPRESSIVE STRENGTH (PSI) $\sigma_c \pm s$	FRACTION OF UNDOPED STRENGTH	RATIO OF WT. AFTER TO WT. BEFORE	NUMBER OF SAMPLES
None	0.0	5,450 ± 200		0.996	4
Fe	0.5	3,975 ± 1,275	0.729	0.996	4
Fe	1.0	2,625 ± 1,925	0.482	0.962	4
Fe	1.5	500 ± 625	0.092	0.986	4
Fe	2.0	4,900 ± 3,950	0.899	0.737	4
Fe_2O_3	0.5	5,825 ± 1,100	1.069	1.000	4
Fe_2O_3	1.0	5,200 ± 1,125	0.954	1.000	4
Fe_2O_3	1.5	5,975 ± 2,775	1.096	1.000	4
Fe_2O_3	2.0	5,225 ± 725	0.959	1.001	4

TABLE XXVII. STRENGTH AND WEIGHT LOSS DATA FOR 90+ WT.% ALUMINA RAMMING MIX EXPOSED TO 99.2% CO - 0.8% H_2S INGAS

DOPANT	ADDED WT.% Fe	COMPRESSIVE STRENGTH (PSI) $\sigma_c \pm s$	FRACTION OF UNDOPED STRENGTH	RATIO OF WT. AFTER TO WT. BEFORE	NUMBER OF SAMPLES
None	0.0	5,700 ± 3,025		0.998	4
Fe	0.5	6,100 ± 2,075	1.070	0.997	4
Fe	1.0	9,700 ± 3,425	1.702	0.987	4
Fe	1.5	9,625 ± 4,175	1.689	0.934	4
Fe	2.0	8,475 ± 2,675	1.489	0.931	4
Fe_2O_3	0.5	6,850 ± 2,450	1.202	0.999	4
Fe_2O_3	1.0	2,550 ± 3,550	0.447	0.678	4
Fe_2O_3	1.5	0 ± 0	0	0.706	4
Fe_2O_3	2.0	675 ± 950	0.118	0.131	4

TABLE XXVIII. STRENGTH AND WEIGHT LOSS DATA FOR 90+ WT.% ALUMINA CASTABLE EXPOSED TO 80% CO - 20% H_2O INGAS

DOPANT	ADDED WT.% Fe	COMPRESSIVE STRENGTH (PSI) $\sigma_c \pm s$	FRACTION OF UNDOPED STRENGTH	RATIO OF WT. AFTER TO WT. BEFORE	NUMBER OF SAMPLES
None	0.0	6,775 ± 2,325		1.005	4
Fe	0.5	8,425 ± 1,825	1.244	1.004	4
Fe	1.0	9,825 ± 4,325	1.450	1.004	4
Fe	1.5	10,450 ± 2,275	1.542	1.002	4
Fe	2.0	9,725 ± 2,900	1.435	1.001	4
Fe_2O_3	0.5	9,050 ± 1,600	1.336	1.003	4
Fe_2O_3	1.0	11,350 ± 4,025	1.675	1.002	4
Fe_2O_3	1.5	17,700 ± 1,550	2.613	1.004	4
Fe_2O_3	2.0	16,750 ± 3,775	2.472	1.003	4

TABLE XXIX. STRENGTH AND WEIGHT LOSS DATA FOR 50+ WT.% ALUMINA CASTABLE EXPOSED TO 80% CO - 20% H_2O INGAS

DOPANT	ADDED WT.% Fe	COMPRESSIVE STRENGTH (PSI) σ_c ± s	FRACTION OF UNDOPED STRENGTH	RATIO OF WT. AFTER TO WT. BEFORE	NUMBER OF SAMPLES
None	0.0	3,475 ± 575		0.999	4
Fe	0.5	3,225 ± 1,825	0.928	0.999	4
Fe	1.0	4,425 ± 1,200	1.273	0.998	4
Fe	1.5	5,325 ± 1,300	1.532	0.998	4
Fe	2.0	4,850 ± 100	1.396	0.997	4
Fe_2O_3	0.5	4,400 ± 750	1.266	0.999	4
Fe_2O_3	1.0	4,075 ± 600	1.173	1.000	4
Fe_2O_3	1.5	6,125 ± 2,225	1.763	0.999	4
Fe_2O_3	2.0	4,325 ± 475	1.245	1.000	4

TABLE XXX. STRENGTH AND WEIGHT LOSS DATA FOR 90+ WT.% ALUMINA RAMMING MIX EXPOSED TO 80% CO - 20% H_2O INGAS

DOPANT	ADDED WT.% Fe	COMPRESSIVE STRENGTH (PSI) $\sigma_c \pm s$	FRACTION OF UNDOPED STRENGTH	RATIO OF WT. AFTER TO WT. BEFORE	NUMBER OF SAMPLES
None	0.0	7,725 ± 2,225		1.000	4
Fe	0.5	6,375 ± 1,675	0.948	0.998	4
Fe	1.0	4,825 ± 1,625	0.717	0.999	4
Fe	1.5	7,725 ± 850	1.149	0.999	4
Fe	2.0	8,075 ± 1,775	1.201	0.999	4
Fe_2O_3	0.5	8,100 ± 2,750	1.204	0.999	4
Fe_2O_3	1.0	10,450 ± 3,025	1.554	0.999	4
Fe_2O_3	1.5	10,500 ± 2,900	1.561	0.999	4
Fe_2O_3	2.0	5,975 ± 2,800	0.888	0.999	4

TABLE XXXI. STRENGTH AND WEIGHT LOSS DATA FOR 90+ WT.% ALUMINA CASTABLE EXPOSED TO 60% CO - 40% H_2O INGAS

DOPANT	ADDED WT.% Fe	COMPRESSIVE STRENGTH (PSI) $\sigma_c \pm s$	FRACTION OF UNDOPED STRENGTH	RATIO OF WT. AFTER TO WT. BEFORE	NUMBER OF SAMPLES
None	0.0	8,700 ± 2,800		1.005	4
Fe	0.5	8,150 ± 1,200	0.937	1.005	4
Fe	1.0	9,075 ± 1,500	1.043	1.003	4
Fe	1.5	8,550 ± 2,025	0.983	1.002	4
Fe	2.0	7,775 ± 1,300	0.894	1.003	4
Fe_2O_3	0.5	8,750 ± 725	1.006	1.000	4
Fe_2O_3	1.0	9,250 ± 475	1.063	1.001	4
Fe_2O_3	1.5	10,625 ± 750	1.221	1.001	4
Fe_2O_3	2.0	12,100 ± 3,050	1.391	1.001	4

TABLE XXXII. STRENGTH AND WEIGHT LOSS DATA FOR 50+ WT.% ALUMINA CASTABLE EXPOSED TO 60% CO - 40% H_2O INGAS

DOPANT	ADDED WT.% Fe	COMPRESSIVE STRENGTH (PSI) $\sigma_c \pm s$	FRACTION OF UNDOPED STRENGTH	RATIO OF WT. AFTER TO WT. BEFORE	NUMBER OF SAMPLES
None	0.0	4,775 ± 1,250		1.002	4
Fe	0.5	4,325 ± 975	0.906	1.000	4
Fe	1.0	4,275 ± 1,350	0.895	0.999	4
Fe	1.5	4,550 ± 550	0.953	0.999	4
Fe	2.0	3,150 ± 875	0.660	0.998	4
Fe_2O_3	0.5	3,850 ± 1,325	0.806	1.000	4
Fe_2O_3	1.0	3,975 ± 875	0.832	1.001	4
Fe_2O_3	1.5	4,175 ± 950	0.874	1.000	4
Fe_2O_3	2.0	4,250 ± 675	0.890	1.000	3

TABLE XXXIII. STRENGTH AND WEIGHT LOSS DATA FOR 90+ WT.% ALUMINA RAMMING MIX EXPOSED TO 60% CO - 40% H_2O INGAS

DOPANT	ADDED WT.% Fe	COMPRESSIVE STRENGTH (PSI) $\sigma_c \pm s$	FRACTION OF UNDOPED STRENGTH	RATIO OF WT. AFTER TO WT. BEFORE	NUMBER OF SAMPLES
None	0.0	6,900 ± 2,175		0.999	4
Fe	0.5	5,125 ± 2,000	0.743	0.999	4
Fe	1.0	8,525 ± 3,175	1.236	0.998	4
Fe	1.5	4,900 ± 975	0.710	0.999	4
Fe	2.0	8,625 ± 2,225	1.250	0.998	4
Fe_2O_3	0.5	9,375 ± 3,025	1.359	0.999	4
Fe_2O_3	1.0	7,775 ± 3,150	1.127	0.997	4
Fe_2O_3	1.5	10,600 ± 2,450	1.536	0.998	4
Fe_2O_3	2.0	11,550 ± 3,500	1.674	0.999	4

APPENDIX II

Apparatus for Examination of CO Disintegration of Refractory Materials.

A. Furnaces

B. Reaction Chambers

C. Gas Delivery System

D. Room to House Test Equipment

E. Safety System

A. Furnaces

The 100 hr. CO disintegration tests are being conducted at atmospheric pressure in two Thermolyne Model FA-1730 muffle furnaces. Durnace doors were modified to accomodate the reaction cells, as shown in Figure 63. Temperature control in each furnace is achieved through the use of a Type K thermocouple connected to a Thermolyne Model Furnatrol I temperature-calibrated set-point, time-proportional controller.

High-pressure tests are being conducted in a specially designed furnace built by the Tem-Pres Division of Leco Corporation, shown in Figure 64. The furnace features heating elements that can be fully protected from flammable gases by an inert atmosphere. Temperature is controlled by a Halmar Electronic Series PA-1 silicon controlled rectifier power amplifier controller that uses a Type K thermocouple.

Evaluation of the rapid test for CO disintegration is being performed in Lindberg Hevi-duty tube furnace able to accomodate a 1 1/4 in. OD tube. A V.P.I. & S.U.-built temperature-calbrated set-point controller is used with a Type K thermocouple to control temperature.

Samples are prefired in a Thermolyne Model F-6025 muffle furnace controlled by a Type K thermocouple tied into a V.P.I. & S.U.-built temperature-calibrated set-point controller.

B. Reaction Chambers

Gas-tight liners, parts of which are shown in Figure 63 for the muffle furnace were built at V.P.I. & S.U. from 1/4 in thick Type 316

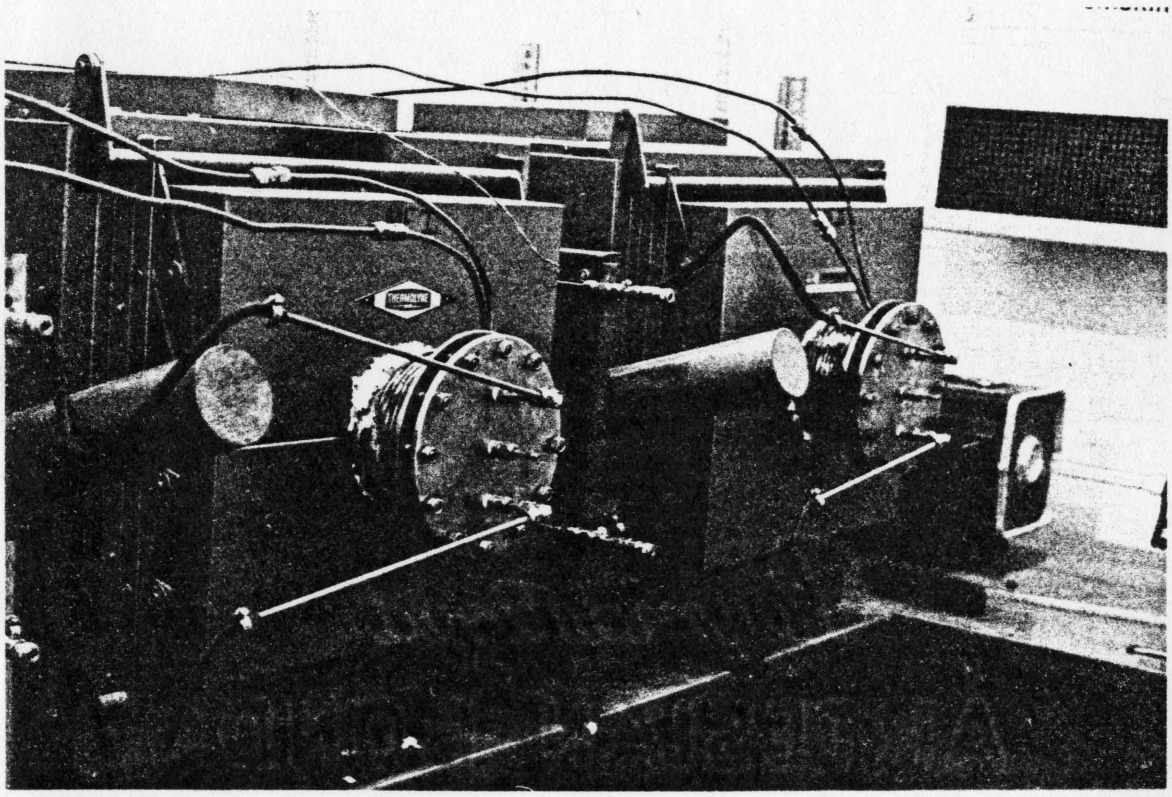

Figure 63. Muffle Furnaces and Liners.

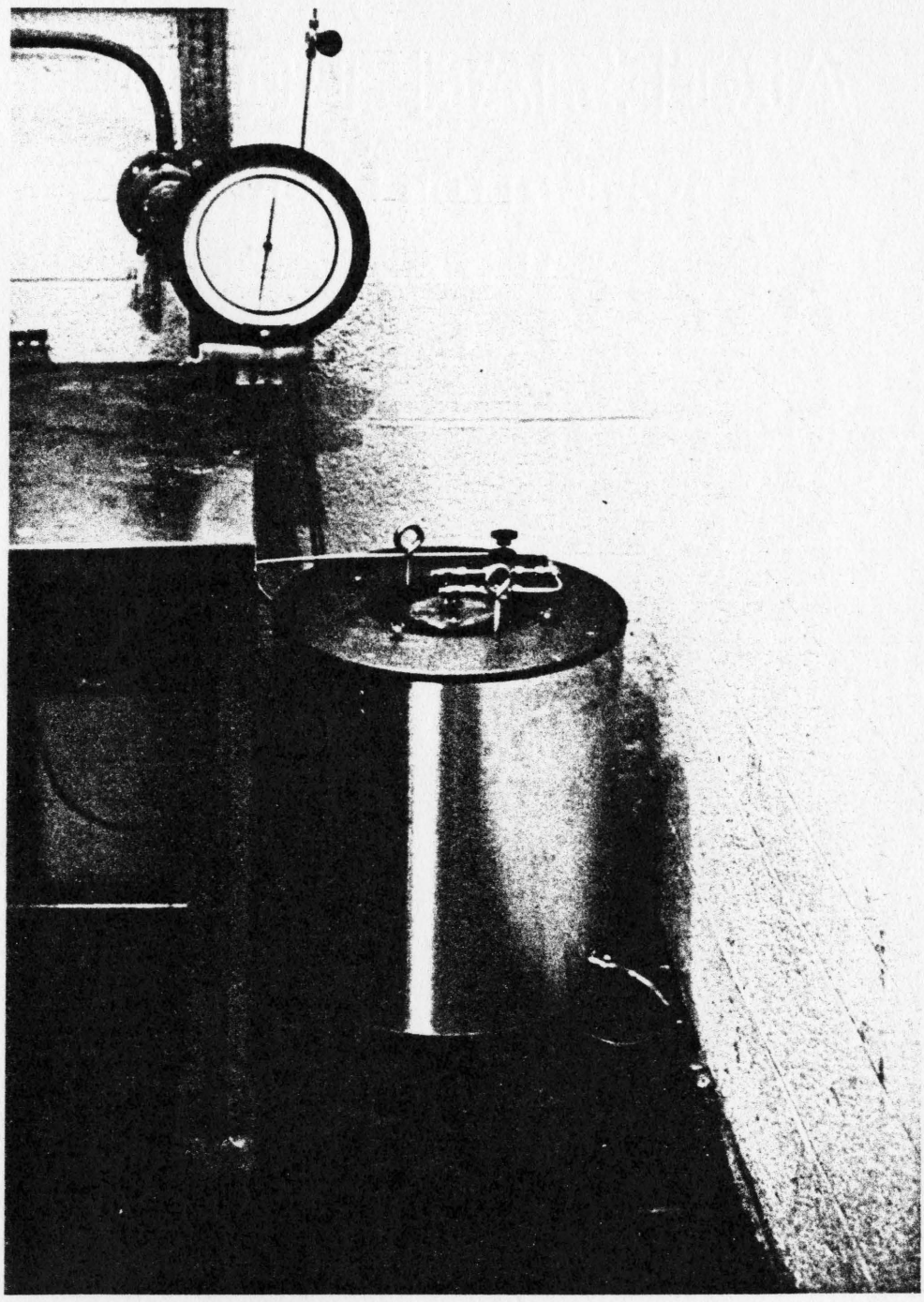

Figure 64. High Pressure Furnace and Cell.

stainless steel. Each liner will hold up to sixty 2 in. x 2 in. x 2 in. samples, which are loaded into the chamber through a 5 in. ID channel that extends through the furnace doors. The end of the channel is closed with a plate bolted against a Viton O-ring seal. This faceplate contains fittings for the gas inlet and outlet tubes, and the thermocouple well. The O-ring seal is protected from excessive temperature by a copper-coil water jacket that extends 3 in. along the outside of the channel, and fibrous alumina[1] packed inside the channel.

The high-pressure cell, shown in Figure 64, from Leco Corporation, Tem-Pres Division, and is made from Type 347 stainless steel. The cell has an 8 in. OD with a 5 in. bore, and can hold at least up to 10 2 in. x 2 in. x 2 in. samples. The cell is rated for 2,000 psi at 500°C.

A 1 in. ID fused silica tube is used in the rapid test experiments. Each end of the tube is drawn to a neck to allow connection of gas inlet and outlet tubing. A ground-glass ball-in-socket joint near one end of the tube is provided for sample access. Coating the joint with an anti-galling lubricant[2] provides a positive seal against gas leaks. The tube is shown, along with the furnace, in Figure 65.

C. Gas Delivery System

Gases are delivered to all four furnaces through 1/4 in. OD Type

1. Fibroflax, Aluminum Company of America, Pennsylvania
2. Silver Goop, Crawford Fitting Company, Ohio

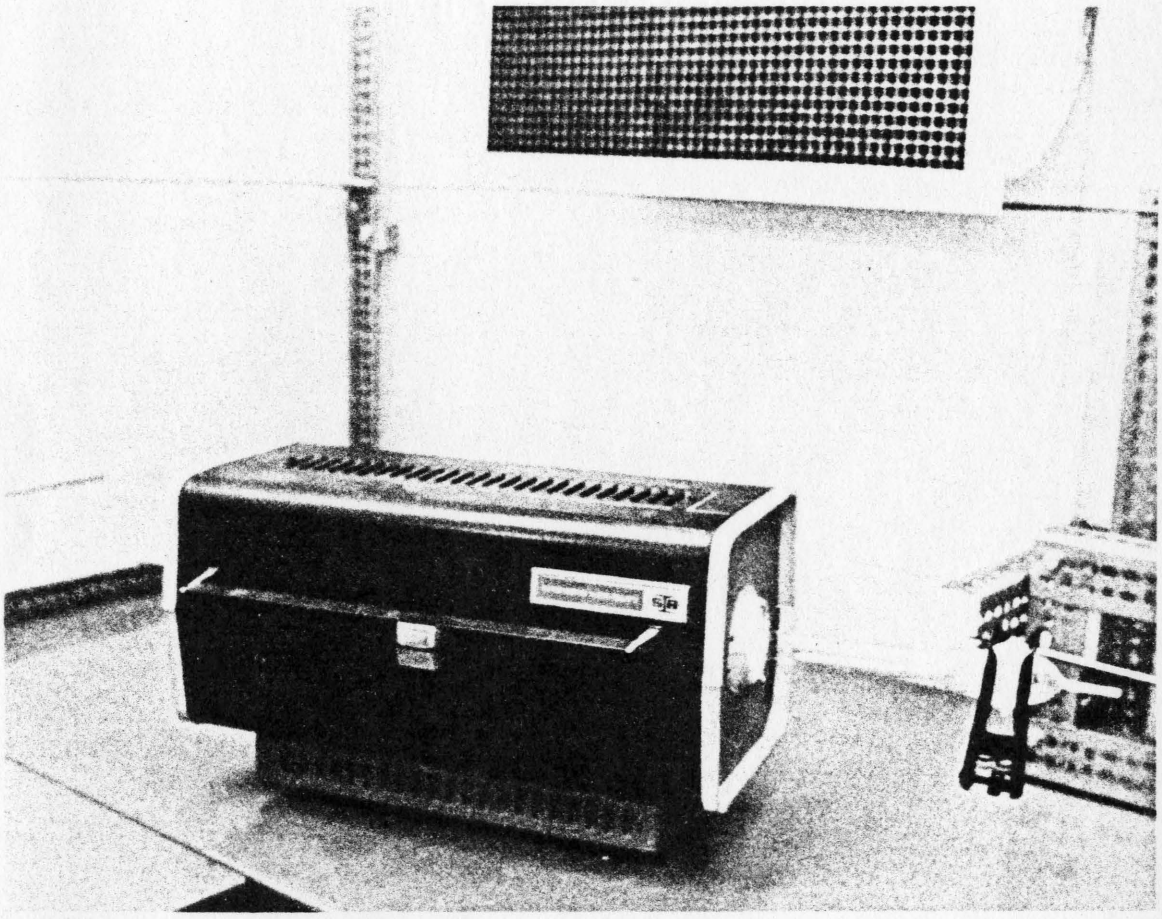

Figure 65. Tube Furnace and Liner.

316 stainless steel tubing. The muffle furnaces and tube furnace, in which tests at atmospheric pressure are conducted, are on a separate gas line from the high pressure furnace, as shown in the schematic diagram in Figure 66. An emergency exhaust line is shared by the atmospheric and high pressure systems.

D. Atmospheric Pressure Systems

Fail-safe equipment, consisting of a pressure switch and check valve (Valve 4), is encountered after passing Valve 3. They are placed at this point so that they will respond to any problems that occur in the atmospheric pressure system. The pressure switch, set to make contact at 10 psi, will initiate system shutdown (turn off furnaces, close air operated valve), if there is over-pressure in the system. The check-valve will allow release of the built-up gases.

Downstream from the pressure switch, gas passes through a cleaning module, to remove any traces of water (Drierite) and carbon dioxide (Ascarite). If these cleaning agents lose their effectiveness while an experiment is in progress, the entire module can easily be changed. Quick-connect fittings are disconnected, shutting off gas flow, then the module is replaced. The gas then passes a pressure gauge which will allow precise measurement of operating pressures. This gauge will also be useful in troubleshooting individual legs if the system in case of emergency shutdown.

Gas is directed to individual furnaces by Valve pairs 5 and 8, 6 and 9, and 7 and 10. For example, closing Valves 7 and 10 would iso-

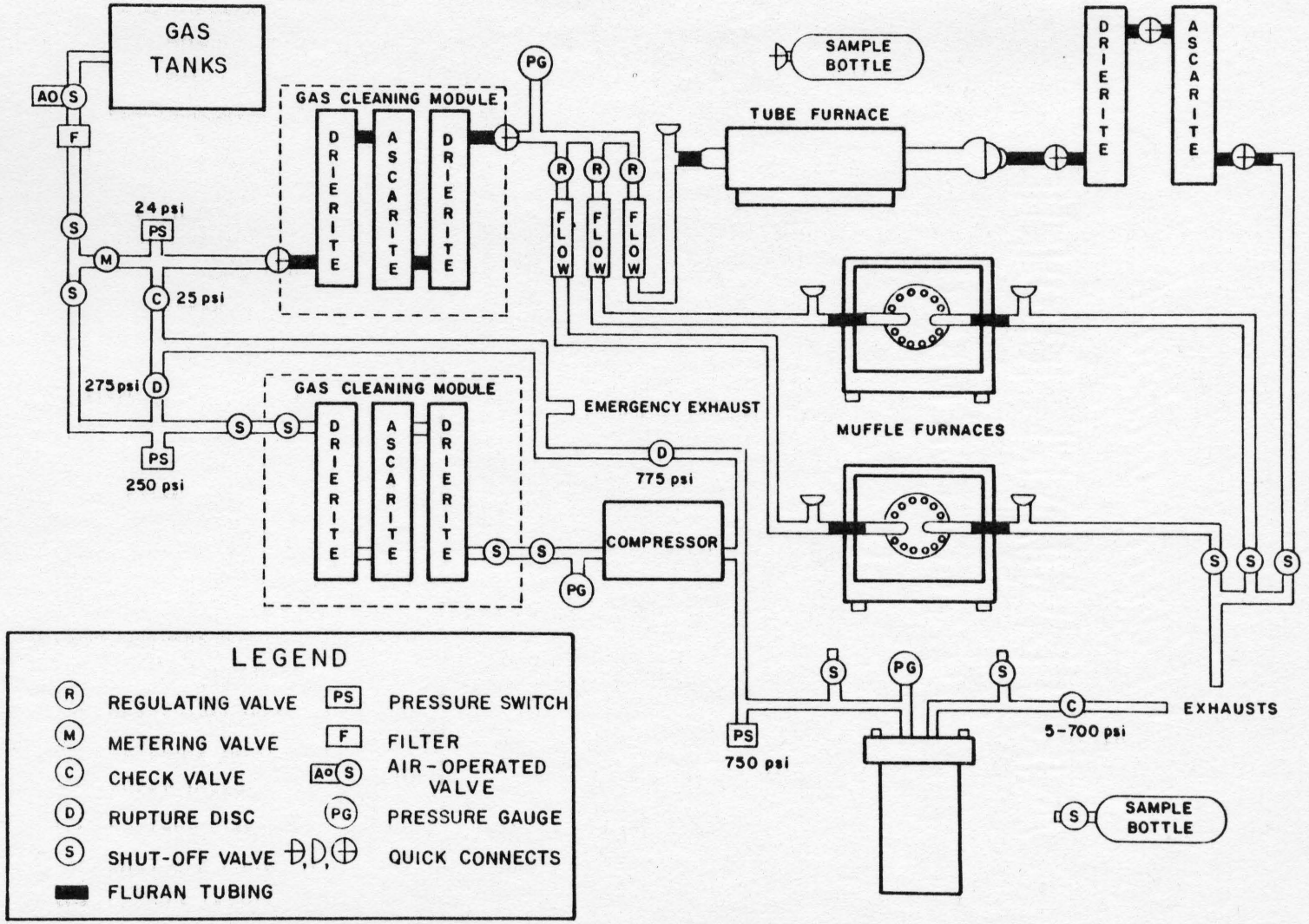

Figure 66. SCHEMATIC DIAGRAM OF APPARATUS

late the tube furnace from the system. Valves 5, 6, and 7 allow some control of gas flow to each furnace. These are provided so that flow rates to each furnace can be maintained regardless of what combination of furnaces is being used. Each leg of the system also has sampling ports on the incoming and outgoing sides of the furnaces. The tube furnace branch is somewhat more complicated than that for the muffle furnaces, because of the nature of the Ascarite column on the exhaust side of the furnace, which must be removed and weighed hourly.

E. High Pressure System

The high pressure system is somewhat similar to the atmospheric pressure system. A pressure switch set at 250 psi and a rupture disc set at 275 psi are located immediate after Valve 2, following the same rational as the failsafe equipment location in the atmospheric pressure system. The gas cleaning module is connected to the system by valves and Swagelok fittings, rather quick-connectors, due to the high pressure (100 to 200 psi) that will be used in the line. Sampling ports will also be accessed with valves 15 and 16 and fittings.

After cleaning, gas pressure is boosted by a Whitey Model LC-10 compressor. This compressor has a special feature, in that it meters the flow of gas through the system. Setting pressure on the inlet and outlet sides of the compressor will determine the flow rate of the gas. Pressure gauges are located to allow proper balance of gas pressure for a desired flow rate.

Pressure in the reaction cell will be regulated with an adjustable check valve (5-700 psi), valve 17. A pressure switch set at 750 psi and rupture disc set at 775 psi are also installed near the cell for added safety.

F. Room to House Test Equipment

In cooperation with the VPI&SU OSHA office, a special 7'3" x 11'6" room was constructed for this project (cost of construction was covered by VPI&SU). Basically the room as a whole has a fire resistance rating of at least 2 hours. All doors and potentially flammable materials are covered with 2 layers of 5/8" gypsum board. The room is provided with explosion venting of approximately 1 ft^2 per 30 ft^3 of room volume. The venting is achieved by placing two blow-out panels near the ceiling of two walls. The air in the room is exhausted at least 20 times per hour through an explosion proof fan; the air intake is located low on a wall away from the exhaust fan in order for the air to flow up and over the experimental equipment. All electrical equipment in the room is explosion proof. In addition, the room contains a sprinkling system set at 165°C and a gas monitor that can be set to sound an alarm at 1250 ppm of CO and H_2 and initiate system shut-down at 2,500 ppm.

A special shed for holding gas tanks has been constructed on the roof of the building approximately 50' away from the test facility. This prevents storing large quantities of gas (and large amounts of stored energy) in an area where personnel will be working.

G. Safety System

Shutdown of the experiment can be initiated by any one of the following conditions: a) excess pressure in the gas lines; b) overheating in either muffle furnace or the high pressure furnace; or c) buildup of CO or H_2 in the test room.

These conditions can be detected, respectively, by pressure switches, thermocouples, and a gas monitor. Signals from any one of these devices will trip a relay, causing all furnaces and the compressor to be turned off and an air-operated valve (Valve 1) on the high pressure line to be closed. The relay can also be tripped manually from outside the test room.

Heating elements in the muffle furnaces and the high pressure furnace are protected from potentially explosive hydrogen concentrations by inert gas. Unlike the high pressure furnace, heating elements in the muffle furnaces cannot be sealed off from the outside atmosphere. For this reason, inert gas is passed through the walls of the furnace and around the heating elements during the test. Inert gas in the high pressure furnace can be left static once operating temperature has been obtained.

As described earlier, in case there is an explosion, the room is designed to dissipate the force of the blast and contain any resulting fires.

APPENDIX III

Calculation of Equilibrium CO/CO_2 Ratio at 500°C

I. Theoretical Background

Classical thermodynamics can be used to determine the relative equilibrium concentrations of gaseous compounds in chemical reactions. This can be done quite easily if ideal behavior of all compounds in the reaction is assumed. Even when there is significant deviation from ideal conditions, calculations based on ideality can provide useful guidelines to aid experimental observations.

For the chemical reaction:

$$\mu_1 R_1 + \mu_2 R_2 + \cdots + \mu_m R_m = \nu_1 P_1 + \nu_2 P_2 + \cdots + \nu_n P_n \qquad (1)$$

where μ_i and ν_j are stiochiometric factors, the equilibrium constant, K, of the reaction is given by:

$$K = \frac{(P_1)^{\nu 1}(P_2)^{\nu 2}\ldots(P_n)^{\nu n}}{(R_1)^{\mu 1}(R_2)^{\mu 2}\ldots(R_m)^{\mu m}} \qquad (2)$$

when ideal behavior (unit activity coefficients) of reactants, R_i, and products, P_j, is assumed. A relationship between the equilibrium constant and the change in enthapy, $\Delta H°$, of the reaction can be found using the Van't Hoff equation:[1]

$$\frac{d\ell n(K)}{dt} = \frac{\Delta H°}{RT^2} \qquad (3)$$

The Kirchoff formula[2] allows the enthapy change of a reaction to be determined from heat capacity data for the reactants and products:

$$\Delta H^\circ = \Delta H_I^\circ + \int \Delta C_p dT \tag{4}$$

where ΔH_I° is a constant of integration and

$$\Delta C_p = \sum_{j=1}^{n} \nu_j C_{P_{Pj}} - \sum_{i=i}^{m} \mu_i C_{P_{Ri}} \tag{5}$$

The constant ΔH_I° can be determined by solving Equation 4 for a known ΔH° at a particular temperature within the range of validity of ΔCp. Enthapy changes at other temperatures within the ΔCp range of validity can then be calculated.

The equilibrium constant can be calculated by replacing ΔH° in Equation 3 with its equivalent in Equation 4 and integrating:

$$R\ell n(K) = \int^{T'} \frac{\Delta H_I^\circ + \int \Delta C_p dT}{T^2} \tag{6}$$

Using the calculated value of K, relative amounts of gaseous reactants and products can then be determined by means of Equation 1.

II. Calculation of Ideal Equilibrium Concentration of CO and CO_2 at 500°

Reaction: $2CO = CO_2 + C$

Data:[3] $C_p = A + Bx10^{-3} T + Cx10^5 T^{-2}$ (Cal)

Compound	H°_{298}(Kcal)	A	B	C
C	0.453	2.18*	3.16*	-1.48*
CO	-26.42	6.79	0.98	-0.11
CO_2	-94.05	10.55	2.16	-2.04

* for graphite, amorphous carbon data unavailable

Calculation:

$$\Delta H^{\circ}_{298} = H^{\circ}_{298CO_2} + H^{\circ}_{298C} - 2H^{\circ}_{298CO}$$

$$= 94.05 + 0.453 - 2(-26.42)$$

$$= -40.76 \times 10^{3} \text{ cal}$$

$$\Delta C_p = C_pCO_2 + C_{pc} - 2C_{p_{co}}$$

$$= (10.55+2.18-(2)6.79)+(2.16+3.16-(2)0.98)x10^{-3}T$$

$$+(-2.04-1.48+(2)0.11)x10^{5}T^{-2}$$

$$= -0.85+3.36x10^{-3}T-3.30x10^{5}T^{-2}$$

$$\Delta H^{\circ}_{I} = \Delta H^{\circ}_{298} - \int^{298}\Delta C_p dT$$

$$= -40.76x10^{3}-\int^{298}(-0.85+3.36x10^{-3}T-3.30x10^{5}T^{-2})dT$$

$$= -40.76x10^{3}+0.85(298)-1.68x10^{-3}(298)^{2}+3.30x10^{5}(298)^{-1}$$

$$= -39,549 \text{ cal}$$

$$R\ell n(K) = \int^{773} \frac{-39,549+\int(-0.85+3.36x10^{-3}T-3.30x10^{5}T^{-2})}{T^{2}} dT$$

$$= \int^{773} \frac{-39,549-0.85T+1.68x10^{-3}T^{2}+3.30x10^{5}T^{-1}}{T^{2}} dT$$

$$= \int^{773}(-39,549T^{-2}-0.85T^{-1}+1.68x10^{-3}+3.30x10^{5}T^{-3})dT$$

$$= 39,549(773)^{-1}-0.85\ell n(773)+1.68x10^{-3}(773)$$

$$-1.65x10^{5}(773)^{-2}$$

$$= 46.53$$

$$K = e^{46.53/1.987}$$

$$= e^{23.42}$$

$$= 1.48 \times 10^{10}$$

$$= \frac{(CO_2)}{(CO)^2}$$

In a given atmosphere composed only of CO and CO_2, (CO) = X, (CO_2) = 1 - X

$$1.48 \times 10^{10} = \frac{1 - X}{X^2}$$

$$1.48 \times 10^{10} X^2 + X - 1 = 0$$

$$X = 8.22 \times 10^{-6} \simeq \frac{(CO)}{(CO_2)}$$

REFERENCES

1. G. N. Lewis, and M. Randall, Thermodynamics, Second Edition, pp. 173 (1961).

2. Ibid, pp. 72 (1961).

3. I. Barin, and O. Knacke, Thermochemical Properties of Inorganic Substances, pp. 116, 162, 163 (1973).

APPENDIX IV

Effect of Iron-Impurity Particle Size on CO Disintegration of the 90+ Weight Percent Alumina Castable Refractory

A. Experimental Results

The results of this experiment are summarized in Figure 67 and Table VI.

B. Discussion

The retained strength of the castable reached a maximum at or near the 35-80 mesh size of iron oxide dopant, as shown in Figure 68 This strength behavior and the corresponding degree of spalling damage, shown in Figure 67, indicate that the particle size of the iron impurity has a definite effect on CO disintegration in refractories. This effect is more complicated than a linear or exponential dependence, as the refractory strength first improves, then degrades as the particle size of the iron inclusion is reduced.

An explanation for the observed strength dependence can be found by close examination of samples doped with different size iron oxide particles. Samples with large dopant particles have a different fracture behavior from samples with small dopant particles. Fracture in samples doped with 12-35 mesh iron oxide occurred as large cracks, generated at dopant sites and propagated through the concrete matrix, as shown in Figure 69 . In samples doped with smaller size iron oxide inclusions, the matrix appeared to flake away, as shown in Figure 70, rather than contain large cracks. Both types of fracture can be seen as the result of carbon deposition about the iron-impurity particles in the refractory.

In the case of the large cracks, impurity particles are large and widely dispersed in the matrix of the refractory. Being large,

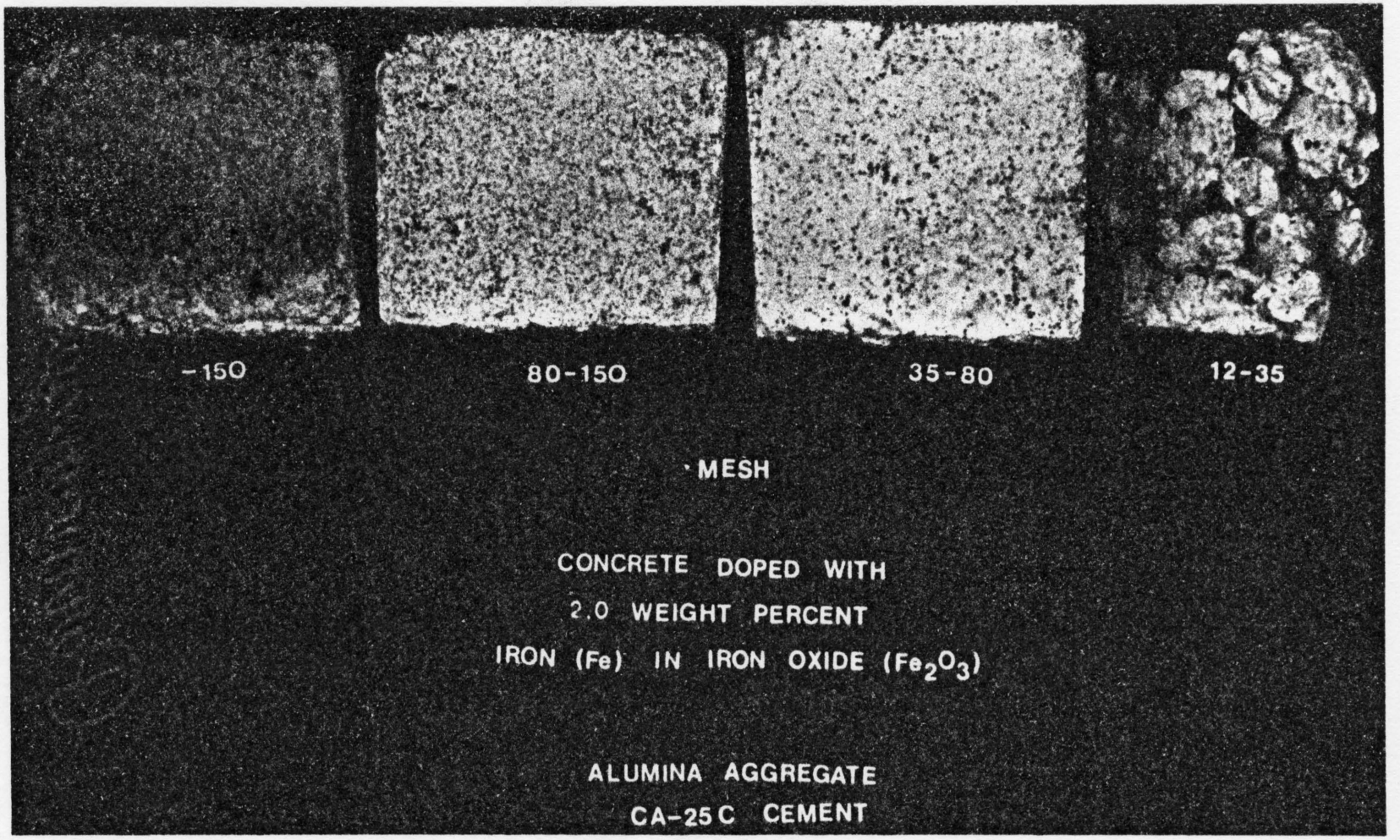

Figure 67. 100 hr. Exposure to CO- Representative Samples of 90+ Wt.% Alumina Castable.

TABLE VI. STRENGTH AND SPALLING DATA FOR 90+ WT.% ALUMINA CASTABLE DOPED WITH VARIOUS PARTICLE SIZES OF IRON OXIDE

Fe_2O_3 Particle Size Distribution	Appearance of Castables	Compressive Strength σ_c ± s (psi)	No. Samples Tested
12 - 35	Complete Disintegration	0	0	4
35 - 80	Light Spalling at Corners	3,950	575	4
80 - 150	Light Spalling at Corners	3,500	775	4
- 150	Light to moderate Spalling at Corners and Edges	3,100	775	4

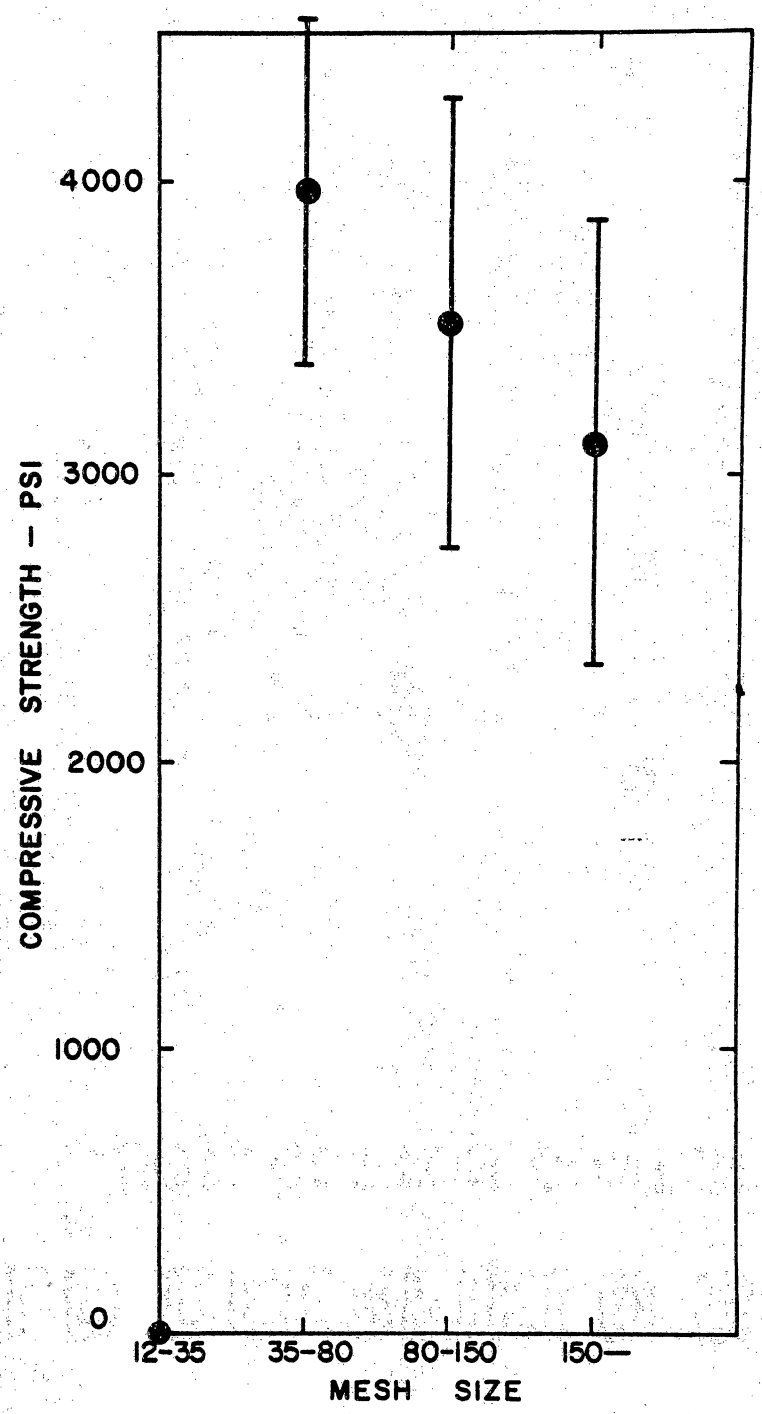

Figure 68. Compressive Strength of 90+ Wt.% Alumina Castable Doped with 2.0 Wt.% Fe_2O_3.

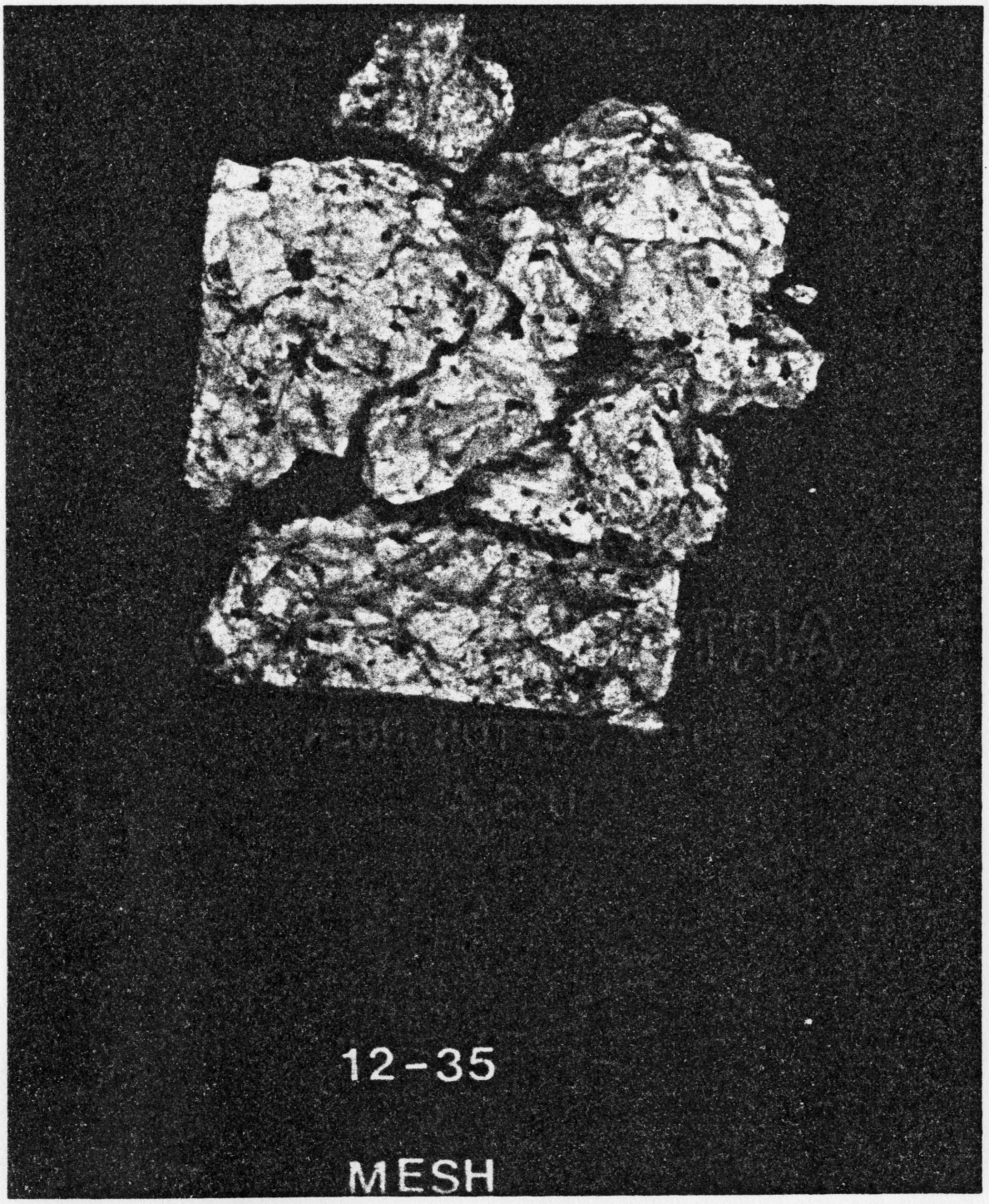

Figure 69. Spalling Damage in 90+ Wt.% Alumina Castable Doped with 12-35 Mesh Fe_2O_3.

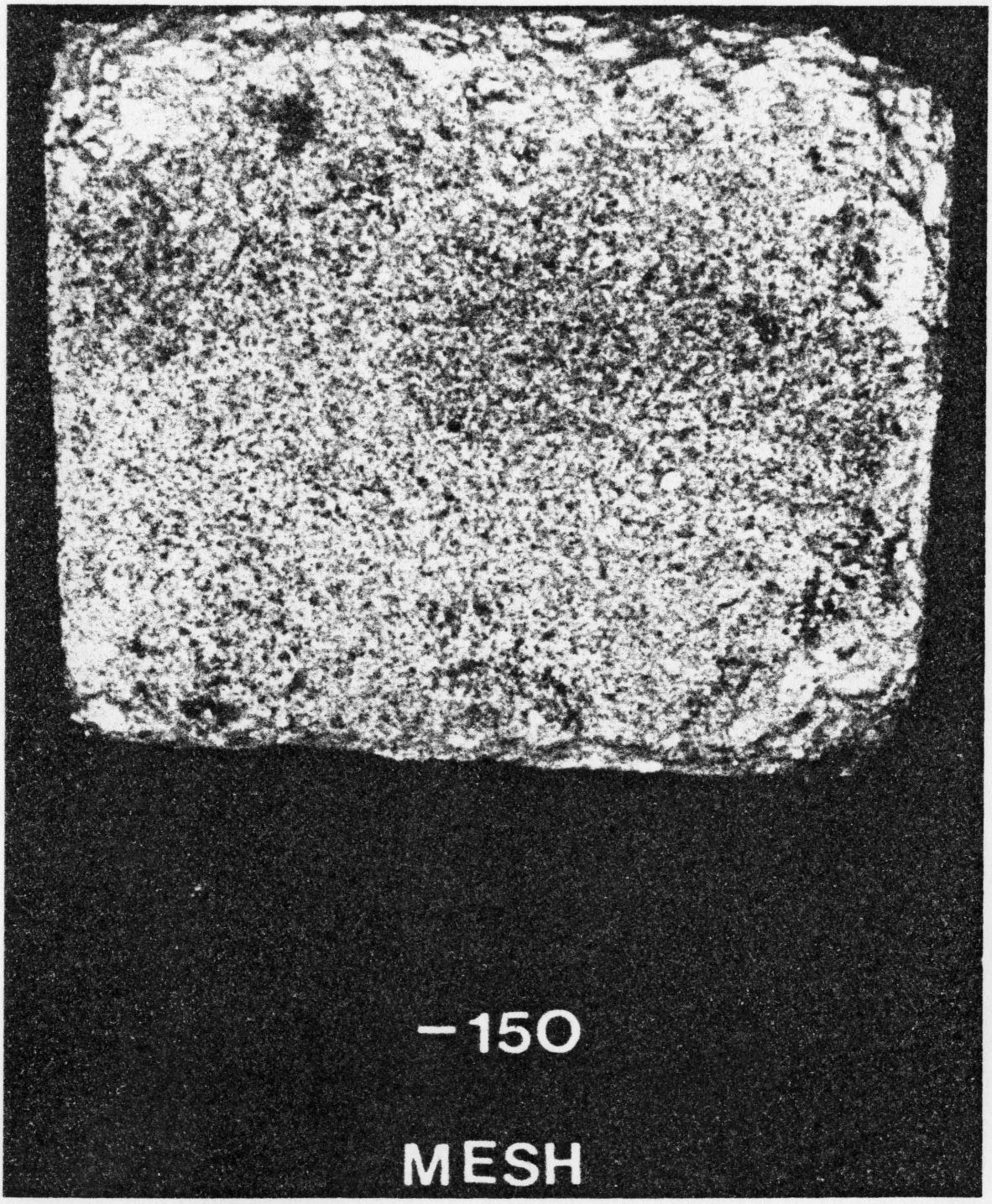

Figure 70. Spalling Damage in 90+ Wt.% Alumina Castable Doped with -150 Mesh Fe_2O_3.

they induce large amounts of carbon to deposit near them. The carbon induces enough strain in the matrix to generate and propagate cracks over large distances.

In the case of the flaking matrix, the impurity particles are small, but, they are closely packed, since they constitute the same volume fraction of the refractory as the larger particles. The small particles do not cause as much carbon to be deposited, therefore, the strains produced in the refractory matrix will not be as great. Cracks will propagate only over short distances, as there is less strain, however, with the closer spacing of the particles, the cracks need not be long in order to intersect one another.

APPENDIX V

Effect of Elevated Gas Pressure on CO Disintegration of Three Monolithic Refractories

A. Experimental Results

1. Visible Effects of 100 Hr. Exposure to CO at 600 PSI

a. 90+ Wt.% Alumina Castable

Samples of the undoped 90+ wt.% alumina castable turned light gray due to carbon deposition. One of the four samples also had a large crack shown in Figure 71a, that was later found to be caused by one small impurity site, shown in Figure 71b.

The three samples doped with 0.5 wt.% metallic iron completely disintegrated in the 100 hr. test, while the three samples doped with 2.0 Fe wt.% iron oxide remained intact. The Fe_2O_3 - doped samples were very dark gray in color and had large amounts of free carbon deposited in surface pores.

b. 50+ Wt.% Alumina Castable

Samples of the undoped 50+ wt.% alumina castable did not turn gray in color, as did the 90+ wt.% alumina castable, however, very small amounts of edge spalling occurred on all four of the samples. In addition, a small portion of the face of one sample spalled revealing a carbon ball.

The three samples doped with 0.5 wt.% metallic iron completely disintegrated. Samples doped with 2.0 Fe wt.% iron oxide remained intact. The edge spalling seen for samples of the undoped refractory did not occur in the Fe_2O_3 - doped samples. They also were lighter in color than the iron oxide-doped samples of the 90+ wt. alumina castable.

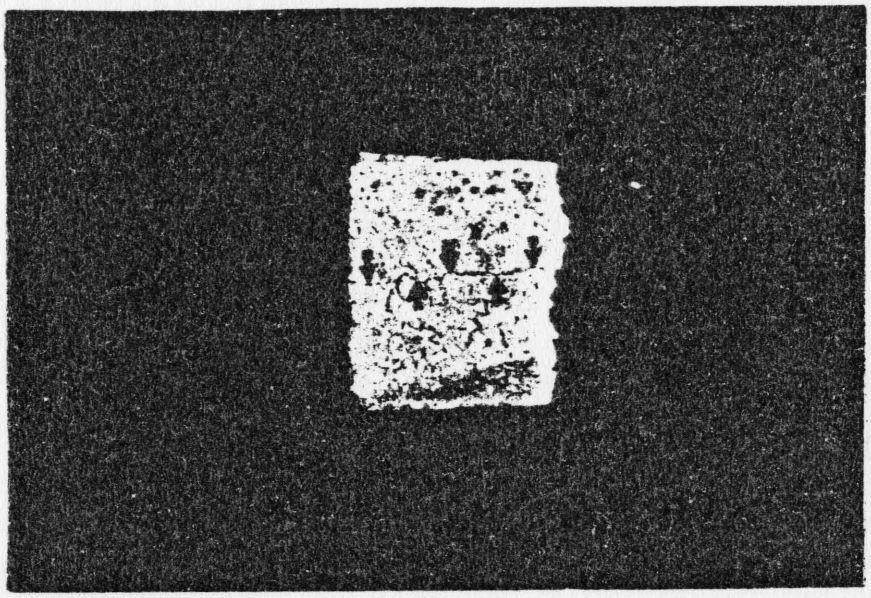

a. Crack running horizontally through center of sample following high pressure CO test, highlighted by arrows.

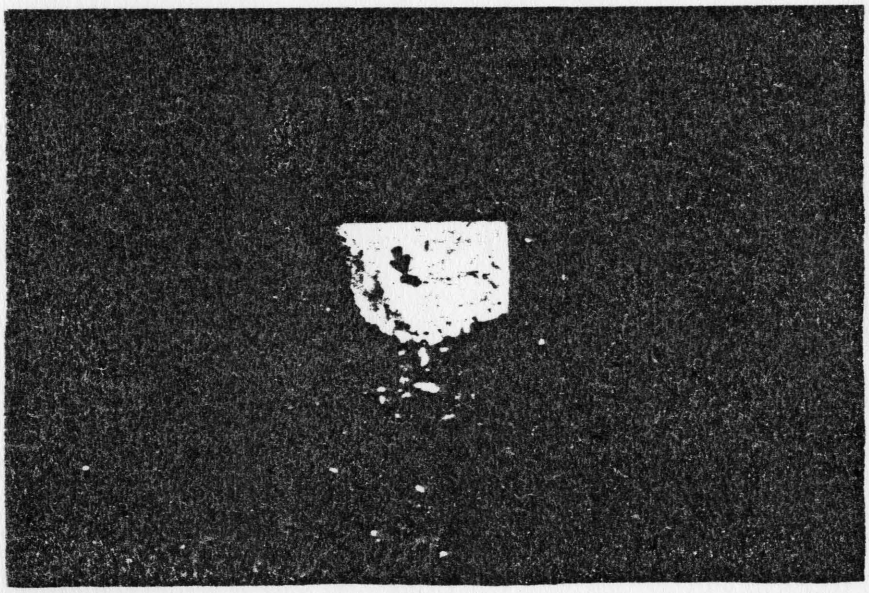

b. Carbon deposit causing crack as seen following compression strength test, highlighted by arrow.

Figure 71. Sample of 90+ Wt.% Alumina Castable Exposed to CO at 600 PSI.

c. 90+ Wt.% Alumina Phosphate-Bonded Ramming Mix

Samples of the 90+ wt.% alumina phosphate-bonded ramming mix doped with 0.5 wt.% metallic iron completely disintegrated. Samples doped with 1.0 Fe wt.% iron oxide turned medium gray and spalled on corners and edges. Undoped samples had no spalling damage and appeared no darker than when exposed to CO at atmospheric pressure.

All intact samples had large amounts of carbon deposition at the surface. This is most likely caused by the presence of small amounts of steel that were picked up from the mold used in preparation of the ramming mix samples, and, it did not appear to penetrate into the refractory or cause any spalling damage.

2. Compressive Strength After 100 Hr. Exposure to CO at 600 PSI

Data for the three monolithic refractories are summarized in Table VII.

a. Strength of Undoped Refractories

The average undoped compressive strengths of both castables are slightly greater than the overall average strengths recorded for these two refractories at atmospheric pressure. In the case of the 90+ wt.% alumina refractory, the average strength after exposure to CO at 600 psi included the strength of the sample severely cracked by carbon deposition about an impurity, apparently present in the raw material. The 50+ wt.% alumina castable had good strength retention after 100

TABLE VII. STRENGTH AND WEIGHT LOSS DATA FOR REFRACTORIES EXPOSED TO CO AT 600 PSI

ADDED DOPANT/WT.% Fe	COMPRESSIVE STRENGTH (PSI) $\sigma_c \pm S$	RATIO WT. BEFORE TO WT. AFTER	NUMBER OF SAMPLES	AVG. UNDOPED STRENGTH AT ONE ATM. (PSI)** $\sigma_c \pm S$
90+ Wt.% Al_2O_3 Castable				
None/p.p	7,675 ± 500	0.999	4	7,150 ± 2,050
Fe/0.5	0 ± 0	0.000	3	
Fe_2O_3	9,725 ± 600	1.007	3	
50+ Wt.% Al_2O_3 Castable				
None/0.0	5,400 ± 1,025	0.999	4*	4,825 ± 1,250
Fe/0.5	0 ± 0	0.000	3	
Fe_2O_3/2.0	7,850 ± 325	1.011	3	
90+ Wt.% Al_2O_3 Phosphate-Bonded Ramming Mix				
None/0.0	6,900 ± 950	1.000	4*	10,050 ± 3,750
Fe/0.5	0 ± 0	0.000	3	
Fe_2O_3/1.0	6,775 ± 2,200	1.006	3	

*Only 3 samples used in strength testing.

**44 samples for each refractory from 100 hr. exposures to various CO-containing atmospheres.

hrs. in CO at 600 psi despite the presence of numerous carbon balls and small amounts of spalling.

The average strength of the undoped 90+ wt.% alumina phosphate-bonded ramming mix in the 600 psi CO test was also within the standard deviation of its overall average undoped strength at atmospheric pressure, however, this strength from the high pressure test is at the lower limit of the deviation.

b. Strength of Refractories Doped with Fe

All three refractories suffered complete disintegration when doped with 0.5 wt.% metallic iron, and thus had no retained strength. Greater amounts of metallic iron in the refractories would again yield complete disintegration with no retained strength.

c. Strength of Refractories Doped with Fe_2O_3

The strength when doped with 2.0 Fe wt.% iron oxide was at least as great as the undoped strength for both castables. This result is similar to what occurred for these two refractories at atmospheric pressure, and, smaller amounts of iron oxide dopant should yield similar strengths to what was observed at 2.0 Fe wt.%.

Strength of the 90+ wt.% alumina phosphate-bonded ramming mix was slightly less when doped with 1.0 Fe wt.% iron oxide than its undoped strength. At atmospheric pressure, samples of ramming mix doped with up to 1.0 Fe wt.% iron oxide also retained essentially the same amount of strength as the undoped refractory. Strength of the iron oxide-

doped ramming mix decreased due to CO disintegration damage at levels of 1.5 Fe wt.% and 2.0 Fe wt.% in the atmospheric pressure tests. Based on the response of the 0.5 wt.% metallic iron and 1.0 Fe wt.% iron oxide-doped ramming mix to CO at 600 psi, the projected response of the ramming mix doped with 1.5 Fe wt.% and 2.0 Fe wt.% iron oxide would be major amounts of spalling at both dopant levels and, possibly, complete disintegration at the 2.0 Fe wt.% level. The spalling damage would decrease the strength at these dopant levels from 70-85% of the undoped strength to less than 50% of the undoped strength.

B. Discussion

1. Selection of Samples

Undoped samples of the three refractories were exposed to CO at 600 psi in order to see if disintegration damage, which appeared to be nonexistent at atmospheric pressure, could be induced. Samples doped with 0.5 wt.% metallic iron suffered some disintegration damage at atmospheric pressure and were included to see to what degree this disintegration was accelerated. Castables doped with up to 2.0 Fe wt.% iron oxide suffered no apparent disintegration in CO at atmospheric pressure, as did the phosphate-bonded ramming mix doped with up to 1.0 Fe wt.% iron oxide. Samples at these highest observed unaffected dopant levels of iron oxide were included to see if pressure would induce CO disintegration.

2. Effect of Pressure on CO Disintegration

a. 90+ Wt.% Alumina Castable

CO disintegration of the 90+ wt.% alumina castable is definitely accelerated by exposure to CO at high pressure, in this case 600 psi. Undoped samples of the refractory turned gray from uniform carbon deposition that was not seen at atmospheric pressure. Furthermore, extremely small amounts (less than, including deposited carbon, 0.05 Vol.% of the sample) of a carbon deposition catalyzing impurity can severely damage the refractory, as shown in Figure 71. In cases where carbon deposition had been shown to occur at atmospheric pressure, namely, for a dopant level of 0.5 wt.% metallic iron, raising gas pressure had the catastrophic effect of causing complete disintegration.

Reduction of iron oxide impurities appeared unaffected by increasing the pressure of the CO. The extra darkness of iron oxide-doped samples can be seen as a composite of the darkening caused in the undoped refractory at 600 psi and the gray color obtained at atmospheric pressure in the iron oxide-doped samples.

The effects observed at high pressure agree with chemical reactions for carbon deposition:

$$2\ CO = CO_2 + C, \tag{1}$$

and for reduction of iron oxide:

$$3Fe_2O_3 + CO = 2Fe_3O_4 + CO_2. \tag{2}$$

In the case of carbon deposition, elevated pressure would increase

carbon deposition, as two moles of gas are replaced by only one in the reaction. On the other hand, in the case of iron oxide reduction, there is no change in the amount of gas present, so pressure would not influence the reaction. This latter result is especially true for the CO disintegration test, which has a CO-saturated atmosphere even at atmospheric pressure.

b. 50+ Wt.% Alumina Castable

CO disintegration in the 50+ wt.% alumina castable is also accelerated by elevated pressure. Carbon deposition in undoped samples of this refractory is not uniform, which it was for the 90+ wt.% alumina castable, and more serious degradation was observed. Carbon in the 50+ wt.% alumina castable tends to form balls. This increases local strains in the refractory and brings on spalling damage sooner. The undoped samples exposed to CO at 600 psi for 100 hr. had spalling damage beginning to occur very near their surfaces. As yet, this damage had not penetrated far enough into the refractory to degrade its mechanical strength.

The addition of a small amount of metallic iron, in this case 0.5 wt.%, caused complete destruction of the 50+ wt.% alumina castable, as it did for the 90+ wt.% alumina castable. Iron oxide-doped samples of the 50+ wt.% alumina castable also behaved the same as similarly doped samples of the 90+ wt.% castable, in that reduction of the iron-oxide impurity was not accelerated by elevated pressure.

c. 90+ Wt.% Alumina Phosphate-Bonded Ramming Mix

CO disintegration of the 90+ wt.% alumina phosphate-bonded ramming mix was also accelerated by high pressure when carbon deposition catalysts were present. Samples doped with 0.5 wt.% metallic iron were completely destroyed. Samples doped with 1.0 Fe wt.% iron oxide suffered small amounts of spalling and no measurable strength degradation. Although the phosphates present do cause some catalysts for carbon deposition to be formed from the iron oxide impurities in the ramming mix, the observed trend is similar to that seen for the castables, in that pressure tends to have little affect on the production of carbon deposition catalysts from iron oxide.

Undoped samples of the refractory had no apparent signs of accelerated carbon deposition under high-pressure CO. There were no signs of carbon deposition in the samples. The strength of the undoped ramming mix may have been slightly degraded, however, it was still within the bounds of statistical error for strength.

Publications and Presentations

The information contained in this thesis has been published in Annual and Quarterly Progress Reports entitled "Investigation of CO Disintegration of Refractories in Coal Gasifiers" under United States Department of Energy contract number EF-77-S-01-2631 with J. J. Brown, Jr. as principal investigator and G. E. Wrenn, Jr. as principal author. Distribution of the reports was limited to the USDOE and other selected agencies and institutions. All reports are available for public examination.

The contents of this thesis have also been the subject of two technical presentations by G. E. Wrenn, Jr., co-authored by J. J. Brown, Jr.:

> "CO Disintegration of High-Alumina Monolithic Refractories for Coal Gasifiers," presented at the Fall Meeting of The American Ceramic Society Refractories Division, Oct. 5-7, 1978, Bedford Springs, Pa., and at the Fall Meeting of The Virginia Section of The American Ceramic Society, Oct. 20, 1978, Roanoke, Va.
>
> "Effect of Pressure on CO Disintegration of High-Alumina Castable and Monolithic Refractories," presented at the Annual Meeting of The American Ceramic Society, Apr. 28-May 2, 1979, Cincinnati, Oh.

The two page vita has been removed from the scanned document. Page 1 of 2

The two page vita has been removed from the scanned document. Page 2 of 2

EFFECT OF VARIOUS GASES ON CO DISINTEGRATION OF MONOLITHIC REFRACTORIES FOR COAL GASIFIERS

by

George E. Wrenn, Jr.

(ABSTRACT)

Three monolithic refractories (a 90+ wt.% alumina Castable, a 50+ wt.% alumina castable, and a 90+ wt.% alumina phosphate-bonded ramming mix) doped with up to 2.0 wt.% Fe and 2.0 Fe wt.% Fe_2O_3 were tested for CO disintegration in a 100 hr. test similar to ASTM C-288. The effects of CO_2, NH_3, H_2, H_2S, and H_2O on CO disintegration were observed.

Prefired samples of all three refractories were found to be susceptible to disintegration in a CO atmosphere when 0.5 wt.% Fe or more was added. Castables doped with up to 2.0 Fe wt.% Fe_2O_3 were not affected by CO, while the ramming mix doped with 1.5 Fe wt.% Fe_2O_3 or more was.

H_2 and H_2O proved most effective in retarding CO disintegration in all three refractories. CO_2, H_2S, and NH_3, in descending order, also retarded CO disintegration in both castables. The retarding effect of up to 15% CO_2 in CO is questionable for the ramming mix. NH_3 did not slow CO disintegration in this refractory and H_2S actually accelerated the disintegration process.

The effect of gas pressure is also found to be especially important, for it greatly accelerates CO disintegration in all three monoliths and appears to be a more significant factor than the disintegration-inhibiting gases.

An optimum iron-impurity size range, neither a maximum nor a minimum, for which CO disintegration resistance was greatest was also found for the 90+ wt.% alumina castable.